Marine community changes after a hurricane disturbance across a natural CO_2 gradient

Birgit Solheim Huseklepp

Master of Science in Biology – Marine Biology
4th semester 2021
Department of Biological Sciences, University of Bergen

Supervisors:
Samuel P. S. Rastrick – Institute of Marine Research
Thorolf Magnesen – Department of Biological Sciences, University of Bergen.

ACKNOWLEDGMENTS:
The material for this thesis was gathered as a part of a project in Dominica run by Operation Wallacea, which is an organization that engages conservation research expeditions, and I am thankful for the opportunity to work with them. The project was brought to me by my main supervisor, Samuel P. S. Rastrick at the Institute of Marine Research. He has been engaged in the project since 2014, and in similar projects for a long time, and has provided me with great knowledge and guidance in the project, for which I am thankful for. Additionally, I wish to thank Helen Rastrick for guidance of species identification. I am also thankful for my internal supervisor, Thorolf Magnesen at the University of Bergen, who has provided support and guidance through the project. I also wish to thank Tina Kutti at the Institute of Marine Research for guidance and discussion of analysis methods. The statistical analysis could not have been conducted without the support of R-code club from bioCEED led by Richard Telford. For my fellow peers, I thank you for your continued encouragement and guidance throughout the project, although it has at times felt like the blind leading the blind. Lastly, I would like to thank my friends and family who have tolerated my relentless ranting about shallow marine CO_2 seep system communities, conundrums on statistical analysis, and extensive speeches on climate change.

Table of Contents

Abstract

Anthropogenic-driven climate change is expected to expose natural communities to various environmental stressors, which in the ocean will be reflected as increasing temperatures, ocean acidification, and altered patterns of extreme weather events. As the ocean functions as a CO_2 sink, oceanic pCO_2 is expected to increase, causing a decrease in pH levels as emissions continue to rise, leading to ocean acidification. By utilizing a natural CO_2 seep system gradient in a shallow marine community of the coast in Dominica as an analogue for future oceanic conditions, the community composition was compared over a four-point time series between 2017 to 2019. During the experiment, the study area experienced a hurricane event, thus allowing investigations of marine community response and recovery following the hurricane event. The community was measured by estimating species coverage from photo-quadrants gathered in transects extending in cardinal directions out from the pCO_2 seep site. Results show that along a natural pCO_2-gradient the community experiences a simplification of species composition as proximity to the CO_2 seep increases. Moreover, the synergistic effects of both the hurricane impact along with naturally higher pCO_2 levels caused a decrease in diversity and an increase of evenness following the hurricane impact, with recovery commencing at a slower pace against the backdrop of high pCO_2 conditions. Notably, the results of this study suggest that hurricane events lead to decreases in diversity, although against a backdrop of ocean acidification, some diversity may already be lost. Therefore, hurricane impacts may show less of an effect on the community composition and diversity of future marine communities due to the overall simplification that has already occurred. The results of this study highlight the challenges marine communities will face as a result of exposure to several environmental stressors, and illustrate the need for more research investigating the combined effect of multiple climatic stressors on marine communities.

1 Introduction

1.1 General Introduction

1.1.1 Climate change

The new Summary for Policy makers from the International Panel on Climate Change (IPCC) confirms that currently observed climate change is driven by anthropogenic greenhouse gas (GHG) emissions (IPCC 2021). Such changes include increasing temperatures on land and in the ocean, sea level rise, reduced sea-ice extent, reduced snow cover, and changes to precipitation levels and extreme weather patterns. Already the impacts of anthropogenic GHG emissions have been observed in all inhabited regions (IPCC, 2021), and with every additional increase in temperature, the projected changes in extreme events, such hurricanes, precipitation, heatwaves and drought, are predicted to increase in frequency and intensity (IPCC, 2021).

1.1.2 Ocean acidification

Especially in the ocean anthropogenic climate forcing entails consequences for several of the physical oceanic properties, including sea level rise, ocean acidification, and changes to wind and oceanic current patterns (Doney et al. 2012). Changes of the physical properties of the ocean will have cascading effects for marine communities, from acclimatization and adaptation of single organisms physiology and behaviour, to community-structure changes, as well as distribution shifts and altered spatial ranges (Hoffmann and Parsons 1991; Hall-Spencer et al. 2008; Doney et al. 2012; Poloczanska et al. 2013). Because of the great volume of seawater, the ocean acts as a buffer for atmospheric CO_2 to such a great capacity that the ocean has now absorbed more than half of all anthropogenic CO_2 from the atmosphere (Sabine et al. 2004). Consequences of this CO_2 uptake will be reflected in the oceanic carbonate chemistry, seeing decreasing pH levels as well as decreasing carbonate-ion concentrations, a process known as ocean acidification (OA) (Caldeira and Wickett 2003, 2005). The process of OA is shown in Equation 1, where CO_2 is taken up by the ocean, and forms carbonic acid (H_2CO_3) through reactions with water (H_2O). The H_2CO_3 molecule loses a hydrogen ion (H^+), leaving a bicarbonate ion (HCO_3^-). Again, a H+ ion is lost from the HCO_3^-, leaving one carbonate ion (CO_3^{2-}) and one H^+ ion:

$$Eq.1: \quad CO_{2(atm)} \rightleftharpoons CO_{2(aq)} + H_2O \rightleftharpoons H_2CO_3 \rightleftharpoons H^+ + HCO_3^- \rightleftharpoons 2H^+ + CO_3^{2-}$$

As oceanic uptake of CO_2 continues, the availability of carbonate ions will decrease due to the buffering capabilities of seawater, where an increase in hydrogen ion availability will drive the chemical composition towards the stable state of bicarbonate. Simultaneously, the increase in hydrogen ions will cause a decrease in pH levels (Hönisch et al. 2012a). With the current GHG emissions, anthropogenic actions could result in pH decline from 8.2 at pre-industrial levels to 7.8 in worst-case scenarios (IPCC 2013). Already, a decrease of about 0.11 units has been observed from 1770 to 2000 (Hoegh-Guldberg et al., 2007; Jiang et al., 2019). Some estimates predict an increase of 150% in hydrogen ions, and a decrease in carbonate availability of 50%

(Doney et al. 2009). Carbonate ion concentrations have now decreased to ~210 μmol kg−1, lower than they have been in the past 420 000 years (Hoegh-Guldberg et al., 2007).

1.1.3 Coral reefs and ocean acidification

Decreasing pH and changes to saturation levels of carbonate ions greatly impact calcifying organisms such as corals, molluscs, echinoderms and coralline algae that rely on constant saturation levels of carbonate ions to grow and maintain their skeleton (Andersson et al., 2008; Anthony et al., 2008; Cohen & Holcomb, 2009; Erez et al., 2011; Hoegh-Guldberg et al., 2007). OA poses a direct threat to for these species, and entails not only impacts on skeletal growth and maintenance (Barkley et al. 2015), but may also impact recruitment rates (Albright and Langdon 2011), cause tissue necrosis (Langdon et al. 2018), impact feeding rates (Towle et al. 2015), compromise the immune responses, and impact necessary sensory organs (Ashur et al. 2017). Furthermore, OA will also impact non-calcareous species, affecting muscle mass and growth in invertebrates (e.g. Keppel et al. 2012) and fish (Baumann et al. 2011). Evidence from both field studies and laboratory studies suggests that the main issues for calcification rates of calcifying organisms is not the overall saturation state of the ocean, but rather changes in the proton gradient between the seawater and the calcifying fluid (Cyronak et al. 2016). While evidence suggests that both calcifying corals and coccolithophores do have the ability to control the carbonate chemistry (Mackinder et al. 2010; McCulloch et al. 2012a), implications occur with increasing H^+ concentrations. To maintain favorable intracellular $CaCO_3$ (calcium carbonate) saturation for calcification rates, the corals must remove increasing amounts of H^+ ions (Allemand et al. 2011). Consequently, it becomes harder for the coral to maintain high saturation of $CaCO_3$ in the calcifying fluid, as the electrochemical gradient between the coral tissue as the intracellular fluids decreases (Cyronak et al. 2016). Thus, the increased uptake of atmospheric CO_2 leads to an energetic issue for calcifying organisms, as they must continually actively or passively transport more and more H^+ ions. Moreover, the decreasing pH levels and aragonite saturations may lead to dissolution or erosion of calcium carbonate structures (Guinotte & Fabry, 2008; Hoegh-Guldberg et al., 2007; Rodolfo-Metalpa et al., 2011).

Although coral reefs only cover about 0.1% of the ocean floor, coral reef ecosystems hosts up to one third of all marine species at some stage in their life cycle (Reaka-Kudla 1997; Reaka-Kulda 2005; Plaisance et al. 2011). Consequently, coral reefs are some of the most biodiverse marine ecosystems (Roberts et al. 2002), and some of the most ecologically important in relation to the services they provide (Hoegh-Guldberg, 2011). Yet, coral reefs are some of the most vulnerable ecosystems on the planet, facing not only challenges of global climate change such as increasing temperatures and ocean acidification (IPCC 2014), but are also subjected to threats on a local scale (Burke et al. 2011). Such local threats include overfishing, agricultural run-off, development of coastal areas that is inconsiderate of the presence of coastal ecosystems, and physical damage caused by human interactions, which were considered the most hazardous events for coral reef ecosystems prior to the 1980s (Glynn 1991). While many of these local hazards remain a challenge for coral reefs, certainly ocean acidification will be one of the greatest threats for coral reefs in the oncoming century (Hoegh-Guldberg et al. 2017). Indeed, should anthropogenic GHG emissions proceed to exceed 500 ppm, calcifying coral reefs will become non-functional, as the carbonate-ion concentration will be too low for coral

species to continue to maintain and grow their skeleton (Hoegh-Guldberg et al., 2007). Future projected changes in carbonate chemistry renders most corals in undersaturated seawater by the end of the century (Zheng and Cao 2014).

Although impactful, OA may not be the only factor leading to the demise of corals and other calcifying organisms. Marine communities will also be greatly impacted by increasing temperatures (Selig et al. 2012), which may increase to such an extent that the maximum temperature threshold for many species may be surpassed (Pörtner and Farrell 2008). Indeed, as oceanic temperatures have increased since the 1980s, damage such as bleaching events to coral reefs has become more frequent (Williams et al. 1990). In the 1980s and 1990s the coral reefs of the Caribbean region endured an extended period of bleaching, both as a result of increasing temperatures, as well as a decrease in the ubiquitous sea urchin *Diadema antillarum* (Hughes et al. 1985). As extreme heatwaves are expected to occur more intensely and more frequently (IPCC, 2021), thermal stress poses are serious threat to coral reefs. Similarly to OA, temperature is also expected to impact the growth rate (Cantin et al. 2010), as well as disease prevalence (Bruno et al. 2007) and more frequent coral belaching (Glynn, 1993). Several environmental stressors, including OA and temperature, as well as deoxygenation and extreme climatic events, pose great threats to biodiversity on their own (Ho, 2020). However, the combined effect of all these climate stressors is likely to cause great ramifications for marine communities.

1.1.4 Hurricanes

Extreme weather is a collective term inclusive of wide range of unexpected, unseasoned or unusually severe climatic events, often referring to events such as heatwaves, coldwaves, droughts, extreme precipitation, flooding and storms (e.g. tropical cyclones, hurricanes) (Stephenson 2008). Compared to other climate drivers, changes of extreme weather patterns in relation to anthropogenic activities has received less attention, much because demonstrating attributions of anthropogenic actions to changing patterns of extreme weather events can be challenging (Trenberth et al. 2015). However, evidence from the past decades demonstrates a change in extreme weather patterns with regards to intensity, frequency and duration in response to anthropogenic greenhouse gas (GHG) emissions (IPCC 2014; National Academies of Sciences Engineering and Medicine 2016).

The north-western region of the Atlantic ocean is a region accustomed to hurricane activity (Goldenberg et al. 2001). Current studies forecast a decrease in hurricane frequency simultaneous with an increase in intensity, with more category 4 and category 5 storms in this region (Bender et al. 2010). At the same time, a weakening in vertical wind shear patterns in this region is predicted to occur (Ting et al. 2019). This deterioration of wind shear patterns allows for an increased intensification of hurricanes approaching the north eastern Atlantic coastline (Ting et al. 2019). This trend concurs with consistent research of pattern changes of tropical cyclones, which may transpire as a global decrease in frequency by 6-34%, but overall an increase of 2-11% in intensity (Knutson et al. 2010). Moreover, correlations between sea surface temperature and tropical cyclone activity in the Atlantic ocean has been observed

(Goldenberg et al. 2001; Emanuel 2007), suggesting that temperature increases may impact hurricane frequency and intensification.

1.1.5 Hurricane impact on coral reefs

Ecosystem disturbance caused by hurricanes has been recognized for a long time, with changes to extreme weather patterns serving as a strong stressor for marine communities (Sainsbury et al. 2018). Repercussions of extreme weather events such as hurricanes on marine communities may cause changes in biodiversity patterns (Wernberg et al. 2013), leading to extensive changes to ecosystem structure and functioning (Cardoso et al. 2008; Graham et al. 2014). Some of the most vulnerable species to hurricane impacts are coral reefs (Gardner et al. 2005). Hurricane event can have immediate effects on corals through physical damage caused by wave surges and strong undercurrents, reduction in water quality (Edmunds 2019), terrestrial runoff leading to algae blooms that cause deoxygenation (Nelson and Altieri 2019), increased turbidity and lowered salinity caused by increased precipitation. Some of these effects may be particularly damaging to the symbiotic algae, the zooxanthella, of the corals (LaJeunesse et al. 2018; Pengsakun et al. 2019) and to the calcification rate of the corals (Manzello et al. 2013; Wijgerde et al. 2014). Against a general trend of decline in coral coverage (Perry et al. 2013), a hurricane impact may lead to an accelerated rate of decline in coverage (Hughes and Connell 1999). Indeed, in the first year following a hurricane event, coral reefs in the Caribbean region can experience a decline in coral coverage of about 17% (Gardner et al. 2005). Contrastingly, hurricanes may cause an initial increase in coral coverage due to the reattachment of broken corals which then grow for some time, until also they resume the general trend of cover decline (Highsmith et al. 1980; Lirman 2000). Notably, damage caused by a hurricane impact is variable, and depends on both the strength of the hurricane, as well as the reef archeology (Harmelin-Vivien 1994). The degree of physical damage also depends on the size and structure of the coral, with boulder and encrusting growth forms doing better in storm events compared with plate and corymblike coral structure (Mah and Stearn 1986; Madin et al. 2014). Moreover, resistance against hurricane impact is higher for communities composed of a higher diversity and richness (Bellwood and Hughes 2001; Newman et al. 2015).

1.2 Specific Introduction

1.2.1 CO_2 seep systems

Investigating effects of climate change, especially OA, on marine species is a challenging task, and has previously been based on laboratory experiments. While such studies provide some insight into the challenges marine species face in relation to climate change, these studies do not accomplish to provide the complexities of marine community responses (Riebesell and Gattuso 2014). Indeed, gaps of knowledge exists relating to moving from single species to community or ecosystem responses (Riebesell and Gattuso 2014). To provide more insight into both individual species responses to OA, as well as community responses, natural CO_2 seep systems have been utilized in recent years to investigate the impact of OA. These seep systems, also known as CO_2 seeps, cause a continuous release of CO_2 which alters the local carbonate chemistry of the seawater (Kerrison et al. 2011; Lin et al. 2019). As the CO_2 seeps out from

the CO_2 seeps, it mixes with seawater, causing an increase in oceanic partial pressure of CO_2 (pCO_2) (µtam). As the ocean accumulates more, the predicted pCO_2 levers are predicted to increase from the current 400µtam to 850µtam (IPCC, 2014). Therefore, shallow CO_2 seeps may be used as natural analogous for ocean acidification. Already such studies have transpired at several locations around the world, including the Mediterranean (Beaubien et al. 2008; Hall-Spencer et al. 2008; Calosi et al. 2013b; Collard et al. 2016; Brown et al. 2017), the central Indo-Pacific region (Fabricius et al. 2011; Lamare et al. 2016; Kenkel et al. 2018), the temperate Pacific ocean (Agostini et al. 2015; Lin et al. 2019), the North East Atlantic ocean (Hernández et al. 2016) and the Caribbean (Enochs et al. 2020). Community level changes have been observed in such studies, with reductions in calcareous species, shifting to communities of species that do not build calcified skeletons, such as algae (Hall-Spencer et al., 2008), and the overall community becoming more homogenous over time (Brown et al, 2017). On an individual level, the energy requirements might shift as a result of living in a more stressful environment of decreased pH (Harvey et al. 2016). However, great variations in ability to adapt have been observed for closely related species of sea urchins, causing a distribution gradient of species of sea urchins based on differences on physiology (Calosi et al. 2013a). Population-level changes have also been observed, with changes in demography and variation in reproductive success (Harvey et al., 2016). Studies such as these ones provide evidence for how community structure will respond to the climatic driver OA.

1.2.2 Study Area: Dominica

One such area where shallow CO_2 seeps are present is Dominica (officially the Commonwealth of Dominica), a young volcanic island of the Lesser Antilles in the Caribbean Sea, characterized by mountains with a steep rock face and dense vegetation (Figure 1). Being situated on the volcanic arc of the Lesser Antilles, Dominica has an active volcanic nature which still forms the island, and this is reflected in the topography of the island and the coastal line (Slinger-Friedman 2017). Dominica has a diverse ecology, where the marine habitats are made up of mainly seagrass beds, but also sandy and rocky substrate, and coral reefs and coral assemblages (Steiner & Willette, 2010). These marine habitats are defined by narrow and steep shelfs that provide restrictions for the euphotic zone which impacts the species reliant on photosynthesis to grow (Steiner, 2015). Due to a lack of energy-dissipating structures present along the coast, the marine communities present here withhold little protection from extreme weather events, such as hurricanes (Steiner 2003). Several shallow-water CO_2 seeps are present in Dominica, such as a seep site located in Champagne Bay (Figure 1). The CO_2 seeps locally decrease the pH due to the release of CO_2. The presence of these seep systems make Dominica an interesting location to investigate the impact of ocean acidification on species composition in a lowered pH-environment (Kerrison et al. 2011). Furthermore, being situated in the tropical region of the western Atlantic ocean, Dominica frequently endure storm events, most recently the Tropical Storm Erika in 2015, and Hurricane Maria in 2017. Intensification and increased frequency of extreme weather has been observed in the most recent storm events of Dominica (Thomas and Benjamin 2018). Such intensification was observed in Hurricane Maria, which hit Dominica at as category 5 (cat-5) hurricane on the 18th of September, 2017, a wind speed that had reached 258 km/h (Brown and Blake 2017). Therefore, Dominica also provides a unique opportunity to study the impact of storm events on marine coastal communities.

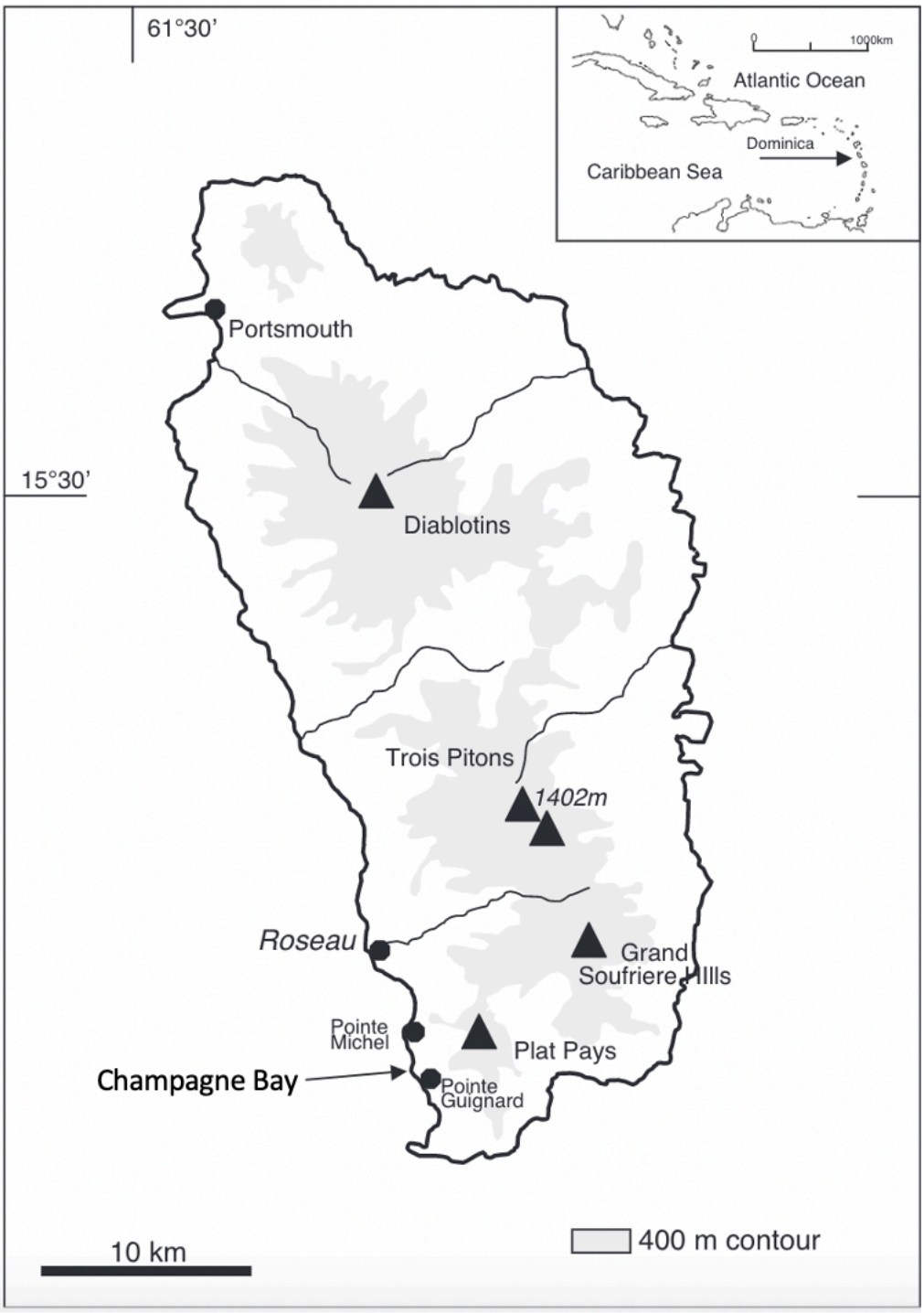

Figure 1: Map of the Dominica. The island is situated in between the Caribbean Sea in the west, and the Atlantic Ocean in the east. Champagne Bay, located in the south-western part of the island, is indicated with an arrow. Map from McCarthy et al., 2005.

1.2.3 Study Community

With a coral reef cover of 49 km^2 (Jackson et al. 2014), Dominica is an island with a moderately high coral coverage. In particular Champagne Bay, the site of this survey, is an area with a high coral coverage compared to other bays along the west coast (Steiner et al. 2007), where the coral reefs are considered to be in 'Fair' condition despite being subjected to overfishing (Kramer et al. 2016). Prevalent corals found in the Champagne area include the fringing

colonies of *Madracis mirabilis*, domes of *Siderastrea siderea*, *Siderastrea radians* and *Porites asteroides*, the fire coral *Millepora* sp., species of the genus *Orbicella* and brain corals of the *Diploria* genus (Steiner et al. 2007; Steiner 2015b). In general, the Caribbean region is enduring a decline in coral coverage and for reef building corals (Perry et al. 2013). The mustard hill coral, *P. asteroides*, is a common coral across the Caribbean region, but research suggests that OA may have an impact on life history traits (Albright and Langdon 2011), while the massive startlet coral, *S. sidera*, has demonstrated a high tolerance for stress (Davies et al. 2016). Both *P. asteroides* and *S. radians* have been reported to continue to recruit in areas of the Caribbean that are exposed to environmental stressors which could be related to climate change (Otaño-Cruz et al. 2019). Comparativley, the mountainous star coral, *Orbicella faveloata*, has been observed to be sensitive to higher levels of pCO_2 (Langdon et al. 2018). The response to climate change of corals in the Caribbean region could be a more homogenization, with decreased biodiversity, while other species thrive. Another cnidarian common to the west coast of Dominica is the sun anemone *Stichodactyla helianthus* (Steiner et al. 2007), which is ubiquitous to the eastern and southern Caribbean (Santhanam 2020). Compared with research from CO_2 seep systems on neighboring islands to Dominica, both scleractinian (reef building corals) and soft corals show reliance towards low pH values and high pCO_2 levels (Enochs et al. 2020).

Concurrent with decades of decline for reef-building corals, sponges have advanced to become the most dominant benthic animal on most reefs (Zea 1993; Colvard and Edmunds 2010; McMurray et al. 2010; Villamizar et al. 2014). The majority of sponges inhabiting the marine environments of Dominica are of the class Demospingiae (Clermont 2008), with erect and encrusting sponges making up an equal amount of coverage in Champagne Bay (Steiner et al. 2007). Compared with corals, some sponges are predicted to do well with declining levels of pH (Duckworth et al. 2012). While the majority of sponges in Dominica tend to inhabit depths of 6-18m (Clermont 2008), Champagne has a prevalent sponge community in more shallow depths of 0-5m as well. Present species include tube sponges such as *Aplysina fitularis* and *Verongula rigida*, encrusting sponges such as *Ircinia felix* and *Svenzea zeai*, sponges with rope forms of *Amphimedon compressa* and *Iotrochota birotulata*, and barrel sponges of *Xestospongia muta* and *Verongula* sp. (Clermont 2008). Further North in the Caribbean Sea *X. muta* has been reported to increase in numbers (McMurray et al. 2010). Some species of boring sponges have also been observed (Steiner et al. 2007; Clermont 2008).

Dominica is also home to the long spined urchin *Diadema antillarum* (Steiner and Williams 2006), which acts a keystone species at Caribbean coral reefs through grazing of macroalgae (Carpenter 1981). Indeed, the substratum in Champagne Bay may be covered by algae, mainly brown turf algae and *Dictyota* sp. (Steiner et al. 2007). Furthermore, several sessile macroinvertebrate species also inhabit Champagne Bay. The area has a high abundance of sessile, tube dwelling annelids of the family serpulidae, including *Bispira* sp. and *Sabellastarte magnifica* (Steiner et al. 2007). The serpulidae build calcite and/or argonite calcium carbonate tubes (Bornhold and Milliman 1973). Similarly to corals, these serpulidae are susceptible to decreases in pH levels in the ocean (Brown et al. 2017). These tubes are built inside crevices of substratum, preferably *P. asteroides* or *Orbicella annularis* in Champagne Bay (Steiner et

al. 2007). Importantly, on Caribbean reefs a decline in macroinvertebrate diversity has been related to loss of coral cover and coral 3D structure (Idjadi and Edmunds 2006; Perry et al. 2013).

1.3 Aims and Hypotheses

Investigating the impact of multiple environmental stressors remains a gap for predicting future persistence of marine community composition during climate change (Riebesell and Gattuso 2014). Other studies of CO_2 seep systems are limited to one environmental driver, namely OA. However, by investigating a community along natural CO_2 gradient in an area that is frequently exposed to storm events provides the unique opportunity to investigate community responses to these two climate stressors simultaneously. This study aims to investigate how a shallow, tropical marine community experiences the combined stress of a hurricane impact as well as ocean acidification. By using a four-point time series between 2017 to 2019 of data from a CO_2 seep system, the seep provides a natural analogue to analyse the community change in response to predicted OA through a photo-quadrant transect analysis. Furthermore, the time series allows for determining ramificaitons of Hurricane Maria, as well as the community recovery following the storm event, while simultaneously being exposed to pCO_2 levels similar to those predicted for the end of the century. This combination of stressors can give a further understanding of how such ecosystems might endure the predicted impacts resulting from anthropogenic climate forcing.

The hypotheses of this thesis are:

1. An observed community shift along the pCO_2 gradient.

Based on previous studies utilizing CO_2 seeps as natural gradients of OA, observations of a community shift away from calcifying organism towards macroalgae have been reported (Hall-Spencer et al. 2008). Although some species display persistence in the face of OA, this study expect to observe that prevalence of calcifying organisms decrease with proximity to the CO_2 seep as pCO_2 levels increase.

2. The hurricane impact will cause a decrease in diversity.

Physical damage following a hurricane event is to be expected, as hurricanes are strong drivers of physical disruption for marine communities (Harmelin-Vivien 1994). Both corals and sponges will lose coverage area, making the environment more homogenous.

3. The combined effect of ocean acidification and hurricanes will lead to decreased diversity and more evenness.

Environmental drivers often have synergistic effects, and the changes to one environmental driver can decrease organisms sensitivity to other drivers (Pörtner and Farrell 2008). Therefore, the impact of these two environmental drivers might have a strong impact on the community composition. The immediate impact of the hurricane will cause physical disruption, leading to decreased diversity across the transects. Not all species will be impacted evenly, as some species may be better equipped at enduring combination of these two stressors.

4. Recovery of species will be slower against a backdrop of increased pCO_2 levels.

Following the time series, a recovery of species is expected to occur. Conceivably, recovery will occur at a faster the further away from the seep site, as the species in this part of the community will be subjected to less environmental impact of pCO_2. Further impacts of the hurricane could cause less pCO_2 tolerant species to have a slow recovery. Such species may also be outcompeted for space by more tolerant species, thereby rendering the space occupied, restricting recolonization of areas that are left bare after the hurricane impact by less stress tolerant species.

The experimental design of this study provides a unique opportunity to gain further insights into how species endure the combined effect of both ocean acidification and a hurricane impact. Gaining more knowledge into how marine communities respond to multiple climatic stressors remains crucial in the endeavor of prevailing healthy marine communities in the future.

2 Methods

2.1 Site Characterization: Champagne Bay

The survey area of this study is known as Champagne Bay, and is situated on the southwestern coast of Dominica (Figure 2). The CO_2 seeps of Champagne Bay are a part of the Plat Pays volcanic complex which confers volcanic activity both on land and in the shallow marine coast (Lindsay et al. 2003). The complex is located in southern part of the island, and is one of seven active volcanic centres in Dominica (Joseph et al. 2019). In these marine seep systems CO_2 seeps out as a continuous stream of bubbles at 1-4m of depth at six locations of focused venting in Champagne Bay, extending to an area about 40m out from shore (Mccarthy et al. 2005). The CO_2 seep chosen for this survey (Point zero = Geographical location: 15.244765, -61.373428) is located at the end of Champagne Beach, in the southern part of Champagne Bay. The seep site is situated about 18m out from land, with a depth of 3m. Transects were laid from point zero extending 30m out from the CO_2 seep following the cardinal directions North East (NE), North (N), North West (NW), West (W), South West (SW) and South (S) (Figure 2). In survey time points 2017 and 2019 transects and accompanying environmental data for NE were not obtained. Transects were not investigated for the cardinal directions heading South East and East, as these transects contain metal contamination (based on previous, unpublished data from the same project). Depth ranged between 2 to 4.5 meters across the transects.

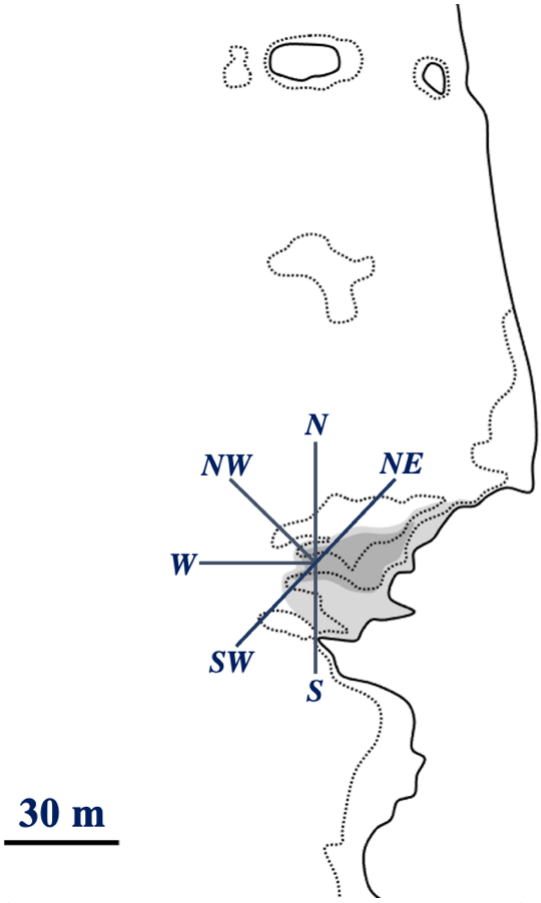

Figure 2: Illustration map of survey area. Seep site located in the southern part of Champagne Bay, indicated with transects extending from point zero in cardinal directions, as indicated by letters NE (North East), N (North), NW (North West), W (West), SW (South West) and S (South).

The gas composition of the seep site at point zero consists mainly of CO_2 which contributes to about 84% of the gasses in the seep (Table 1), thus making it a high-CO_2 seep. All other gases contribute minimally, with nitrogen (N_2) being the second-most contributing gas with about 10% (McCarthy et al., 2005). Hydrogen sulphide (H_2S) has minimal contribution to the seeping gasses (McCarthy et al., 2005), and become non-detectable along the transects extending in all cardinal directions (Pers. comm. Samuel J. S. Rastrick at the Institute of Marine Research (IMR)).

Table 1: Proportions of gas composition at the CO_2 seep site in Champagne Bay used as site zero in this survey (McCarthy et al., 2005).

Gas	Proportion (%)
Carbon dioxide (CO_2)	~ 84
Nitrogen (N_2)	~ 10
Hydrogen sulphide (H_2S)	~ 4
Methane (CH_4), hydrogen chloride (HCl), oxygen (O_2) and Argon (Ar)	~ 2 (minor concentrations)

2.2 Photo-quadrant survey

2.2.1 Collection of environmental data (pH and temperature logging)

Temperature, salinity and pH levels were obtained by a handheld multimeter (labquest 2, vernier). Measurements were taken every other meter along the transects concurrent with the photo-quadrant transects. In March 2018, pH measurements were only sampled every five meters. Total alkalinity (TA) was measured every week during survey times by titration (after Fitzer et al. 2012). TA measurements were collected at the point zero of the seep site and at a reference site about 100m north of the seep site. Levels of pCO_2 were calculated using the free-access carbonate system calculations software CO2SYS (Lewis and Wallace 1998) with formulations from Dickson and Millero (1987), which are applicable over a wide range of salinities.

2.2.2 Field work: Benthic habitat mapping

Photo-quadrat surveys were performed between 2017 and 2019 at four different time points; June/July of 2017, March of 2018, June/July of 2018, and June/July of 2019. Survey material was collected by researchers and research assistants affiliated with Operation Wallacea. Photo-quadrats were obtained by filming a continuous video using a GoPro camera (GoPro Hero4 Black) fitted with underwater housing. The camera was fixed to two rods that extended 2 meters above a 1x1 meter quadrat. The camera was angled 90 degrees onto the quadrant to allow for analysis of benthic coverage to be recorded. The quadrat was moved at 1 meter intervals 30 times successively along the transect, with care taken to avoid overlap between successive quadrats.

2.2.3 Image analysis

Prior to performing analyses of species coverage from the material gathered in the transects, a 10x10 grid was added digitally to the $1m^2$, dividing the quadrat frame in each image into 100 smaller squares. Each square in the grid represented 1% of the total grid, and species presence within each square were assigned values of 0%, 0.5% or 1%. Accordingly, species coverage was determined down to 0.5% precision. Species coverage between 0.5% and 1.0% was rounded up based on if the species covered more than or less than 0.75% of the square. Therefore, any species or substrate type present within a quadrat would obtain at least 0.5% coverage, even though it might have covered less than half of the square. Coverage within each quadrat was exactly 100%. For sessile macroinvertebrates, such as sea urchins, anemones and annelid worms, individual count data was also registered, in addition to species coverage. Species identification, coverage percentages and macroinvertebrate counts was controlled twice for each transect.

Additionally, transect images were used to describe the bottom substrate in the transects. Bottom substrate was divided into five classes (Table 2) based on the European standard for mapping bottom substrate (EN 16260 2012). The five classes present at the study location include bedrock, bedrock covered with thin layer of sediment, very coarse sediment, coarse sediment, and dead coral. Sediment type was recorded in three different categories 'Hard', 'Soft' or 'Mixed', with primary, secondary and tertiary substrate class indicated for each quadrant.

Table 2: Substrate categories with description.

Type of Substarte	Description
Bedrock	Exposed bedrock and large boulders, >63cm
Bedrock with thin layer of sediment	
Very coarse sediment	63-630mm
Coarse sediment	Sand and gravel, 0.0063-6.3cm
Dead coral	

2.3 Statistical Analysis

All statistical analyses were conducted using statistical programming language 'R' (version 4.1.0) () in 'RStudio' (version 1.4.1717) (R Core Team 2021). All plots were made using the package 'ggplot2' (Wickham 2016).

2.3.2 Analysis of the study environment

Linear interpolations were conducted for all the environmental variables to allow for statistical analysis of the species data. The environmental variables from summer of 2017, summer of 2018 and summer of 2019 all had measurements sampled every other meter. In March of 2018 environmental parameters were only sampled every five meters. All environmental variables were interpolated in 'R'. Additionally, a linear model was fitted to determine if total alkalinity (TA) was significantly different between the seep site and a reference site 100m away from the seep site. Model selection was conducted by using Akaike Information Criterium (AIC) (Akaike 1998), AIC weights (Wagenmakers and Farrell 2004) and adjusted R-squared values

(Appendix 2). Akaike Information Criterium (AICc) is a measure of goodness of fit for models, where a lower number suggests a better fit model. Probability of having a true model is given with the AIC weight. AIC weights were compared using the 'MuMIn' package (Bartoń 2020). The adjusted R-squared value describes the variance of the independent variables fitted, where a higher number indicates a better fitted model. The selected model interface formula was:

$$1)\ TA\ model <- \ lm(Total\ alkalinity \sim site + \ survey\ time\ point)$$

with raw TA data as a response variable to independent variables of site and year. An analysis of variance (ANOVA) was performed to determine differences between groups. A post hoc Tukey test was carried out using the package 'emmeans' (Lenth 2021) in 'R'.

2.3.3 Species richness, diversity indices and evenness across the gradient

Species coverage data was transformed to species richness in the 'vegan' package (Oksanen et al., 2020) in 'R'. Species richness, coral richness and sponge richness was calculated for all transects across all survey time points. Diversity indices of Hill-Shannon (Hill 1973), also known as the exponential of Shannon's entropy, and Hill-Simpson (Hill 1973), also known as the inverse of Simpson's concentration index, were calculated for species data across all survey time points. Pielou's evenness (Pielou 1966) was also calculated. Calculations of diversity and evenness were carried out in 'R' using the 'vegan' package, based on calculations shown in Table 3. Hill diversity metrics are becoming the preferred metrics to apply, as they represent simple calculations that are logically reasonable (Roswell et al., 2021).

Table 3: Equations for Shannon diversity, Simpson diversity and Pielou's evenness, where where p_i is the proportion of species i *and* S *is the number of species so that* $\sum_{i=1}^{S} p_i = 1$*, and* b *is the base of the logarithm* (Oksanen 2020).

Index:	Calculation:
Hill-Shannon (exp(H′))	$exp\ (H') = e^{-\sum_{i=1}^{S} p_i \ln(p_i)}$
Hill-Simpson (D)	$D = \frac{1}{\sum_{i=1}^{S}(p_i)^2}$
Pielou's Evenness (J)	$J = H/\ log(S)$

Models were fitted to test if the species richness, diversity or evenness was impacted by both the pCO_2 levels and the hurricane event. The impact of the hurricane was tested by fitting survey time point as an explanatory variable. Response variables of the models included the community data from all years measured as total species richness, coral richness, sponge richness, Hill-Shannon diversity index, Hill-Simpson diversity index and Pielou's evenness. As well as survey time point (year) serving as explanatory variable, pCO_2 and substrate category was also included in the model as explanatory variables. Temperature and salinity were considered constants due to marginal variability. The observed variability would have little to no biological impact but could lead to overfitted models and uncertainty. Distance from the seep site was not included as an independent variable, as the objective of the study was to determine the impact of pCO_2 levels on communities, not distance from vents. All other environmental variables were found to be correlated with pCO_2, and were therefore excluded

from the model (Appendix 3). For species richness, coral richness and sponge richness three separate generalized linear models (GLM) were fitted, as GLMs enable the use of linear models in cases where the response variable has non-normal distribution (McCullagh and Nelder 1989). In this case, the models were fitted with quasi-Poisson distribution to account for overdispersion in the data. The fitted model was:

$$2)\ Richness_{mod} <- glm(richness \sim survey\ time\ point + pCO_2 + substrate\ category, family = quasipoisson)$$

with total richness, coral richness or sponge richness serving as response variable, and survey time point, pCO_2 level (µtam) and substrate category (hard, soft and mixed) as response variables. Post hoc Tukey tests were carried out using the package 'emmeans' (Lenth 2021) in 'R'.

Diversity and evenness indices were fitted with linear models (LM), where Hill-Shannon diversity, Hill-Simpson diversity or Pielou's evenness served as response variables in three separate models. The model interface of these LMs were:

$$3)\ Speices\ indices_{mod} <- lm(species\ indices \sim survey\ time\ point + pCO_2 + substrate\ category)$$

with the explanatory variables of survey time point, pCO_2 and substrate category. An ANOVA was performed to test if there were significant differences between the variables. Post hoc Tukey tests were carried out using the package 'emmeans' (Lenth 2021) in 'R'.

2.3.4 Multivariate Analysis

Benthic community composition in relation to the pCO_2 gradient was assessed using a constrained direct gradient multivariate analysis conducted in 'R' using the 'vegan' package. These analyses methods entail ordering community composition along axes according to their similarity, or dissimilarity (Gauch 1982). Sites with similar species composition are positioned close together, while sites that are dissimilar are positioned further apart. Similarly, species that are governed by similar environmental conditions, are also positioned close. In direct gradient analyses the species composition is directly related to the constraining variables, which are the environmental parameters. The species composition matrix is fitted through regression against the environmental variables, and thus such methods can be described as a set of multiple linear regressions. One such method of direct gradient analysis is canonical correspondence analysis (CCA) (ter Braak 1986). CCA models assume unimodality of the data, which is common in ecological data, and this method is therefore the most widely applied multivariate direct gradient analysis to apply. Another direct gradient analysis is a redundancy analysis (RDA) (Rao 1964), which is a method assumes a linear relationship between response variables.

Common practice when conducting statistical analyses, including multivariate analyses, is to transform data to reduce the impact of outliers, particularly for species data where rare species may imply stronger significance of relationships (Legendre and Gallagher 2001). Similarly,

dominant species may also impact the statistical analysis. Therefore, applying a transformation on the species data may reduce such issues. As the species data was recorded in percentages, an Arcsine transformation (Sokal and Rohlf 1995) was conducted before the multivariate analyses were preformed. Also known as the arcsine square root transformation, this transformation was calculated as arcsine of the square root of the proportion of species coverage divided by 100. This type of transformation is common for proportional data, and was therefore chosen as species composition was recorded in percentage coverage.

To determine if a linear (RDA) or a non-linear (CCA) method should be applied to the data, a Detrended Correspondence Analysis (DCA) (Hill and Gauch 1980)was conducted for the species data using the ´vegan´ package. DCA removes the curvature (arch effect) observed in the data through detrending, thus removing all systematic dependence between axes. The DCA returns a list of axis lengths, which can be used to determine the ordination method. If axes lengths of the DCA are of values less than 2, a linear approach is suitable, while values above 2 warrants the application of a non-linear method (Lepš and Šmilauer 2003). Based on the results of the DCA, an RDA was chosen as the best choice for the analysis. As with other linear regression methods, RDAs are subjected to issues with correlated variables. Therefore, reducing the number of variables as much as possible is desirable (Oksanen 2015) to achieve parsimony. A correlation plot was made (Appendix 3) to determine correlation between explanatory variables. As pCO_2 was the desired explanatory variable to investigate in this survey, it was selected in favour of all correlated variables, including distance from the CO_2 seep and pH levels. Additionally, temperature, salinity and total alkalinity did not vary across the gradient, and were therefore also excluded as explanatory variables. Henceforth, to test the similarity of site, representing species composition in each quadrat of each survey time point, the fitted model interface was:

$$4)\ RDA_{full\_mod} <- rda(species \sim survey\ time\ point + pCO_2 + substrate\ category)$$

with species as response variable, and survey time point, pCO_2 and substrate category (‘hard’ or ‘mixed’) as explanatory variables. Permutational multivariate analysis of variance (PERMANOVA) were performed to determine the partitioning of variation across a multivariate data. Additionally, separate multivariate analyses were made for each survey time point to investigate the impact of pCO_2 levels and substrate type on species. A DCA was conducted on the species matrices, and RDA was chosen as the most suitable model. These models all had the same interface, which was:

$$5)\ RDA_{separate\_mod} <- rda(species \sim pCO_2 + substrate\ category)$$

with arcsine transformed species data as response variable, and pCO_2 and substrate category (‘hard’ or ‘mixed’) as explanatory variables. PERMANOVAs were performed. Biplots were made for all of the separate ordination models.

Owing to the high dominance of brown turf algae in the dataset, the ordination plots of the species made for the separate years did not show much variation in between species responses to the explanatory variable. Because of this, brown turf algae was removed from the species matrix to reduce the overpowering weight of the high coverage brown turf algae governed. To make up for the huge gaps in the dataset created by removing the brown turf algae, the species data was standardized by dividing by the margin total. After that the species matrices for the separate years were arcsine transformed, before a DCA was performed to determine the most suitable constrained multivariate analysis to be applied. Removal of the dominant weight of brown turf algae in the data altered data to be non-linear (unimodal), and a CCA was deemed the most suitable analysis. Again, separate models for each survey time point were made with same model interface as for the RDAs:

$$6)\ CCA_{separate\_mod} <- cca(species \sim pCO_2 + substrate\ category)$$

with species data as response variable, and pCO_2 and substrate category as response variables. PERMANOVAs were conducted afterwards. A full model including survey time point as an explanatory variable was also made for species data without the brown turf algae using the same steps as described above. This CCA has a model interface of:

$$7)\ CCA_{full\_mod} <- cca(species \sim survey\ time\ point + pCO_2 + substrate\ category)$$

with arcsine transformed species data from all survey time points as response variable to the explanatory variables of survey time point, pCO_2 and substrate category. PERMANOVAs were conducted. Biplots were made for all of the separate ordination models.

The ´vegan´ package was used to test goodness of fit of the RDAs and the CCAs. The goodness of fit of the models were tested by investigating the variance inflation of the constraining variables, as well as comparing the adjusted r-squared values and the r-square values. A Monte-Carlo permutation tests were carried out to investigate the robustness of the models. All biplots were made using the 'ggvegan' package (Simpson, 2019).

2.3.5 Hurricane impact on sessile macroinvertebrates

To test the hurricane impact on count numbers of sessile macroinvertebrates a multivariate analysis was conducted as described in the paragraph above. The DCA revealed that a CCA was the most suitable model for the macroinvertebrate count data. The model interface was:

$$8)\ Macroinvertebrate_{mod} <- cca(macro\ count\ data \sim survey\ time\ point + pCO2 + substrate\ category)$$

with macroinvertebrate count data as response variable, and survey time point, pCO_2 measurements and substrate category serving as response variables. The goodness of fit of the model was tested by the same method as described above, and the robustness was tested with a Monte-Carlo permutation test. PERMANOVAs were performed to determine the partitioning of variation across a multivariate data.

3 Results

3.1 Environmental parameters

The linear interpolated pCO_2 measurements were plotted for all transect directions across all survey time points to display the pCO_2 environment in all years (Figure 3). The gradient ranged from above 1000µtam to bellow 500µtam across most transects for all survey time points. Additionally, the raw pCO_2 data was also plotted, which show the same trend (Appendix 4).

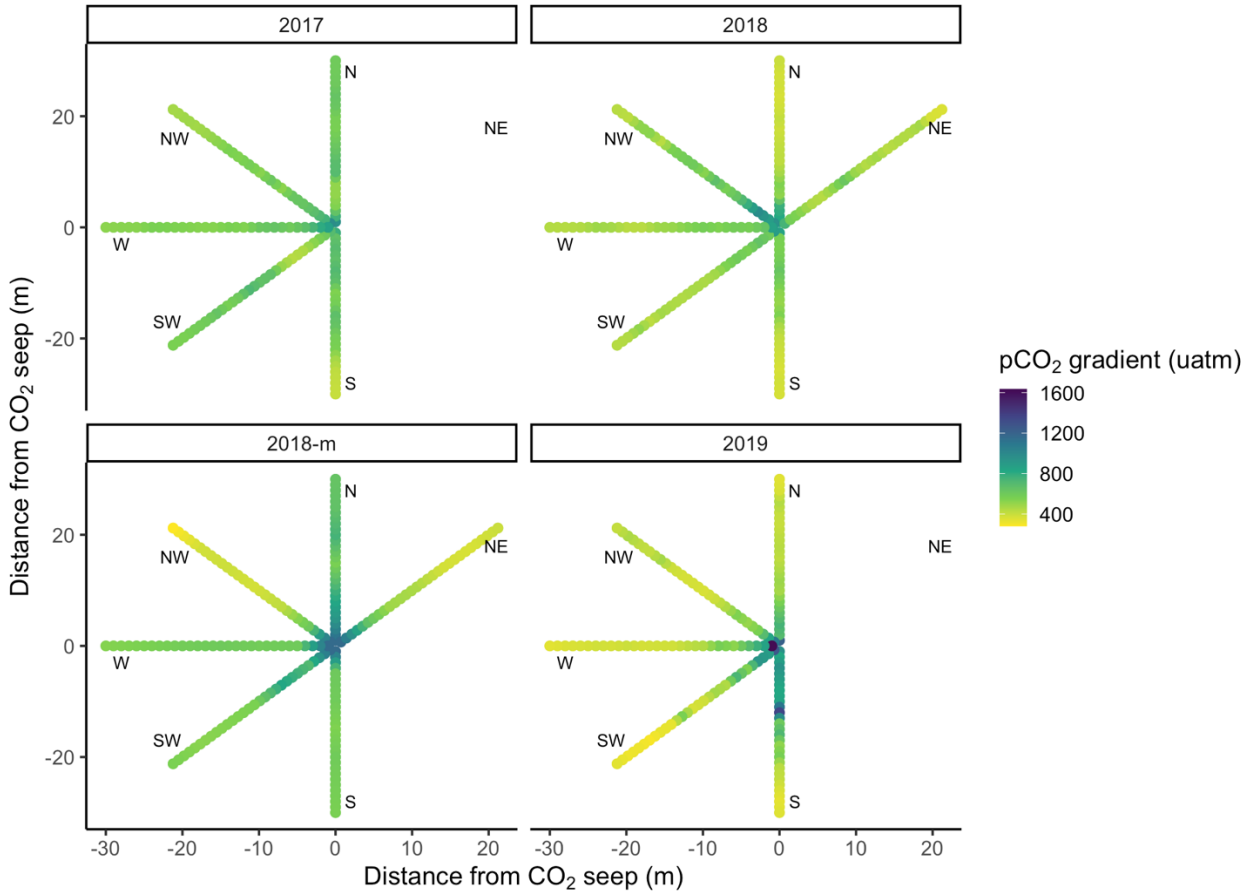

Figure 3: pCO_2 gradient from all survey time points. pCO_2 (µtam) was measured for every cardinal direction, as displayed by labels NE for North East, S for South, SW for South West, W for West, NW for North West and N for North. This was plotted for every survey time point, as indicated by the panes on top of the graphs, with 2017 for the summer of 2017, 2018-m for March of 2018, 2018 for the summer of 2018 and 2019 for the summer of 2019.

The CO_2 seep site was not found to impact TA, as values did not vary significantly between reference site and seep site within survey time points (ANOVA: $F_{4,48}$ =14.13, p-value: 1.087e-07, Appendix 5), with a narrow range detected at the seep site and the reference site (Table 4). A post hoc Tukey test revealed that the summer of 2018 was significantly different from all other survey time points, while all other survey time points did now show any statistical difference between them (Appendix 6). Additionally, temperature and salinity showed little variation across the range or between survey time points (Table 4).

Table 4: Temperature, salinity and total alkalinity. Ranges of maximum and minimum temperature (C°) and salinity (ppt) are given for each survey time points. Mean total alkalinity (µmol/kg) is given for the CO_2 seep site, and at a reference site 100m away for each of the survey time points.

Survey time point	Temperature (C°)		Salinity		Total Alkalinity (µmol/kg)	
	Mean	Max	Min	Max	Seep (mean)	Reference (mean)
2017	29.45	30.3	29.4	30.8	2361.3	2387.9
2018 (March)	28.0	30.3	29.5	31.9	2385.4	2389.7
2018	28.1	31.0	27.9	30.3	2242.7	2248.6
2019	29.3	30.2	29.0	30.0	2352.1	2360.8

3.2 Benthic community cover

Photo-quadrats from 44 transects were analyzed from across the time series, of which 10 were collected from 2017, 12 collected from March of 2018, 12 were collected from the summer of 2018, and 10 were collected from 2019. 2017 and 2019 had one less transect, as the transect heading North East was not recorded in either of these years. For all survey time points transects were recorded twice, allowing two replicates of all cardinal directions. This includes transects heading in the cardinal directions of North, North West, West, South West and South. Importantly, in the summer of 2018 the transect heading North East is missing quadrat 6-8 for both replicates. Additionally, the transect heading South is missing quadrat 7 for both replicates. In 2019 the transect heading South was shorter compared with all other transects, ending at 24 quadrats for both replicates.

A total of 48 species were observed across all survey time points (Table 5). Of these, 19 species were corals, whereof 16 were scleractinian corals, two corals were soft corals, and one species was a hydrocoral (not a true coral). Furthermore, 16 sponge species were found, and 4 macroalgae species. Additionally, calcifying algae was detected. A total of seven macroinvertebrate species were recorded, of which two were cnidarians, one echinoderm, and four species of polychaeta. Two of the polychaeta worms were from the family Sabellidae (*Sabellastarte* spp. and *Bispira* spp.).

Table 5: Surveyed species. Scientific name and common name of all species found in the survey, with maximum pCO_2 levels, minimum pH levels and minimum distance from the CO_2 seep site. Red colour: species that will not survive above 850µatm and below levels of 8.0 pH. Orange: species present between 7.8 and 8.0 pH levels. Green: Species present above 850µatm and below 7.8 pH levels.

Scientific Name	Common Name	Maximum pCO_2 levels (µatm)	Minimum pH levels	Minimum distance to seep
HARD CORALS – Scleractinia				
Agaricia spp.	Lettuce coral (???)	506	8.14	23
Colpophyllia natans (Houttuyn, 1772)	Boulder brain coral	926	7.91	3
Dichocoenia stokesii (Milne-Edwards & Haime, 1849)	Elliptical star coral	600	8.08	15
Diploria sp. (Milne-Edwards & Haime, 1848)	Grooved brain coral	1160	7.82	1
Madracis mirabilis sensu Wells, 1973	Yellow finger coral	614	8.07	23

(Duchassaing & Michelotti, 1860)				
Montastraea cavernosa (Linnaeus, 1767)	Great star coral	920	7.91	3
Orbicella annularis (Ellis & Solander, 1786)	Boulder star coral	695	8.02	9
Orbicella faveolata (Ellis & Solander, 1786)	Mountainous star coral	821	7.96	4
Porites astreoides (Lamarck, 1816)	Mustard hill coral	1160	7.82	1
Porites colonensis (Zlatarski, 1990)	Honeycomb plate coral	623	8.06	25
Porites divaricata (Le Sueur, 1820)	Thin finger coral	757	7.99	2
Porites porites (Pallas, 1766)	Finger coral	687	8.03	7
Siderastrea siderea (Ellis & Solander, 1786)	Massive starlet coral	1255	7.79	1
Siderastrea radians (Pallas, 1766)	Lesser starlet coral	885	7.93	2
Solenastrea bournoni (Milne-Edwards & Haime, 1849)	Smooth star coral	686	8.03	4
Stephanocoenia intersepta (Esper, 1795)	Blushing star coral	687	8.03	4
CORALS – Anthoathecata (hydrocoral)				
Millepora spp. (Linnaeus, 1758)	Fire coral	1635	7.69	1
CORALS – Alcyonacea				
Gorgonia spp. (Linnaeus, 1758)	Common sea fans	446	8.18	19
Pseudopterogorgia spp (Kükenthal, 1919)	Sea plume	543	8.11	13
SPONGES – Demospongia / PORIFERA				
Agelas spp (Duchassaing & Michelotti, 1864)		708	8.01	5
Amphimedon compressa (Duchassaing & Michelotti, 1864)	Erect rope sponge	745	8.01	4
Aplysina cauliformis (Carter, 1882)	Row pore rope sponge	580	8.09	26
Aplysina fistularis (Pallas, 1766)	Yellow tube sponge	985	7.89	1
Chondrilla nucula (Schmidt, 1862)	Chicken-liver sponge	772	7.98	5
Cliona spp (Grant, 1826)	Boring sponge	690	8.02	5
Halisarca caerulea (Vacelet & Donadey, 1987)	Star encrusting sponge	588	8.08	15
Iotrochota birotulata (Higgin, 1877)	Green finger sponge	719	8.01	11
Ircinia felix (Duchassaing & Michelotti, 1864)	Stinker sponge	1047	7.87	2
Ircinia spp (Nardo, 1833)		937	7.91	3
Oceanapia bartschi (de Laubenfels, 1934)	Rough tube sponge	695	8.02	10

Siphonodictyon spp (Bergquist, 1965)	Variable boring sponge	598	8.07	6
Svenzea zeai (Alvarez, van Soest & Rützler, 1998)	Sven Zea's sponge	639	8.05	16
Verongula rigida (Esper, 1794)	Pitted sponge	1356	7.76	1
Verongula spp. (Verrill, 1907)	Netted barrel sponge	687	8.03	12
Xestospongia muta (Schmidt, 1870)	Giant barrel sponge	549	8.11	14
MACROALGAE				
Dictyota spp. (Lamouroux, 1809)		1635	7.69	1
	Brown turf algae	1635	7.69	1
	Calcifying algae	1635	7.69	1
	Green turf algae	1096	7.86	1
	Unidentified green algae	981	7.92	1
CNIDARIAN				
Stichodactyla helianthus (Ellis, 1768)	Sun anemone	640	8.05	15
Condylactis gigantea (Weinland, 1860)	Condy anemone	532	8.11	15
ECHINODERMATA				
Diadema antillarum (Philippi, 1845)	Long-spined sea urchin	572	8.09	19
POLYCHAETA				
Loimia medusa (Willey, 1905)	Medusa worm	1635	7.69	1
Hermodice spp. (Kinberg, 1857)	Fireworm	1101	7.84	1
Sabellastarte spp. (Krøyer, 1856)	Giant feather duster worm	945	7.91	1
Bispira spp. (Krøyer, 1856)	Social fether duster	686	8.03	12

Mean benthic coverage across all transects from survey time points was plotted against distance from the CO_2 seep site (Figure 4). Brown turf algae makes up most of the coverage across all survey time points. In the survey time points after the hurricane impact, the brown turf algae makes up an even larger part of the mean coverage across the transects. Brown turf algae had the highest coverage in March of 2018, when mean coverage across all quadrats 80% (±7.39). Comparatively, mean brown turf algae coverage was 65.7% (±15.5) before the hurricane impact, and 77.2% (±9.36) and 76.6% (±8.27) in the summer of 2018 and 2019 respectively. In the summer of 2017, more of the coverage is made up of different species compared with the time points after the hurricane impact. Calcifying algae makes up more of the mean coverage in 2017 compared with the following survey time points. More bare rock is present following the hurricane impact in March of 2018 and summer of 2018 compared with before the hurricane impact in the summer of 2017.

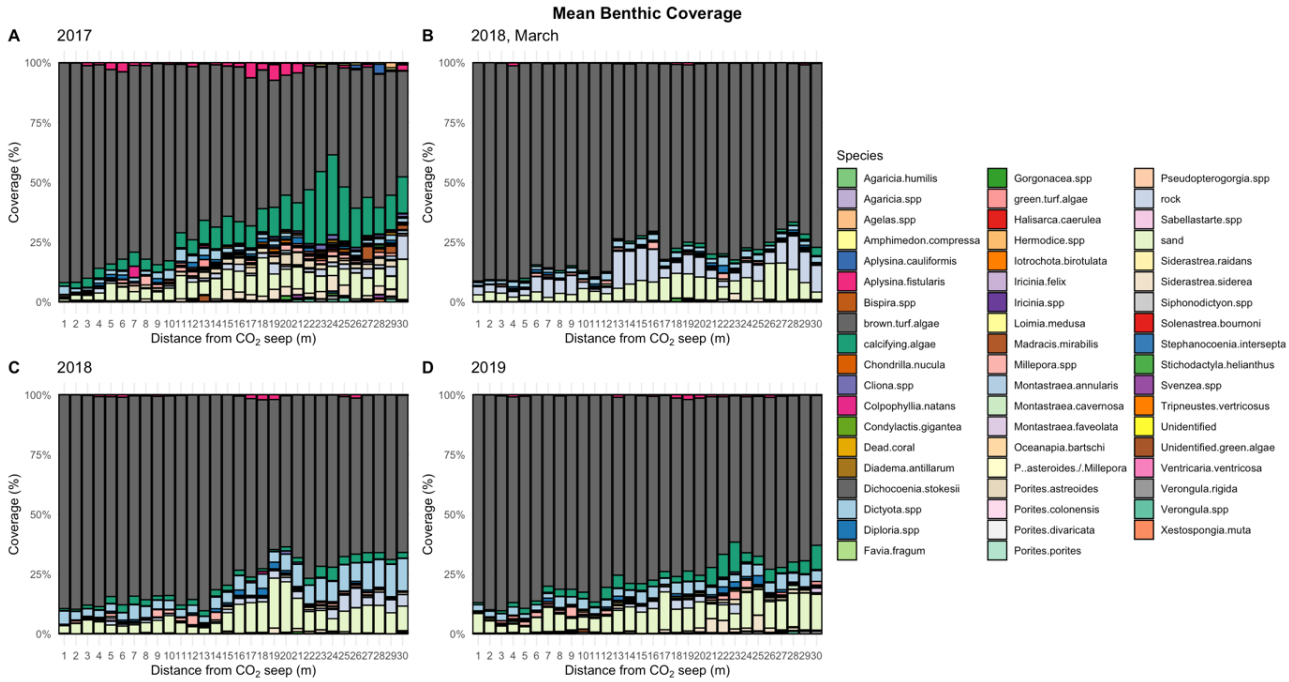

Figure 4: Mean benthic coverage across all survey time points. Benthic coverage is shown in different colours, and includes all types of benthic coverage found along the transects, also substratum such as sand, rock and dead coral. Mean benthic coverage in 2017 (A), before the Hurricane Maria hit the survey area. Mean benthic coverage in March of 2018 (B) shows the coverage in the survey area six months after the hurricane impact. Mean benthic coverage in the summer of 2018 (C) shows the coverage about 10 months after the hurricane. Mean benthic coverage in 2019 (D) shows the coverage almost two years after the hurricane impact.

3.2.1 Coral coverage

Mean coral coverage per quadrat was larger in 2017, being 7.16% (±3.62) before the hurricane impact in 2017, but reduced to 2.23% (±1.44) and 2.76% (±1.24) in March of 2018 and the summer of 2018 respectively. In 2019, the coral coverage increased to 3.66% (±3.03).
Mean coral coverage across all transects from all survey time points was divided into groups of six consecutive quadrats to display coral coverage change across the transects (Figure 5).

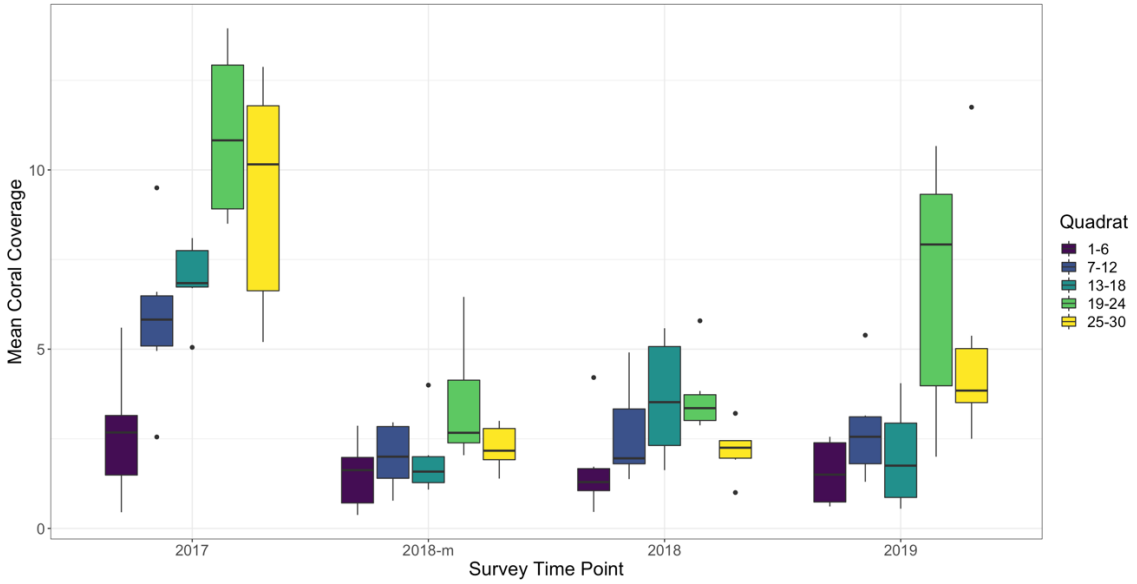

Figure 5: Mean coral coverage across transects from all survey time points. Coral coverage from each survey time point was divided into five groups of quadrats, with each group being made up of 6 quadrats. Groups are displayed in colours. Median coral coverage is displayed by the horizontal line in each individual box, while the whiskers (vertical lines) display maximum and minimum values of coral cover. Outliers are represented by black dots.

3.2.2 Sponge coverage

Before the hurricane impact, in 2017, the mean sponge coverage per quadrat was 4.14% (±3.11). The sponge coverage was drastically reduced in the year after the hurricane impact, with mean sponge coverage per quadrat only being 0.73% (±0.5) in March of 2018, and 0.82% (±0.62) in the summer of 2018. By 2019, mean sponge coverage had increased to 1.48% (±0.79). Mean sponge coverage across transects from all survey time points was divided into groups of six consecutive quadrats to display sponge coverage change across the transects (Figure 6). Across all transects the sponge coverage was reduced in the survey time points after 2017 following the hurricane impact.

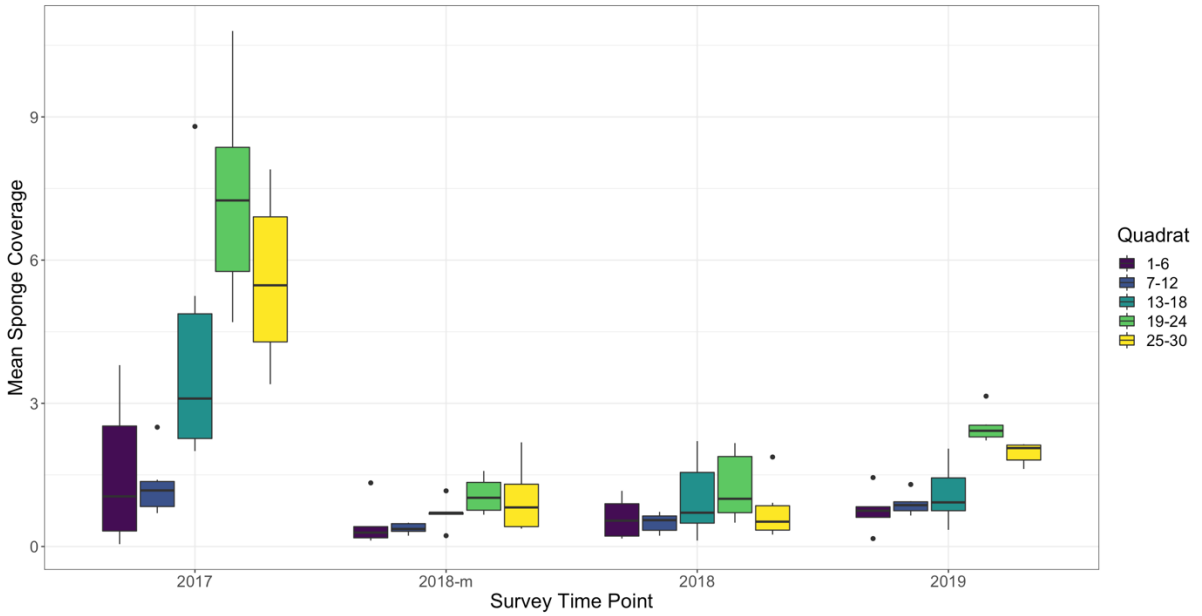

Figure 6: Mean sponge coverage across transects from all survey time points. Mean sponge coverage from each survey time point was divided into five groups of quadrats, with each group being made up of 6 quadrats. Groups are displayed in colours. Median sponge coverage is displayed by the horizontal line in each individual box, while the whiskers (vertical lines) display maximum and minimum values of mean sponge cover. Outliers are represented by black dots.

3.3 Richness, Diversity and Evenness

3.3.1 Richness

Species richness was found to be significantly different for pCO_2 values and survey time points, but not for substrate category (quasi-Poisson GLM with logit link function: 'Survey time pont' F = 171.0484, p < 2e-16, 'pCO_2' F = 84.3990, p<2e-16, 'Substrate category' F = 1.9141, p = 0.1479, Appendix 7). A post hoc Tukey test revealed that all survey time points had statistically significant species richness numbers, apart from March of 2018 and the summer of 2018 (Appendix 8). Coral richness showed the same trend as overall species richness did, with survey time point and year being significantly different, but not substrate category (quasi-Poisson GLM with logit link function: 'Survey time pont' F = 79.3845, p < 2.2e-16, 'pCO_2' F = 26.3753, p = 3.254e-07, 'Substrate category' F = 0.4275, p = 0.6522, Appendix 9). Coral richness before the hurricane impact, in 2017, was found to be significantly different from all other survey time points after the hurricane impact in the post hoc Tukey test (Appendix 10).

Also sponge richness was significantly different across survey time point and pCO_2 value, but not for substrate category (quasi-Poisson GLM with logit link function: 'Survey time pont' F = 78.3277, p <2e-16, 'pCO_2' F = 92.2186, p <2e-16, 'Substrate category' F = 0.0228, p = 0.9775, Appendix 11). A post hoc tueky test showed that sponge richness was significantly different between all survey time points (Appendix 12).

3.3.2 Diversity

Diversity metrics of Hill-Shannon and Hill-Simpson indices were calculated. Hill-Shannon diversity was found to be significantly different in response to the explanatory variables of survey time point, pCO_2 measurements and substrate category (ANOVA: $F_{6,1259}$ = 88.09 p-value < 2.2e-16, Appendix 13). A post-hoc Tukey test revealed that the survey time point before the hurricane in 2017 was significantly different from all other years, while the other survey time points did not show any statistical significant difference between them (Appendix 14). Hill-Shannon diversity was higher in quadrats further away from the seep site, and Hill-Shannon diversity showed a larger range in 2017 and 2019 compared with March of 2018 and summer of 2018 (Figure 7). For the fitted explanatory variables Hill-Simpson diversity was also found to be statistically different (ANOVA: $F_{6,1259}$: 69.97, p-value < 2.2e-16, Appendix 15). The post-hoc Tukey test revealed the same trend for Hill-Simpson diversity as for Hill-Shannon, with the diversity of 2017 being different from all other survey time points, while no statistical difference was observed between the other survey time points (Appendix 16).

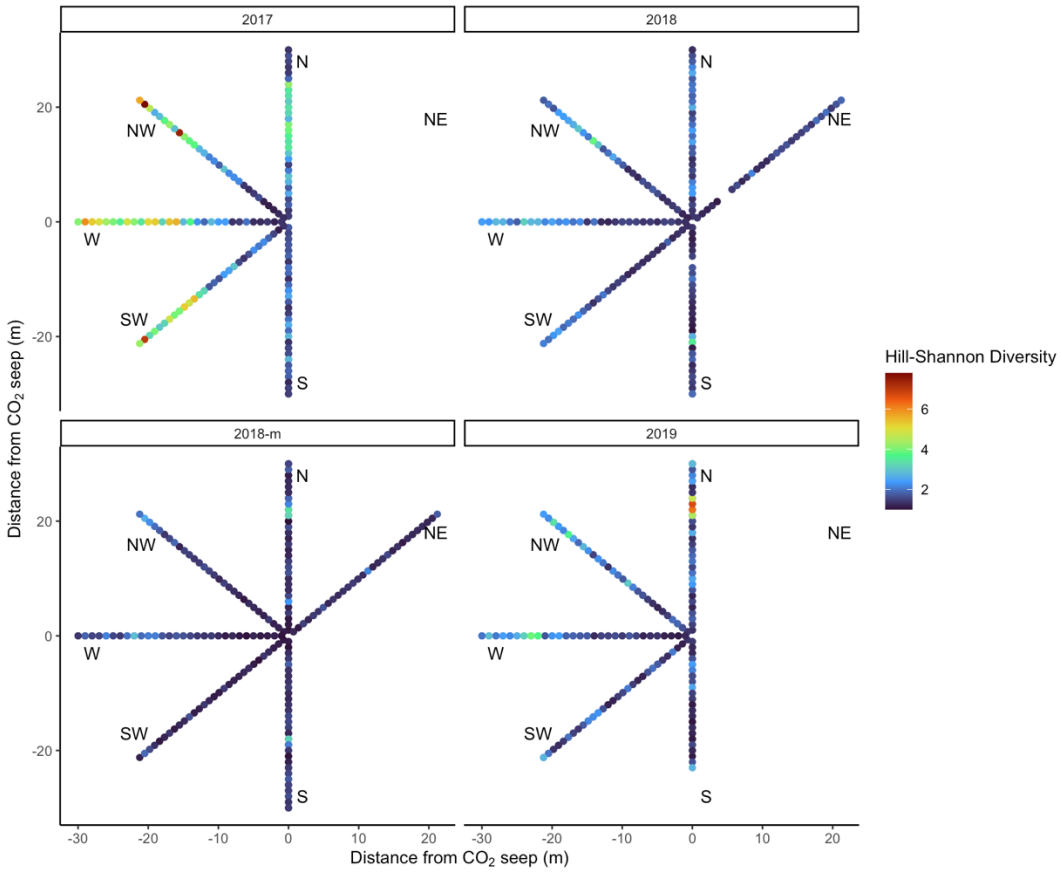

Figure 7: Hill-Shannon diversity across transects from all survey time points. Hill-Shannon diversity was plotted for all cardinal directions as displayed by labels NE for North East, S for South, SW for South West, W for West, NW for North West and N for North. The diversity metric was plotted for every survey time point, as indicated by the panes on top of the graphs, with 2017 for the summer of 2017, 2018-m for March of 2018, 2018 for the summer of 2018 and 2019 for the summer of 2019.

3.3.2 Evenness

Pielou's evenness was found to statistically different for the explanatory variables (ANOVA: $F_{6, 1258} = 81.88$, p-value: < 2.2e-16, Appendix 17). The post hoc tueky test revealed that all years were statistically different from one another, apart from the summer of 2018 and the summer of 2019 ($LM_{post\text{-}hoc}$: p = 0.5743, Appendix 18). 2017 shows little evenness, while March of 2018 shows the most evenness across the transects (Figure 8).

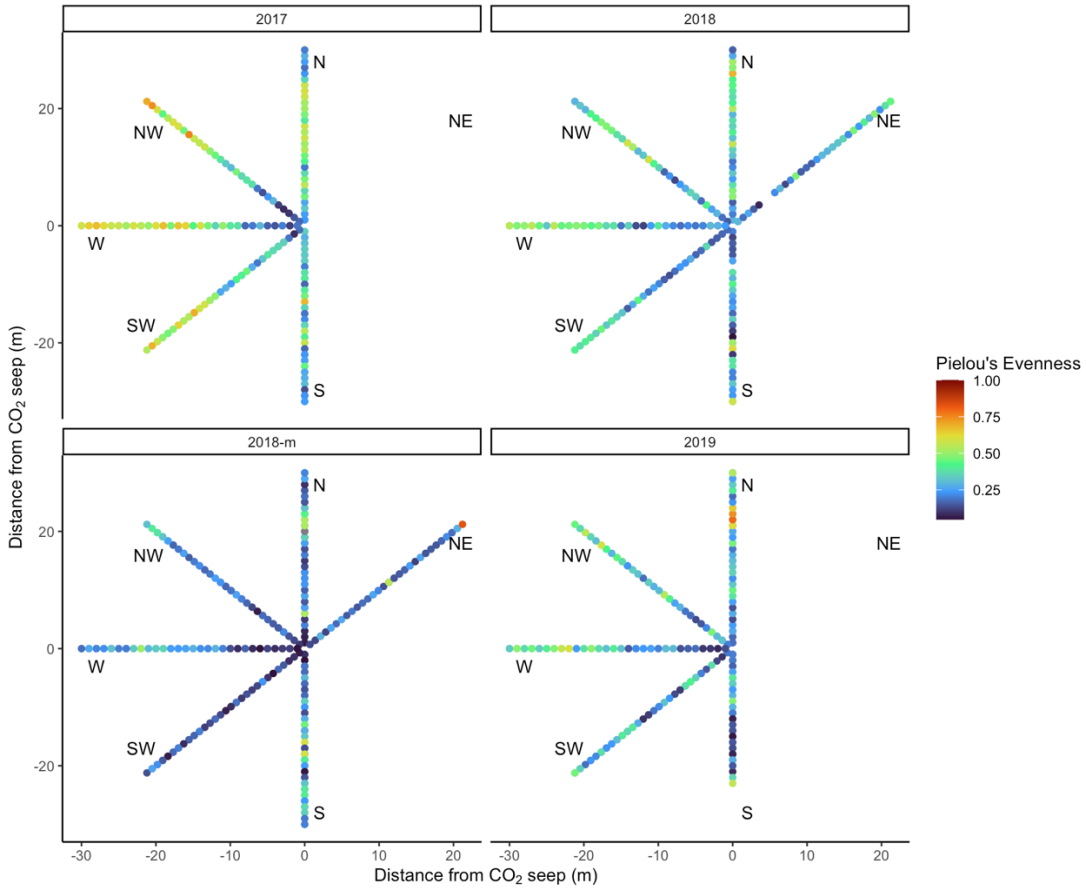

Figure 8: Pielou's eveness across transects from all survey time points. Pielou's evenness diversity was plotted for all cardinal directions as displayed by labels NE for North East, S for South, SW for South West, W for West, NW for North West and N for North. The evenness metric was plotted for every survey time point, as indicated by the panes on top of the graphs, with 2017 for the summer of 2017, 2018-m for March of 2018, 2018 for the summer of 2018 and 2019 for the summer of 2019.

3.4 Species composition

In all multivariate ordination plots the species names were shortened to reduce clustering on the plots (Appendix 19). The separate RDA models made for each survey time point were highly weighted by brown turf algae across all survey time points, while all other species showed high similarity for the fitted environmental variables (2017: Appendix 20; March of 2018: Appendix 21; summer of 2018: Appendix 22; 2019: Appendix 23). In these RDAs the model the variance explained by the constrained axes was larger in survey time points after the hurricane impact, compared with the summer of 2017 before the hurricane impact (Appendix 24). pCO_2 shows a strong, significant gradient in all survey time points (Appendix 25). In both the fitted CCA and RDA models, the eigenvalue for the constrained axes indicated that little variance was explained by the fitted model compared with the unconstrained variables (RDA eigenvalues: Appendix 27; CCA eigenvalues: Appendix 28).

3.4.1 Species composition in 2017

The CCA model for all species except brown turf algae in the summer of 2017 showed two gradients in the community structure, where 2.3% of inertia (Chi-square) could be explained by the explanatory variables in the model (Appendix 28). Of this variance, 1.42% of the variance could be explained by the first canonical axis (CCA1), while 0.88% could be explained by the second canonical axis (CCA2). The fitted CCA model was revealed to be robust ($p = 0.001$) with the Monte-Carlo permutation test. The correlation between the community composition and the fitted canonical axes were found to be statistically significant for the pCO_2 gradient (PERMANOVA: $p < 0.05$), but not for substrate category (PERMANOVA: $p = 0.068$) (Appendix 29). The strength and direction of the relationship between the species and the explanatory variables are illustrated in the CCA biplot (Figure 9). The opposing positioning to the pCO_2 gradient of *S. helianthus, Gorgonia* spp. *Pseudopterogorgia* spp., *M. mirabilis,* and *X. muta* in the biplot reflects a strong negative relationship with the variable. *Oceanapia bartschi* shows a stong relationship with 'Hard' substrate, while *S. bournoni, X. muta* and *A. cauliformis* show a strong relationship with 'Mixed' substrate. *Hermodice* spp. and *P. divaricata* shows some relationship along the pCO_2 gradient. Species that cluster in the middle of the canonical space do not show any particular relationship with any of the explanatory variables included in the model.

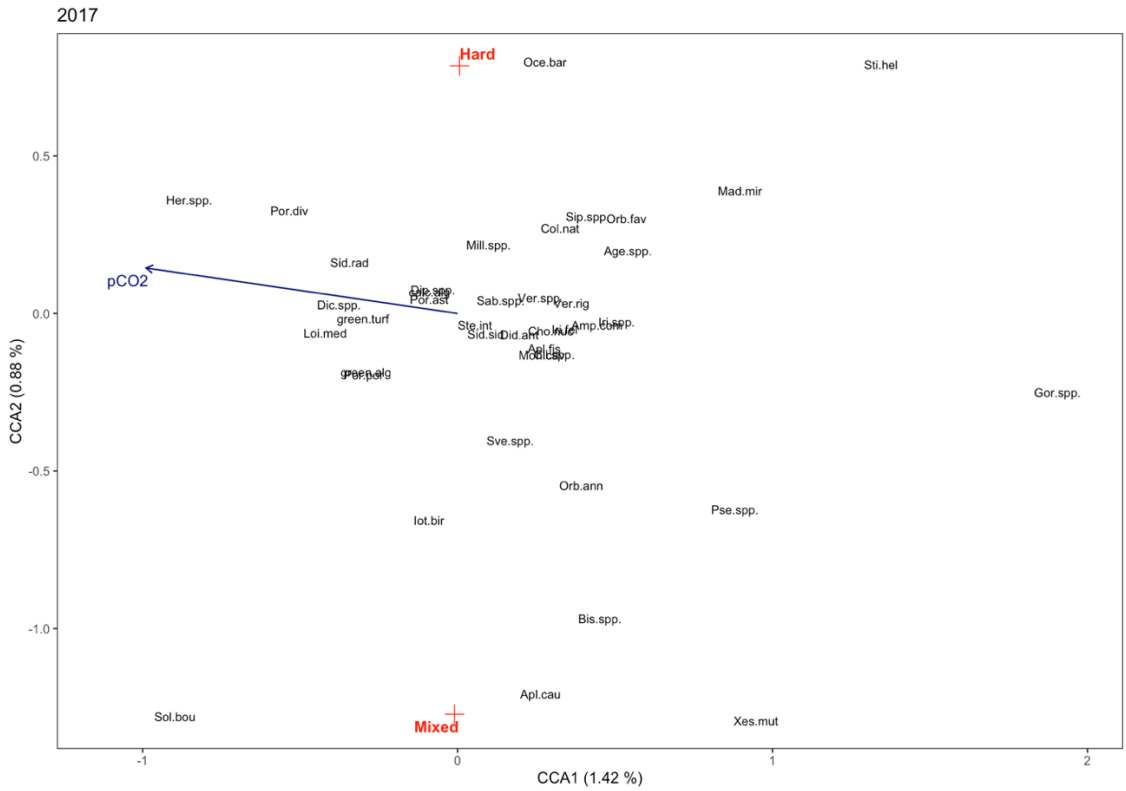

Figure 9: Canonical Correspondence Analysis (CCA) for all species except brown turf algae in the summer of 2017. A biplot was made to display the species responses to the response to environmental variables. Factor level variable substrate category (indicated by labels 'Hard' or 'Mixed') are indicated by red crosses. pCO_2 measurements are represented by the blue arrow, with arrow length and direction corresponds with the variance which can be explained by that explanatory variable. The direction of the arrows indicates an increasing magnitude of the variable.

3.4.2 Species composition in March of 2018

The CCA model for all species except brown turf algae in March of 2018 showed two gradients in the community structure, where 2.1% of inertia (Chi-square) could be explained by the explanatory variables in the model (Appendix 28). Of this variance, 1.58% of the variance could be explained by the first canonical axis (CCA1), while 0.49% could be explained by the second canonical axis (CCA2). The fitted CCA model was revealed to be robust (p = 0.002) with a Monte-Carlo permutation test. The correlation between the community composition and the fitted canonical axes were not statistically significant for the pCO_2 gradient (PERMANOVA: p = 0.097), but were significant for substrate category (PERMANOVA: p < 0.05) (Appendix 29). The strength and direction of the relationship between the species and the explanatory variables are illustrated in the CCA biplot (Figure 10). In March of 2018 several species show a strong relationship with 'Mixed' substrate, including *S. bournoni, S. radians* and *O. bartschi.* Substrate category 'Hard' show a strong relationship with *I. birotulata*. While *Diploria* sp., shows some positive relationship with the pCO_2 gradient, *P. porites* and *Siphonodictyon* spp. show a strongly negative relationship towards pCO_2.

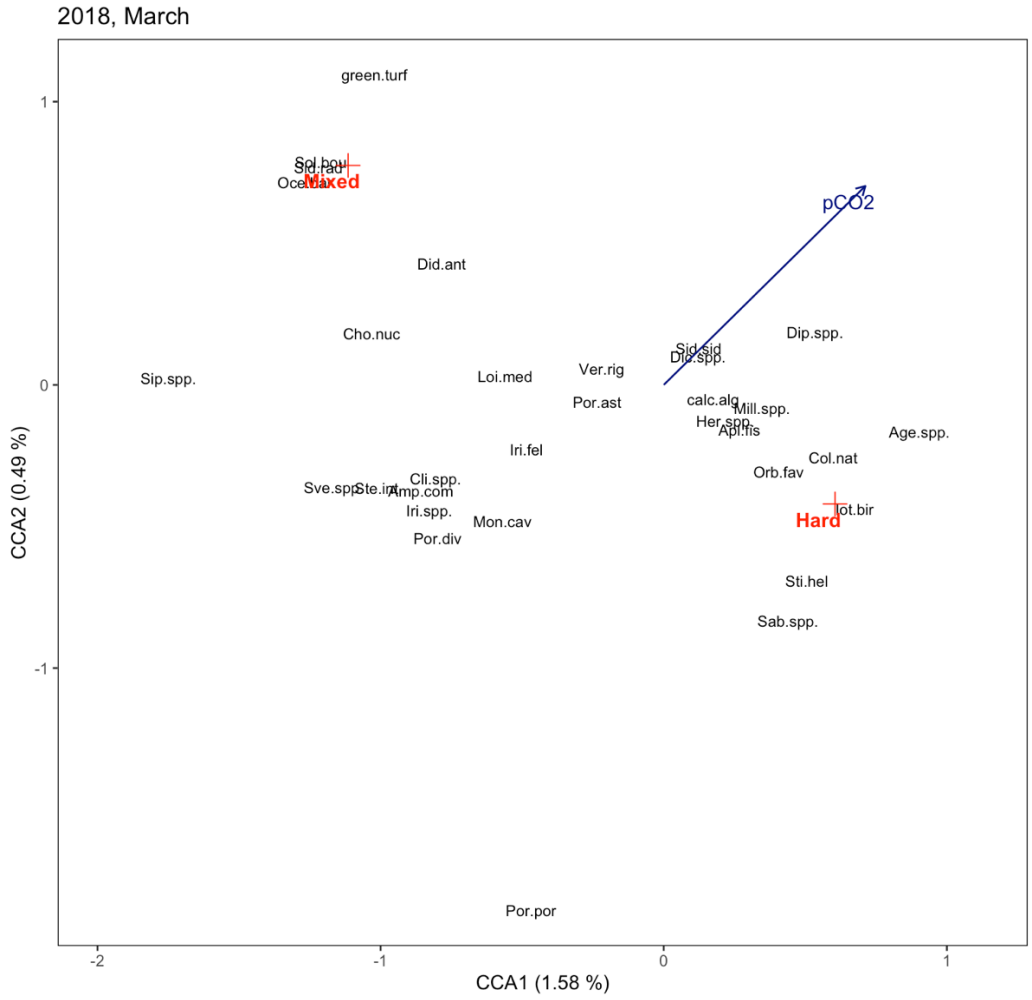

Figure 10: Canonical Correspondence Analysis (CCA) for all species except brown turf algae in March of 2018. A biplot was made to display the species responses to the response to environmental variables. Factor level variable substrate category (indicated by labels 'Hard' or 'Mixed') are indicated by red crosses. pCO_2 measurements are represented by the blue arrow, with arrow length and direction corresponds with the variance which can be explained by that explanatory variable. The direction of the arrows indicates an increasing magnitude of the variable.

3.4.3 Species composition in 2018

The CCA model for all species except brown turf algae in the summer of 2018 showed two gradients in the community structure, where 2.7% of inertia (Chi-square) could be explained by the explanatory variables in the model (Appendix 28). Of this variance, 2.16% of the variance could be explained by the first canonical axis (CCA1), while 0.54% could be explained by the second canonical axis (CCA2). The fitted CCA model was revealed to be robust (p = 0.001) with the Monte-Carlo permutation test. The correlation between the community composition and the fitted canonical axes were found not statistically significant for the pCO_2 gradient (PERMANOVA: p = 0.154), but was statistically significant for substrate category (PERMANOVA: p < 0.5) (Appendix 29). The strength and direction of the relationship between the species from the different years and the explanatory variables are illustrated in the CCA biplot (Figure 11). A positive relationship is observed between *V. rigida* and pCO_2. *Siphonodictyon* spp. and *Sabellastarte* spp. are found close together on the left side of the canonical space, showing similar responses to the fitted explanatory variables. Similarly, *C. nucula* and *A. compressa* are also found together in the canonical space.

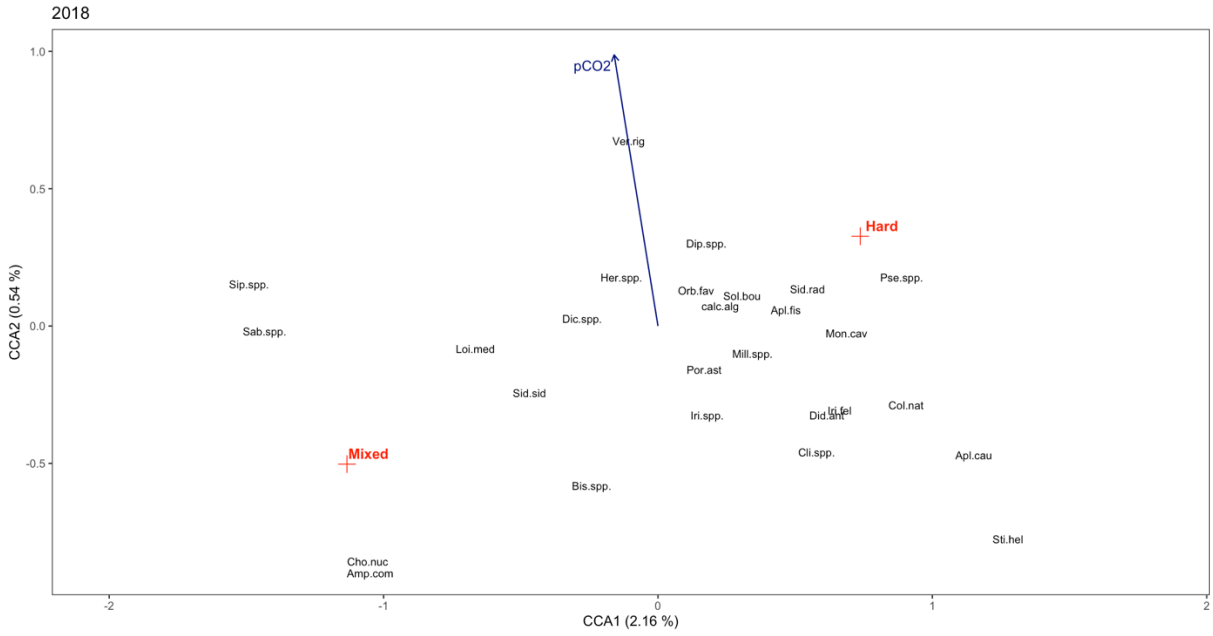

Figure 11: Canonical Correspondence Analysis (CCA) for all species except brown turf algae in the summer of 2018. A biplot was made to display the species responses to the response to environmental variables. Factor level variable substrate category (indicated by labels 'Hard' or 'Mixed') are indicated by red crosses. pCO_2 measurements are represented by the blue arrow, with arrow length and direction corresponds with the variance which can be explained by that explanatory variable. The direction of the arrows indicates an increasing magnitude of the variable.

3.4.4 Species composition in 2019

The CCA model for all species except brown turf algae in the summer of 2019 showed two gradients in the community structure, where 2.42% of inertia (Chi-square) could be explained by the explanatory variables in the model (Appendix 28). Of this variance, 1.5% of the variance could be explained by the first canonical axis (CCA1), while 0.93% could be explained by the second canonical axis (CCA2). The fitted CCA model was revealed to be robust (p = 0.001) with the Monte-Carlo permutation test. The correlation between the community composition and the fitted canonical axes were found to be statistically significant for the pCO_2 gradient

(PERMANOVA: $p < 0.05$), and also for substrate category (PERMANOVA: $p < 0.5$) (Appendix 29). The strength and direction of the relationship between the species and the explanatory variables are illustrated in the CCA biplot (Figure 12). In 2019 two of the polychaeta species *Hermodice* spp. and *Sabellastarte* spp., as well as *Millepora* spp. show a strong positive relationship with the pCO_2 gradient. The unidentified green algae shows a strong positioning to the far left side in the canonical space. Surrounding the 'Mixed' substrate are two clusters consisting of *Gorgonia* spp., *P. porites*, and *M. cavernosa* on the one side, and *S. bournoni, Agelas* spp., *O. annularis*, and *O. bartschi.*

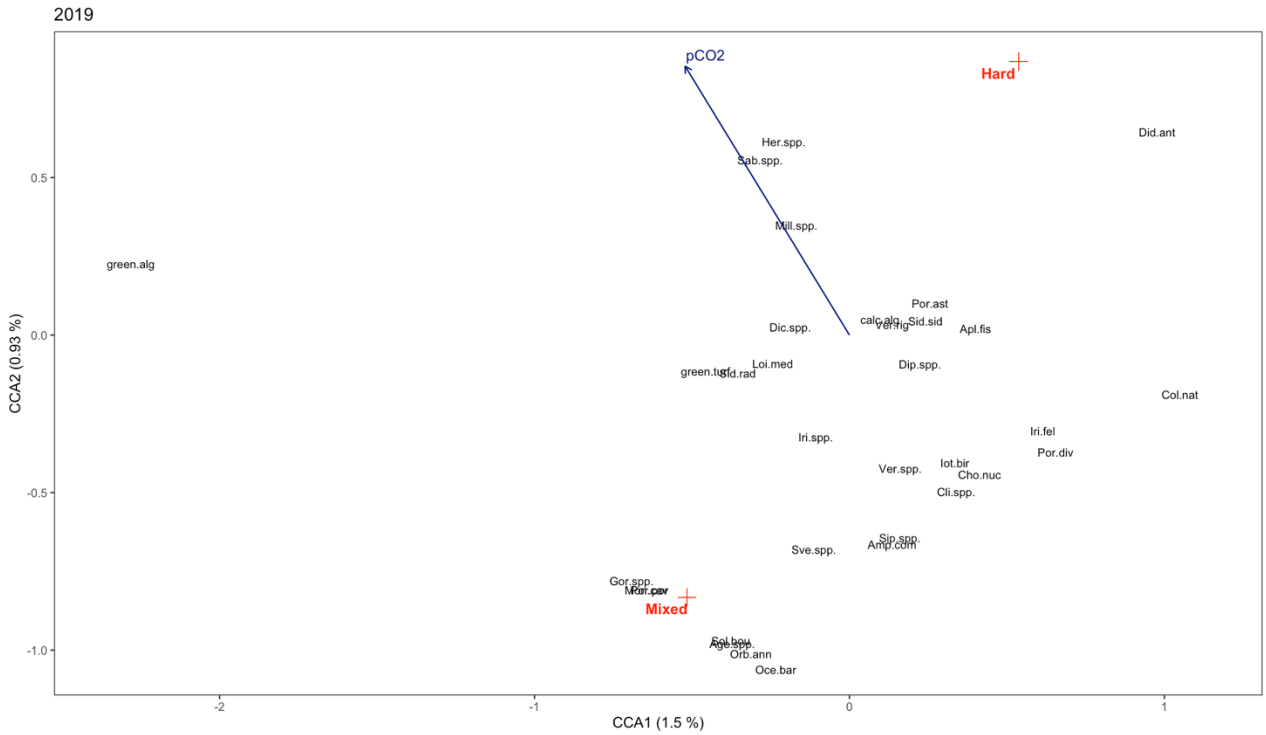

Figure 12: Canonical Correspondence Analysis (CCA) for all species except brown turf algae in the summer of 2019. A biplot was made to display the species responses to the response to environmental variables. Factor level variable substrate category (indicated by labels 'Hard' or 'Mixed') are indicated by red crosses. pCO_2 measurements are represented by the blue arrow, with arrow length and direction corresponds with the variance which can be explained by that explanatory variable. The direction of the arrows indicates an increasing magnitude of the variable.

3.5 Impact of hurricane on site similarity

The RDA across all years revealed 5 gradients in the community structure, where a total variance (inertia) of 19% could be explained by the explanatory variables in the model (Appendix 24). Of this variance, 13.99 % of the variance could be explained by the first canonical axis (RDA1), while 3.83% could be explained by the second canonical axis (RDA2). The fitted RDA model was revealed to be robust ($p < 0.001$) with the Monte-Carlo permutation test. The correlation between the community composition and the fitted canonical axes were found to be statistically significant (Appendix 25). The strength and direction of the relationship between the sites from the different years and the explanatory variables are illustrated in the RDA biplot (Figure 13). The pCO_2 gradient shows a strong gradient, with sites from the survey time points following the hurricane impact showing a shift closer towards pCO_2.

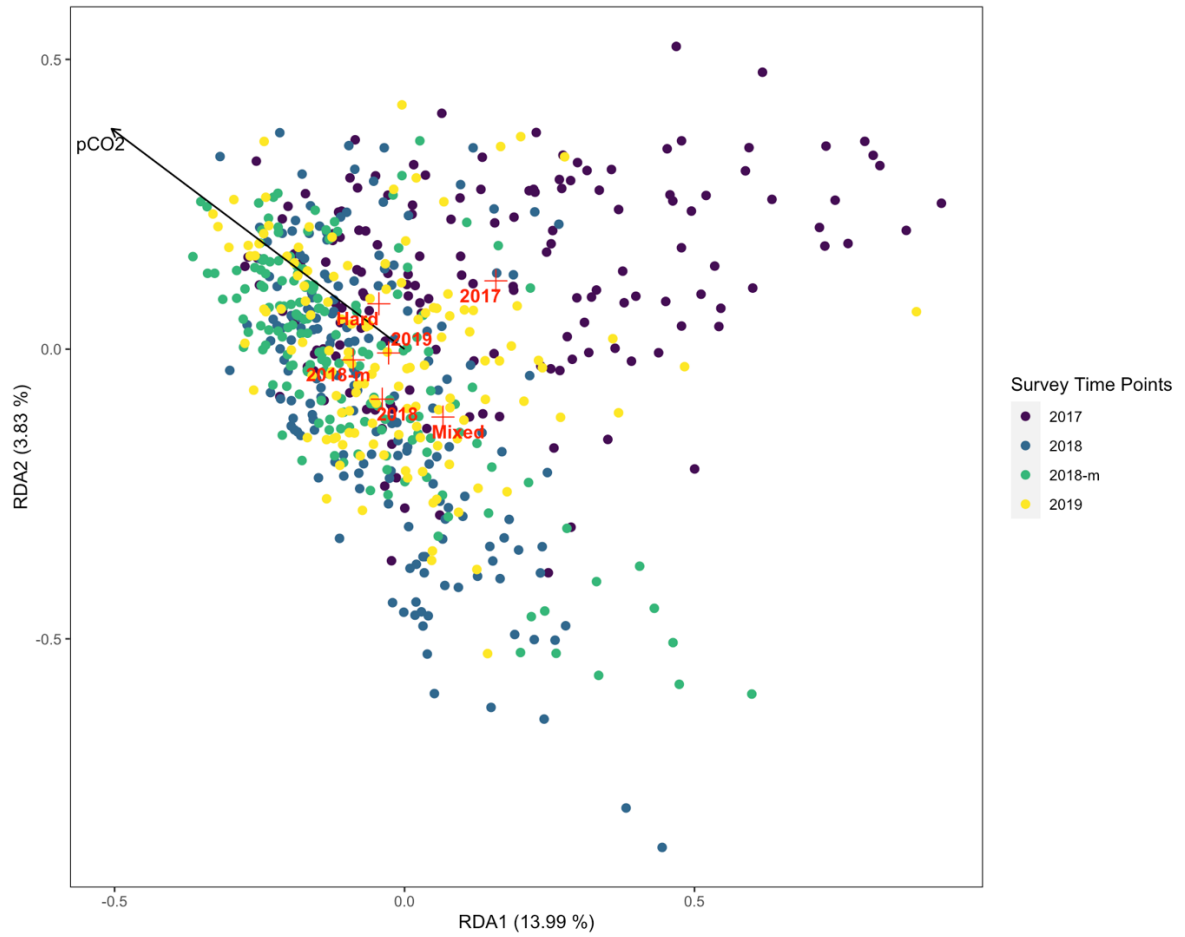

Figure 13: Redundancy analysis (RDA) for sites across all survey time points. A biplot was made to display the similarities of sites in response to explanatory variables. Centroids, coordinates for factor level variables, are indicated with red crosses. Factor level variables include survey time point (indicated by labels '2017', '2018m', '2018' and '2019') and substrate category (indicated by labels 'Hard' or 'Mixed'). pCO_2 measurements are represented by the blue arrow, with arrow length and direction corresponds with the variance which can be explained by that explanatory variable. The direction of the arrows indicates an increasing magnitude of the variable. Sites, represented as coordinates of the sites in the space of explanatory variables, with sites in from different survey time points being displayed in different colours.

More similarity between sites was observed when brown turf algae was removed from the multivariate analysis. The CCA across all years where brown turf algae was removed from the species matrix revealed 5 gradients in the community structure, where a total variance (inertia) of 3.5% could be explained by the explanatory variables in the model (Appendix 28). Of this variance, 1.78% of the variance could be explained by the first canonical axis (CCA1), while 0.79% could be explained by the second canonical axis (RDA2). The fitted CCA model was revealed to be robust ($p < 0.001$) with the Monte-Carlo permutation test. The correlation between the community composition and the fitted canonical axes were found to be statistically significant (Appendix 29). The strength and direction of the relationship between the sites from the different years and the explanatory variables are illustrated in the RDA biplot (Figure 14). pCO_2 showed a small impact on site composition. Sites from 2019 and 2017 show similar patterns, with more spread of sites in the canonical space, while sites from March and summer of 2018 show little variation between them.

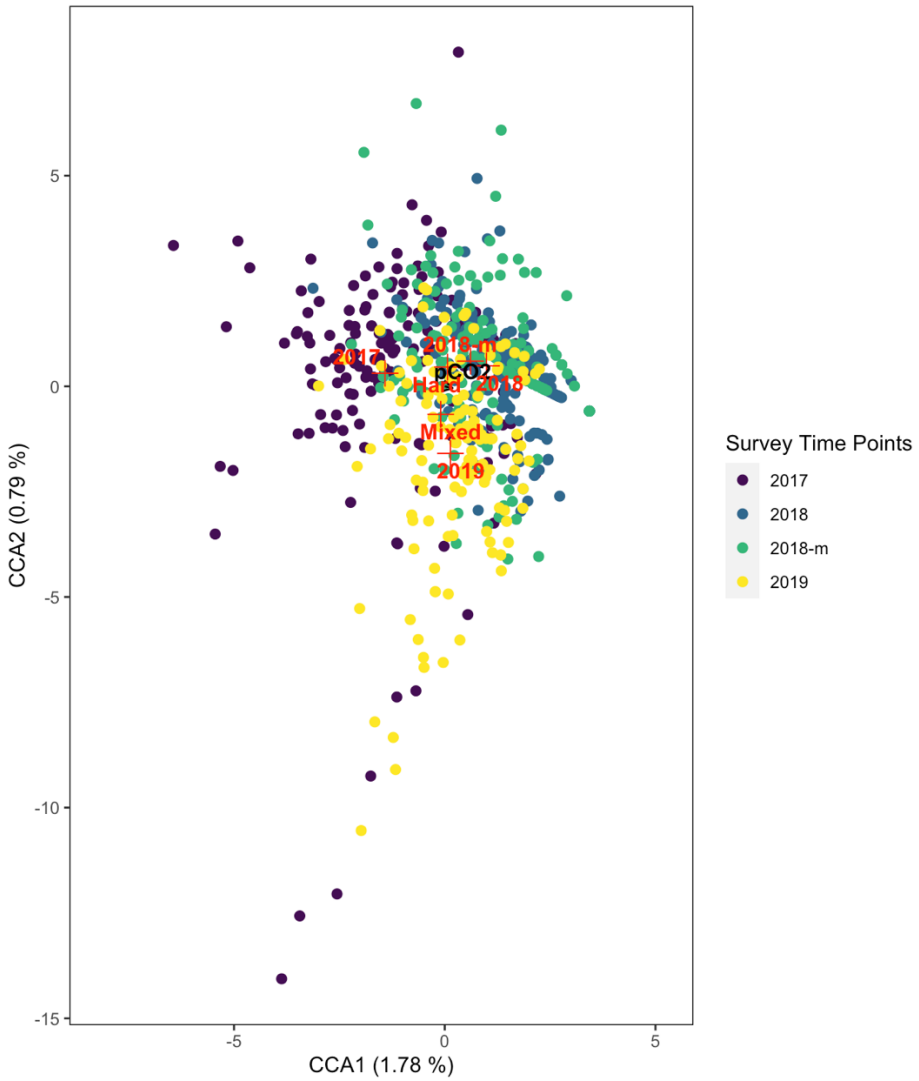

Figure 14: Canonical correspondence analysis (CCA) for sites across all survey time points. A biplot was made to display the similarities of sites when brown turf algae was removed in response to explanatory variables. Centroids, coordinates for factor level variables, are indicated with red crosses. Factor level variables include survey time point (indicated by labels '2017', '2018m', '2018' and '2019') and substrate category (indicated by labels 'Hard' or 'Mixed'). pCO_2 measurements are represented by the blue arrow, with arrow length and direction corresponds with the variance which can be explained by that explanatory variable. The direction of the arrows indicates an increasing magnitude of the variable. Sites, represented as coordinates of the sites in the space of explanatory variables, with sites in from different survey time points being displayed in different colours.

3.6 Hurricane Impact on Sessile Macroinvertebrates

The CCA model for macroinvertebrate count numbers showed six gradients in the community structure, whereof 11.5% of inertia (Chi-square) could be explained by the explanatory variables in the model (Appendix 28). Of this inertia, 6.22% of the inertia could be explained by the first canonical axis (CCA1), while 3.93% could be explained by the second canonical axis (CCA2). The fitted CCA model was revealed to be robust ($p = 0.001$) with the Monte-Carlo permutation test. The correlation between the community composition and the fitted canonical axes were found to be statistically significant for survey time point (PERMANOVA: $p < 0.05$), for the pCO_2 gradient (PERMANOVA: $p < 0.05$), and also for substrate category (PERMANOVA: $p < 0.5$) (Appendix 29). The strength and direction of the relationship between the species and the explanatory variables are illustrated in the CCA biplot (Figure 15). The biplot shows that several species are found at a higher frequency in 2017 before the

hurricane impact, including *C. gigantea*, *D. antillarum*, *Sabellastarte* spp. and *Bispira* spp. One polychaeta, *Hermodice* spp., was found to be more related to March of 2018, while the sun anemone, *Stichodactyla helianthus*, was found not to be related with 2019.

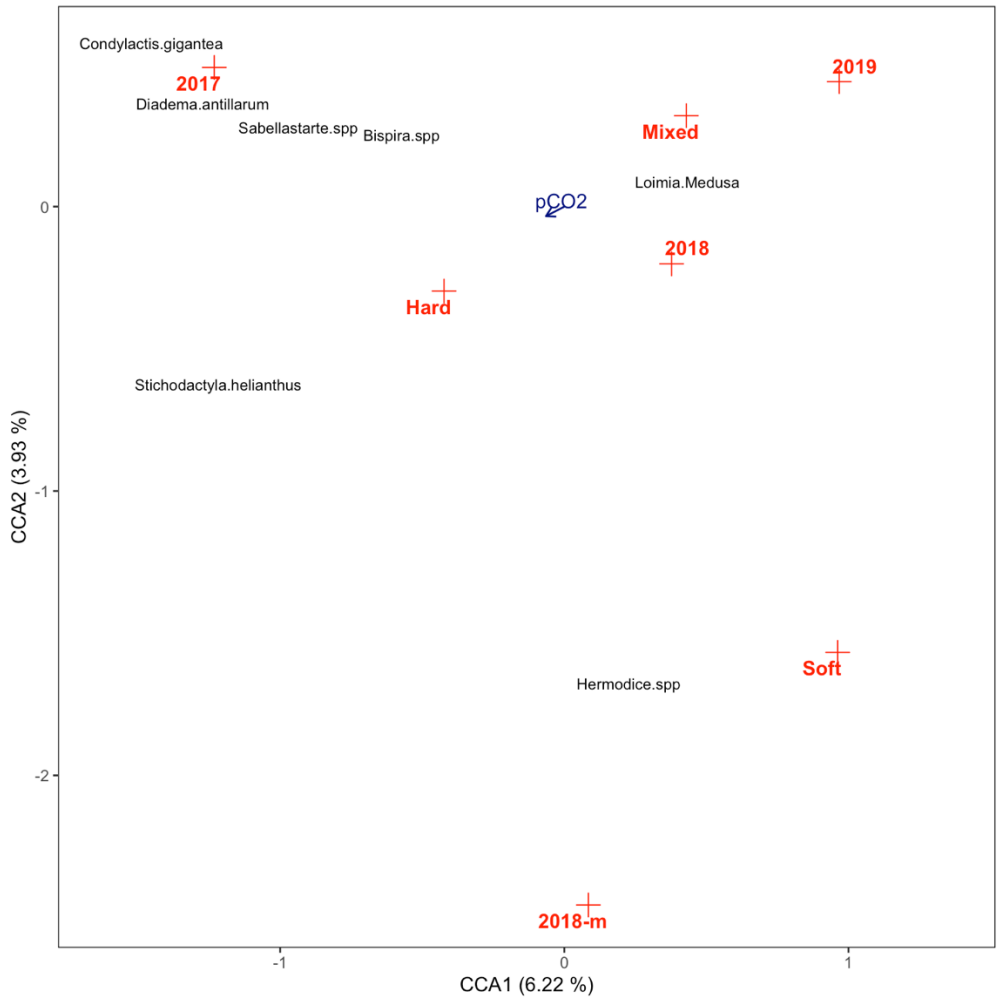

Figure 15: Canonical Correspondence Analysis (CCA) for macroinvertebrate count numbers. A biplot was made to display the species responses to the response to environmental variables. Factor level variables include survey time point (indicated by labels '2017', '2018m', '2018' and '2019') and substrate category (indicated by labels 'Hard' or 'Mixed'). pCO_2 measurements are represented by the blue arrow, with arrow length and direction corresponds with the variance which can be explained by that explanatory variable. The direction of the arrows indicates an increasing magnitude of the variable.

4 Discussion

4.1 Community response to Ocean Acidification

Community composition will be altered in response to the climatic driver of ocean acidification. Never before has the ocean endured such rapid and great changes to its carbonate system as observed in current day (Hönisch et al. 2012b). The amplitude of the global biogeochemical cycle of CO_2 is increasing in response to climatic changes (McNeil and Sasse 2016). This augmentation to the carbon cycle is predicted to cause CO_2 exposure above physiologically detrimental levels for marine animals in the Atlantic, Pacific and Southern Ocean (McNeil & Sasse, 2016). Based on similar research (e.g. Hall-Spencer et al., 2008; Sunday et al., 2017), this study expected an observable community shift away from calcifying species towards macroalgae as pCO_2 levels increased with proximity to the seep system. This type of community shift was observed across all the transects and all survey time points. Corresponding with observations from similar research (Hall-Spencer et al., 2008), macroalgae make up most of the benthic coverage in the quadrats with the highest pCO_2 levels. As the pCO_2 levels decrease towards current-day oceanic levels, the diversity along the transects increase (Hill-Shannon: $p < 0.05$, Hill-Simpson: $p < 0.05$), and the evenness of the transects decrease (Pielou's evenness: $p < 0.05$). Furthermore, more calcifying organism were present in quadrants with lower pCO_2 measurements, indicating that the calcifying organisms are affected by pCO2 levels. To date, several studies have investigated the community change that occurs along a pCO_2 gradient, with focus on coral species (Fabricius et al. 2011; Crook et al. 2011; Inoue et al. 2013). All studies found that there will be a community shift towards less Scleractinian corals (reef building corals) being present, lowered recruitment (Fabricius et al., 2011), and a decrease in diversity nearer the seep site, relating to lowered pH levels and increasing pCO_2 levels (Brown et al. 2017).

However, several corals and sponges in this survey were found in proximity with the seep site (Table 5), thereby suggesting a tolerance for higher levels of pCO_2 of these species. Both corals and sponges have a lower mean coverage near the seep site observed near the seep site (Figure 5, Figure 6), but also individual organisms exhibited a smaller coverage area in the quadrats nearest to the CO_2 seep. For example, a coral of the genus *Diploria* was observed in the quadrat nearest the seep site. At this closeness to the seep site, the *Diploria* coral only covered about 1% of the quadrat. Comparatively, a colony of *Diploria* sp. recorded in quadrat 19 (i.e., 19m away from the seep) showed a coverage of about 30% of the quadrat. Other species that displayed similar patterns include the corals *P. asteroides*, *Millepora* sp., *S. siderea* and *S. radians*, and the sponges *V. rigida*, *A. fistularis*, *Iricinia* spp. and *I. felix*. The *Porites* genus appear to be a genus of corals that are relatively tolerant to living in high pCO_2 environments (Fabricius et al. 2011). Abundance of *Porites asteroides* is currently increasing in the Caribbean (Green et al. 2008), prompting the suggestion that this species may become prominent in future reef assemblages. Importantly, some species have demonstrated an increase in calcification rates at low energetic cost in response to temperature increases, and may therefore be able to counteract OA to some degree (McCulloch et al. 2012a). Mitigation through increased calcification rates has been observed in corals of the genus *Porites,* however, this increase does not sustain with the additional stress of increasing seawater temperatures

(Cole et al. 2018). Simultaneously, OA can impact several life history traits of *P. asteroides*, which further impacts the recruitment rates (Albright and Langdon 2011). Mitigation through increased calcification is also observed for some deep-sea and cold-water corals, which are already living in an environment that has a decreased saturation of carbonate ions (McCulloch et al. 2012b). Furthermore, some corals found in more temperate regions have found solutions to deal with OA, such as increased feeding rates observed in the threatened *Acropora cervicornis* (Towle et al. 2015). Other scleractinian corals, including *M. faveolata* and *P. asteroides*, can obtain fatty acids from their symbiotic zooxanthella, thus serving as a significant source of fatty acids for corals (Teece et al. 2011). Indeed, organismal modification of local carbonate chemistry may enable some calcifying species to successfully grown and maintain calcified structure in the face of OA (Roleda et al. 2012).

Considering that sponges have become some of the most abundant taxa on Caribbean coral reefs (Rüstler, 2004), it is noteworthy that only a few species appear to do well in the survey area of this study. These include *A. fistularis*, *Iricinia* sp., *I. felix* and *V. rigida*. Interestingly, a study preformed in vitro of the sponges *A. cauliformis*, *A. fistularis* and *I. birotulata* found that these species showed little impact from predicted changes in seawater temperature and pH changes (Duckworth et al. 2012). However, in this study neither *A. cauliformis* or *I. birotulata* are found at pH levels below 8.09 or 8.01 respectively. This could suggest that there are other drivers present in the natural system that were not investigated in the lab which may act limiting on the sponges in the seep system community. With the predicted decreases in pH in the worst-case scenario from the IPCC (2021), these sponges will not sustain as the ocean becomes more acidified. Another sponge which may not do well in future oceans is *Cliona* sp., a boring sponges that prefer to settle in carbonate rich environments (Rosell and Uriz 1992), and have been shown to have reduced attachment rates at pH levels of 7.8 (Duckworth et al. 2012). Indeed, in this study the sponge is not found at pH levels below 8.02, suggesting that this sponge may not be present in future shallow marine communities if the pH levels decrease to the projected 8.0 (IPCC, 2014). Increased levels of pCO_2 can have a great impact on settlement rates of a wide range of benthic organisms (Cigliano et al. 2010). Moreover, species such as *Clinoa* sp. that prefer to settle in carbonate rich environments may struggle in the future, as the carbonate habitat-building species may cease to sustain in response to the cumulative forces of climate change. In addition to *Cliona* spp., also the serpulidae which prefer to settle in crevices of corals (Steiner et al. 2007), may struggle.

Macroalgae, tend to do well in along naturally acidified gradients, probably due to the increase of CO_2 released from CO_2 seeps. Moreover, turf algae presence reduces the photochemical efficiency of neighbouring corals, thereby lowering the overall fitness of the corals (Vermeij et al. 2010). Indeed, turf algae can decrease the density of the symbiont zooxanthella and tissue thickness of corals (Quan-Young and Espinoza-Avalos 2006). This gives turf algae an advantage, and may explain some of the extreme dominance observed of brown turf algae. Comparatively, calcifying algae showed a coverage gradient that decreased towards the seep site in the community present before the hurricane impact. This observation coincides with observations from seep sites in the Mediterranean and in Japan (Peña et al. 2021), where calcifying algae lost both coverage and diversity with increasing proximity to the CO_2 seeps.

Other species that show strong aversions to the CO_2 seep are *Bispira*, *Aplysina cauliformis*, *M. mirabilis*, *Gorgonia* sp. and *Pseudopterogonia* sp., which are all found in quadrats that are more distant from the CO_2 seep, indicating that the environmental conditions near the seep are unfavorable for these species. Notably, a shift towards more soft coals in response to periodically high levels of pCO_2 has been observed in Japan, suggesting that soft corals can tolerate acidified environments over shorter periods (Inoue et al. 2013).

4.2 Community response to Hurricane Impact

The hurricane impact on the community composition was measured by comparing species coverage across time series from before and after Hurricane Maria. A loss of diversity, coral and sponge coverage area and an increase in evenness was observed after the hurricane impact. This corresponds with other research which concludes that extreme weather events can be a driver of biodiversity patterns in marine ecosystems (Wernberg et al. 2016), with frequency and intensity having a strong impact on future species distribution and ecosystem structure (Wernberg et al. 2013). Reduction in coral cover at the Great Barrier Reef has also been connected with extreme weather events, including storm events (De'ath et al. 2012). The majority of the damage from Hurricane Maria is likely a result of the physical damaged caused by the storm event itself, as well as strong wave surges in the time period around the storm event. Notably, these results oppose research conducted at St. Thomas of the Virgin Islands, where Hurricane Irma and Hurricane Maria did not have a significant impact on coral coverage (Gochfeld et al. 2020).

In response to Hurricane Maria, several species notably reduced in coverage area or were completely removed from the area long the survey quadrats. Simultaneously, brown turf algae coverage expanded to about 80% mean coverage per quadrat in March of 2018, 6 months after the hurricane impact. Due to high dominance of brown turf algae, the RDA model fitted for all the survey time points (Figure 13) mainly demonstrates site differentiation of brown turf algae coverage of each survey time point. Before the hurricane impact, in 2017, the sites, or rather the species composition in each quadrat, showed a larger dissimilarity reflected in more distance between sites in 2017. After the hurricane impact, the sites in March of 2018 and the summer of 2018 show a larger similarity, indicating that the species composition, or rather the brown turf algae coverage, within these sites is more similar. Comparatively, by 2019 the sites show a slight skew towards the sites of 2017, which could suggest a return towards site composition present before the hurricane impact. Undoubtedly brown turf algae drives the main site differentiation observed, as in the CCA model fitted when brown turf algae was removed, the site compositions of the survey time points show more similarity between them. Increasing abundance of macroalgae following hurricane impacts has been observed across the Caribbean region for decades (Edmunds 2019). Notably, near the seep site, the brown turf algae remains the dominant group across the survey period.

Several diversity metrics were investigated in this study. Species richness, or number of species, can be an important diversity metric for structural complexity of ecosystems (Sunday et al., 2017). In this survey species richness, coral species and sponge richness was investigated across all survey time points and against pCO_2 measurements. Species richness was found to

be significantly different across all survey time points and for the pCO_2 gradient ($p < 0.05$). The same trend was found for coral richness and sponge richness, with mean coral coverage and sponge coverage being reduced following the hurricane impact (Figure 5 and 6). Additionally, Hill-Shannon and Hill-Simpson diversity metrics were investigated. The Hill-Shannon diversity, also known as Hill number 1, has been identified as a diversity metric that can serve as a good choice when investigating gradients in biodiversity (Roswell et al., 2021), and is based on the weighted geometric means of the proportional abundances. In this survey, the Hill-Shannon diversity was found to be statistically different between all survey time points, with Hill-Shannon numbers being higher in 2017 before the hurricane compared with after the hurricane impact. All other survey time points were not found to be different from each other. The same statistical outcome was found for Hill-Simpson diversity, with larger Hill-Simpson and Hill-Shannon numbers found in 2017 compared with all other years. Thus, the diversity present before the hurricane impact was larger than then diversity present following the hurricane impact. In contrast, Pielou's evenness was found to be statistically different between all survey time points, apart from the summer of 2018 and 2019 (Appendix 18), indicating that evenness of species coverage did not change significantly between these two survey time points. This could suggest that little recovery occurred between the summer of 2018 and 2019. 2017 was the time point with the most diversity, followed by 2019, while March of 2018 and summer of 2018 showed low diversity and high evenness. This gives evidence to an observed simplification effect caused by the hurricane. Before the hurricane hit, the 2017 site composition showed more dispersion (more dissimilarities), but following Hurricane Maria, the sites show more similarity and less spread. Notably, the sites in 2019 show more less similarity between sites compared with March 2018 and summer 2018. Several diversity indices were used in this study to emphasize the observed trends. Indeed, the inclusion of several indices can be more powerful (Roswell et al. 2021).

Based on previous research, the growth form of an organism could affect the impact the hurricane event imposes. For corals, boulder type corals and encrusting growth forms tend to do better, compared with species that have more of an erect growth form (Mah and Stearn 1986; Madin et al. 2014). Many corals showed reduced coverage area in the year following the hurricane impact. However, the encrusting base of the corals *P. asteroides* and *Millepora* sp. allowed for some resilience to the hurricane impact, although erect features were lost. Comparatively, encrusting sponges may see an increase in coverage area, while erect sponges experience a decrease (Gochfeld et al. 2020). Interesting that calcifying algae shows a strong decrease in coverage between years, despite the benefit of having an encrusting nature which could be more resistant to hurricane impacts. This could suggest that the decline in calcifying algae is related to other aspects of the hurricane impact, such as increased turbidity or terrestrial run-off. Moreover, benthic substrate, including sand and rock, makes up a larger proportion of the coverage in the two time points following the hurricane. In March of 2018 both sand and rock are prevalent. However, in the summer of 2018 the rock coverage is reduced again, suggesting a recolonization of the substratum.

4.3 The combined effect of Hurricanes and Ocean Acidification, and the future for Dominican reefs

4.3.1 Community response of two stressors

The combined effect of OA and the hurricane impact was assumed to lead to a decrease in diversity and an increase in evenness across the transects, not just in the quadrats near the seeps where diversity is already low due to high pCO_2 levels. The synergistic effect of OA and hurricanes are observed to cause a simplification of the marine community in this study. Interestingly, as the community composition near the CO_2 seep site is already more homogenous, the effect of the hurricane was less impactful on the community composition around the seep site. Therefore, should the pCO_2 levels decrease from the average levels of 400 µatm to the predicted ~850 µatm in the future (IPCC, 2014), hurricane impacts may appear to impact the community composition less. As this plausible scenario may occur on top of an already overall simplification caused by OA, disruption by hurricane events may seem less impactful. Simplification following hurricanes may be a general response in marine environments, as a response to storm events has already been established in kelp forests, reflected in loss of diversity and decreases in higher trophic levels (Byrnes et al. 2011). Simplification as a response to OA has been observed in other research (Agostini et al. 2021). Therefore, the combined effect of the hurricane and OA may cause overall simplification to be maintained for longer periods than observed in this study, where recovery effects are observed after almost two years. This study finds that the species that are the most restricted in expanding their coverage towards the seep site are also the species that are the most impacted by the storm event. As other species lose their coverage proportions, brown turf algae sees and immediate increase in coverage area.

The canonical axes created in the CCA models indicated that the fitted variables explain very little of the positioning of the species in the canonical space. Canonical axes of low values are common in ecological studies applying multivariate statistics. Although little variance (inertia) could be explained by the axes, all of the fitted multivariate models were found to be significant for survey time point, indicating that the species composition was significantly different across all survey time points. Investigations of the CCA biplots, in the multivariate analyses where the brown turf algae was removed, do not reveal any recurring clusters of species across the survey time points. Yet some species do show the same patterns of positioning in each survey time point. Even after the hurricane impact, *P. asteroides, Millpora* sp., *Diploria* sp., *V. rigida, S. siderea* and *S. radians* are more often could in the middle of the biplot, indicating that their position in relation to the fitted environmental variables in the community is somewhat consistent through the survey time period. Comparatively, *C. nucula*, *A. compressa* and *Gorgonia* sp. are often found in the peripheral parts of the biplots, suggesting they show a stronger relationship with the fitted variables. Notably, less species are present in the survey time points after the hurricane compared with before.

4.3.2 Recovery

Recovery of coral and sponge species was assumed to occur at a slower pace close to the seeps to the backdrop of pCO_2. Indeed, habitat recovery rate following a disturbance event can occur

at a slower rate owing to the adverse biological impacts of OA (Gaylord et al., 2015). Moreover, there is little evidence to suggest a full recovery of reef communities until about 8 years after the initial impact (Gardner et al. 2005), with damage to corals increasing with intensity and frequency of impacts (Gardner et al., 2005). Although some uncertainty remains regarding increase or decreasing frequencies of hurricane impacts, the evidence does suggest that the intensities of hurricanes will increase (Bender et al. 2010). Thus, the impact of hurricane event may cause increasingly more damage on coral reefs, which will require increasingly more time to recover. In this survey coral and sponge cover showed a faster recovery of coverage area at distances further from the CO_2 seep (Figure 5, Figure 6). This suggests that the recovery rate of corals and sponges is impacted by the pCO_2 levels of the surrounding waters. Additionally, interspecific responses to pCO_2 may cause successional delays in acidified environments (Brown et al., 2017).

Brown turf algae appears not to have been greatly impacted by the hurricane, and an increase in coverage percentage may actually indicate that the algae benefits from the demise of other species in the face of OA and hurricanes. This concurs with other research, funding that turf algae in general tends to grow quickly and does well under stressful conditions (Airoldi 1998). Similarly, fast recovery of other photosynthesizing species has also been observed in the invasive seagrass *Halophila stipulacea*, which saw a rapid recovery and expansion of coverage in Puerto Rico after Hurricane Maria (Hernández-Delgado et al. 2020). Conversely, the brown macroalgae *Dictyota* sp., a common species on tropical and subtropical reefs worldwide (Clerck et al. 2006; Bogaert et al. 2020), does not show similar trends of rapid expansion. Rather, almost a year after the hurricane impact, in the summer of 2018, the *Dictyota* sp. gains more coverage area. However, the following year, 2019, this coverage area is again reduced, while other species gain coverage area again. This indicates that the *Dictyota* sp. does not compete well against the brown turf algae. As successional changes begin to revert the community back towards previous diversity levels, the *Dictyota* sp. subsides as other species regain coverage.

Another reason as to why brown turf algae may have expanded its coverage to such great extents may be due the reduction in *Diadema antillarum* sea urchin. Based on the CCA from the macroinvertebrate count numbers, *D. antillarum* was found to be more abundant in 2017 before the hurricane impact, compared with the following survey time points. Acting as a key species grazing on algae, clearing space for other species to settle, *D. antillarum* is an important species on Caribbean reefs (Carpenter 1981). The adverse effects, including physical damage and demise, as a result of hurricane events can greatly reduce numbers of sessile macroinvertebrates, although *D. antillarum* abundances have shown some resilience in response to disturbance event such as hurricanes (Mumby et al. 2006). However, in this study there appears to be less *D. antillarum* present following Hurricane Maria, which is similar to trends observed in the Florida Keys after Hurricane Irma hit at the same time as Hurricane Maria (Simmons et al. 2021). The decline of *D. antillarum* in the survey site led to decreased restriction of brown turf algae by urchin grazing. Moreover, the distribution of keystone species, such as *D. antillarum* can have an impact of how the seep system community is composed. In this study the urchin is only found at a distance from the CO_2 seep in the parts of

the transects that display higher pH and lower pCO_2 measurements. Consequently, as turf algae is naturally suppressed through grazing mechanisms at coral reefs (Hughes et al. 2007), if *D. antillarum* is not present in closer proximity to the CO_2 seep system, clearing space for corals and other species through grazing will not occur close to the seep. A similar trend of urchin absence near a seep system in Italy has also been observed, where an urchin species is thought to be restricted from gracing near the seeps through the physiological limitation of the need to maintain acid-based homeostasis (Calosi et al. 2013a; Small et al. 2016). Low pH has been shown to cause high levels of carbonic acid in body fluids and tissues (Przeslawski et al. 2008; Fabry et al. 2008). Based on the separate CCA ordination plots from the different survey time points, *D. antillarum* shows slight aversion from the pCO_2 gradient, which coincides with observation that the urchin is only found at a distance of 19m or more from the CO_2 seep site.

The almost complete appropriation of coverage is observed by the brown turf algae reduces the chances for other species already present in the area to resettle or gain coverage again, while also reducing the chances of new species to settle in the area. Interestingly, in 2007 a survey investigating the abundance of species along the western coast of Dominica did not find any *Gorgonia* sp. present in Champagne Bay (Steiner et al. 2007), However, in this study several individuals of *Gorgonia* sp. were recorded along the southern-going transect. Settlement of new species may not occur if the coverage is completely dominated by a few species. Furthermore, if future circulation patterns change dramatically, such settlements of new species may not be as easily facilitated, as oceanic circulations drive larvae propagation (Harley et al. 2006). The condy anemony, *Condylactylis gigantea*, was only present in 2017, and had prior to that not been observed in the project study area (Pers. comm. Helen Rastrick at IMR, 2021), but following the hurricane impact, the species was not observed again in any of the survey transects.

The sponge *Aplysina fistularis* was observed regularly across all of the survey time points in most of the transects. It was recorded in close proximity to the CO_2 seep, as well as towards the end of the transects. Reduction of coverage area and of 3D structure was observed for the species following the hurricane event, however, commencement of recovery occurred in the summer of 2018 and 2019. Thus, *A. fistularis* appears to be somewhat species tolerant to both OA and storm events. This may owe to the fact that *A. fistularis* is a sponge that utilizes silica for their spicules. Siliceous sponges thought to be more resilient to OA (Bell et al. 2013; Vicente et al. 2016). In Papua New Guinea siliceous spicules did not reduce along the pH gradient (Fabricius et al. 2011).

4.3.3 Future community composition in marine costal environments of Dominica

Ocean acidification and other climatic drivers will change the community composition of shallow marine communities of Dominica. Research conducted of marine communities near other CO_2 seep sites suggests that encrusting-type corals may do better in the future (Fabricius et al. 2011). In Champagne Bay the encrusting corals of *Porites asteroids* and the firecoral *Millepora* sp. do well, also after the hurricane impact. One reason for this may be due to the fact that encrusting corals have thicker tissue (Loya et al. 2001). Notably, a reduction of 3D structure was observed due to physical damage caused by Hurricane Maria, although such

observations were non-quantifiable with the survey technique of this study. Another coral which may play a more important part in future reef architecture are the coral of genus *Montastraea*, such as *Montastraea cavernosa* in Champagne Bay, which is becoming an increasingly more dominant species at reefs cross the Caribbean region (Perry et al. 2013). The shift towards *Montastraea* corals can be advantageous for the complexity of coral reefs, as the genus tends to facilitate reef complexity (Alvarez-Filip et al. 2011). Note that the species *Orbicella faveloata* and *Orbicella annularis* previously belonged to the genus *Montastraea* (Budd et al. 2012), and can therefore be considered of equal importance for reef structure. *Orbicella faveloata* has been found to have an increased bleaching resistance, relating to the species of the symbiotic algae (Manzello et al. 2019), may therefore have a better change at persisting in the face of OA. Additionally, as mentioned above, both the genus *Montastraea* and *Porites* have been found to be more resistant to OA through fatty acid accretion from their zooxanthella (Teece et al. 2011). Indeed, also at vent systems of neighboring islands were *O. faveloata*, *M. cavernosa* and *P. asteroides* found in areas that experience periods of increased acidification (Enochs et al. 2020). Therefore, corals of these two genera may become vital species in future reefs in Dominica. Interestingly, the sea fans of the *Gorgonia* sp. survived the hurricane without major losses, despite having a structure that would suggest otherwise. Phase shifts away from scleractinian corals that build 3D environments towards a community consisting of more soft corals and macroalgae has become more commonplace, particularly in the Caribbean region (Roff and Mumby 2012). However, although the *Gorgonia* sp. did well in response to the hurricane impact, the species does not appear to do well with OA.

Furthermore, sponges have been predicted to become more prevalent in future marine coastal communities (Bell et al. 2018), and do play important ecological roles (Diaz and Rützler 2001). However, although sponges may thrive as coral reefs deteriorate, also they will eventually be impacted by the same issues that corals face (Rützler 2004). Of the four sponge species that do well in this study, *A. fistularis* is likely to become the most prominent species in future community compositions of Dominica based on the tolerance to OA, as well as the rate of recovery observed in this study. However, most of the coverage could end up being covered by brown turf algae in response to increasing pCO_2 measurements. The appropriation of coverage area by brown turf algae functions as a simplification mechanism also for the macroalgal composition in the community (Harvey et al. 2021). High dominance of brown turf algae in high pCO_2 environments lead to decreased biomass, diversity and complexity of the community, with a lack of other macroalgal species, thus leading to an overall simplification occurring also within macroalgal assemblages (Harvey et al. 2021).

Dominica will likely endure a simplification of their marine coastal communities, as diversity will decrease in response to climatic stressors. Issues arise with simplification of marine ecosystems. Biodiversity is often measured in species richness in ecological studies, and often relates to the quality and stability of the ecosystem or community being described (Worm et al. 2006). Reduced richness leads to overall reduction in ecosystem functioning (Törnroos et al. 2015, Worm et al. 2006). Thus, the marine communities may no longer serve the same benefits should they endure severe simplification. Moreover, it is not only OA and hurricanes that will impact the marine life in the future. Increasing atmospheric CO_2 is also associated

with increasing temperatures, as well as decreases in dissolved oxygen concentrations (Gruber 2011). Marine communities across the globe will all be impacted by these three factors of OA, warming and decreasing dissolved oxygen, with regional differences (Gruber 2011). Furthermore, OA and ocean warming can be viewed as irreversible events, as it may take centuries to recover back to current-day levels (Gruber 2011), by which time it may be too late for several of the prevalent species in present oceans. Certainly, it can be speculated that coral reefs may not persist in future oceans, as corals may be rendered non-functional by 2050 should global atmospheric CO_2 emissions exceed 480ppm (Hoegh-Guldberg et al. 2007).

As stated in De'ath et al. (2012) regional policies cannot protect coral reefs from the global impact of anthropogenic driven climate change. Protection of coral reefs should be focused onto reefs of high complexity, as these tend to support more species diversity (Alvarez-Filip et al. 2011). Such reefs may be recognized by key species, such as the common *Montastraea* (Alvarez-Filip et al., 2011). Ecosystem-based approaches to protection may serve as the best strategy to sustain marine ecosystems (Keller et al. 2009). Additionally, restoring keystone species that serve important ecological roles on coral reefs, such as *D. antillarum*, can be an efficient and cost-effective strategy to implement (Precht and Precht 2015). Moreover, management such as implementation of non-dive zones and no-take zones, does in general allow for more healthy reefs (Graham et al. 2020). Establishing management practices of reefs can help mitigate some of the climate change challenges, such as food security. Notably, densities of reef fish, and consequently the associated fisheries, were strongly impacted by the tropical storm Erica in 2015 and Hurricane Maria in 2017 (Pinnegar et al. 2019). Additionally, prospects of acclimatization or adaptation should be considered for species persistence in the face of climate change. However, if such adaptations occur rapidly enough to allow for maintenance of ecosystem function and services remains unclear (Sunday et al. 2014). In light of the findings of this study, the additive impact of changes in two environmental drivers may cause such stress, that such adaptation may not take place as species will struggle to just stay alive.

4.4 Experimental design and future directions

4.4.1 Photo-quadrant methodology

In this study a time series of photo-quadrant were analysed to determine the impact of two environmental stressors on benthic community coverage. This method is widespread in the field of ecology. Application of photo-quadrant has been used to determine coral coverage, and can also be used to investigate recruitment, growth and mortality (Jokiel et al., 2015).
A known concern associated with photo-quadrat analyses is addressing cryptic or rare species. To combat this, is has been found that when combining photo-quadrat analyses with field observations of more rare or uncommon species, issues with identification may be avoided (Preskitt, Vroom & Smith, 2004). However, this requires the employment of skilled researchers with knowledge of rare or cryptic species specific to the region. This requires that research projects are funded properly to allow for the engagement of experts, which is often uncommon. Therefore, as species identification in this study is based on photo-quadrats of medium resolution, some erroneous identification issues could be present in the dataset. Another issue

with photo-quadrat surveys is the time it takes to process the material. Despite being a relatively inexpensive method that requires little equipment and is easy to conduct in the field, photo-quadrat surveys are time consuming in work, as the videos/photos obtained from the survey must be analysed. In some cases, as with this study, the grid must be added manually, which is also a very time consuming work. However, in recent years more photographic analysis software has been developed to make photo-quadrat grid analyses more effortless to conduct, such as the software photoQuad (see Trygonis & Sini, 2012). Additionally, some software may also help with issues of identification, for example by offering colour-correcting features. Application of such software may allow for faster data analysis, while also reducing the chance of erroneous species identifications.

Determining 3D loss of species that act as structural habitat builders was not in the scope of this study. Although analysis of 3D structure loss could have provided further insight into how the hurricane impacted the species across the time series, this would have required additional equipment as well as time to obtain such data. Standard photo quadrants are recorded at a 90^{o} angle down towards the substrate. To be able to determine 3D structures of species, the camera is typically angled at 45^{o} towards the substrate. Other methods include utilizing artificial intelligence (AI) systems, which can provide a cost-effective approach with about 97% identification certainty (González-Rivero et al. 2020). The inclusion of such technology could have allowed for assessment of how different growth forms of species may be impacted by extreme weather events or physical consequences of OA, such as bioerosion. Moreover, application of 3D approaches could have allowed for further understanding of the synergistic impacts of how these two environmental drivers act.

4.4.2 Using CO_2 seeps as natural analogues of ocean acidification

CO_2 seep systems are not perfect analogues. Some CO_2 seeps are subjected to variability to variability of pH and pCO_2 levels (Kerrison et al., 2011). In some areas variability of pH is related great fluxes of acidification rates relating to tidal changes near the CO_2 seep systems, resulting in extended periods of high acidification as observed in Enochs et al. (2020) and Inoue et al. (2013). Moreover, some sites near CO_2 seeps have been found to show similar diel variation in pH as is common in ambient coastal waters (Kerrison et al., 2011). Diel variation of current-day pH levels has been observed to impact coral growth (Enochs et al. 2018). Notably, in this study the ranges of temperature, salinity and total alkalinity did not show any variability between measurements gathered in March of 2018 compared with environmental variables from the other survey time pints. In general, CO_2 seep systems are viewed as suitable for studies wanting to engage natural laboratories for investigating OA (Kerrison et al. 2011), but variability of pH and pCO_2 measurements should be considered for choice of study area, as well as diel variation in other variables. In this study, the survey location was chosen specifically due to the little variation of other environmental parameters.

4.4.3 Data Analysis

Notably, the models used in this survey are at risk of being too liberal. Spatial autocorrelation is the assumption that closeness in spatial scales will cause more similarities of measured units, while distance between measured units will cause these units to diverge more. In this survey,

the experimental design is compromised by the use of transects extending in many directions from point zero. Consequently, the measured quadrats that are closer to the CO_2 seep are also closer together, compared with the transects that are measured at the end of the transects. In other words, following autocorrelation theory, all quadrats at 1m away from the seep will be more similar to one another, as the distance between these quadrats is much smaller. Opposingly, all quadrats at 30m away from the seep will be further away from each other and will therefore be more dissimilar from one another. Signs of autocorrelation was observed for the LMs and the GLMs. For example, underdispersion was detected during explorative analyses of the data. This was attempted to be corrected for by including a quasi-Poisson distribution term in the model. For the multivariate analyses, testing for spatial autocorrelation is not achievable by any feasible methods, and was therefore excluded from the analysis. Because of this, the statistical results from this study should be treated with caution.

In the fitted multivariate models that used species coverage data, the species data was arcsine transformed. Although it has been suggested to discontinue the use of arcsine transformations (Warton & Hui, 2011), the application of arcsine-based transformation may be more appropriate when the data is analysed in a multivariate analysis. The advantage when using arcsine-based transformations, is that it stabilizes variance and does not require continuous correction for zero counts (Lin & Xu, 2020). Comparatively, a log transformation, which is preferred for linear regressions, where values of negative infinity will occur when a species is not present (0% coverage), and positive infinity will arise when a sample consist of only one species (100% coverage). Therefore, applying an arcsine transformation was deemed suitable for the purposes of this study.

Because the macroinvertebrate count data only consisted of seven species, one multivariate model was selected to view the impact of the explanatory variables, as opposed to fitting seven separate GLMs with quasi-Poisson distribution. Conversely, to view the community change occurring in each survey time point, separate multivariate analyses were made for each survey time point to display the community composition. Another way the multivariate analyses could have been conducted would have been to separate out groups of species based on functional role or taxa. In a study preformed in the Florida Keys the response variable of the fitted CCA model was hard coral coverage, with macroalgae, sponge coverage and environmental drivers as response variables (Maliao et al. 2008). However, as this study aimed to determine the community response to two stressors, all species were fitted as response variables in the models fitted in this study. However, it is conceivable that due to the high coverage of brown turf algae in the study area, it is likely be a strong predictor of coral coverage.

It is generally desirable to fit models with as few explanatory variables as possible, as to avoid overfitting of the model. At the same time, conventional model selection methods, for example based on AIC and AIC weights, tend to favour models that include multiple variables over those that include fewer variables, causing overfitted models to be selected. The models of this study were all fitted with few explanatory variables. Based on the correlation between variables that was observed, many of the environmental variables showed correlation. Because this survey wanted to investigate the impact of pCO_2 on the species, it was chosen in favour of the

other correlated variables. Temperature and salinity were excluded based on biological reasoning. As these two variables show a very narrow range, the biological impact of these two variables was considered to have little influence on the species present along the transects. Although, it should be mentioned that temperature is predicted to increase to about 31C°, which is the thermal maxima for several species. Based on the reasons listed above, model selection was based on biological reasoning as opposed to utilizing conventional model selection techniques.

4.4.4 Future studies

To gain further understanding of how storms and other extreme weather events affect ecosystems, long-term observations and studies conducted in various types of ecosystems across spatial and temporal scales are required (Jentsch, Kreyling & Beierkuhnlein, 2007). Research investigating the impact of multiple climatic drivers are required to allow for implementing policies that can protect vulnerable habitats, or habitats that provide specific ecosystem functions and services of importance. For marine communities to persist in the future, knowledge of how communities and ecosystems respond to multiple environmental drivers must be obtained (Riebesell & Gattuso, 2014). Moreover, understanding single organism or collective communities capacities to adapt to these predicted changes will be key (Riebesell & Gattuso, 2014; Chevin, Lande & Mace, 2010). Few corals and sponges show the potential do adapt to predicted changes at a rate fast enough to keep up with the predicted rate of climate change. Additionally, although acclimatization can facilitate adaptation by allowing time for adaptation to take place (Chevin, Lande & Mace, 2010), but acclimatization may also be costly for species that are driven to their limits through acclimatization (Calosi et al. 2013b).

Researching how climate change will impact communities and ecosystems across a range of local and regional scales can become important, as local variation and site-specific nature may impact modelling results if not a wide range of ecosystems are presented (Ummenhofer & Meehl, 2017). For example, changes in ambient pCO_2 levels will not be globally uniform, and is dependent on the levels of future GHG emissions (IPCC, 2014; Gallego et al., 2018). Therefore, investigations of climatic impact should occur across all latitudes.

Investigating the effects of multiple environmental drivers on marine environments remains a gap in investigating the impacts of future climate change (Ribersell & Gattuso, 2014), and few studies have investigated the long-term effects of multiple climatic drivers. Yet, research focusing on multiple environmental drivers can result in essential information regarding the future of marine communities. Few studies have investigated the long-term effects of multiple climatic drivers on community or ecosystem, with the exception of ocean acidification and temperature (e.g. Duckworth et al. 2012). Challenges of investigating community or ecosystem responses to multiple stressors is the accessibility to natural communities in environments that can be exposed to several environmental stressors. The application of CO_2 seep systems in investigating OA is limited to one climatic driver, and therefore limited knowledge can be gained with regards to future oceans (Ribersell & Gattuso, 2014). However, in certain areas these natural gradients may be subjected to other environmental drivers also, as with the survey area of this study. The results of this study provides further knowledge of how the synergistic

effect of a hurricane impact impacts the community structure of a naturally acidified environment. However, usually, gradient analyses such as the one preformed in this study are limited to one stressor, and only because of the sampling location was this study able to investigate the impact of two climatic stressors on a shallow marine community.

There are several approaches to investigating the impact of multiple drivers. One such approach is using a collection of mosaic across multiple stressors. By applying a mosaic approach created by overlapping abiotic environmental gradients, several climatic drivers can be investigated simultaneously. As multiple climatic drivers in the ocean are predicted to change concurrent with one another, multiple stressor mosaics will drive environmental change (Gibson-Reinemer & Rahel, 2015). Multivariate mosaics can occur through inconsistencies in abiotic and biotic drivers, causing local differences in conditions for species to perform in (Kroeker et al., 2016). Already mosaics investigating the impact of multiple climatic stressors have been conducted, finding an increase in mosaic complexity, suggesting that the mosaic composure of future marine environments can act as both barriers and facilitators of species distribution in the future (Laughlan & Nagelkerken, 2019). Other studies have demonstrated the need for knowledge of how interactions of environmental mosaics can drive intraspecies differences (Kroeker et al., 2016).

Additionally, with advances in technology, new methods may be developed and become more available for common use in research. Environmental DNA (eDNA) is a technique that can be applied both for research purposes as well as for conservation (Thomsen & Willerslev, 2015) and management use (Gilbey et al., 2020). eDNA is a method that samples the DNA present in the water column. The use of eDNA has been proposed to facilitate reconstruction of marine food webs in response to increasing changes in climatic drivers (D'Alessandro & Mariani, 2021), and for conducting biodiversity surveys (Shaw, Weyrich & Cooper, 2015). The use of eDNA can reveal biodiversity changes relating seasons, and may also be useful in detecting biodiversity presence before and after extreme weather events occur (Berry et al., 2019).

4.5 Concluding remarks

The goal of this study was to investigate the combined impact of two environmental stressors related to anthropogenic driven climate change, namely ocean acidification and impact by storms on a Caribbean coral reef community. The results indicate that overall, a simplification is observed in response to ocean acidification, comparative to results found in seeps systems in Japan (Agostini et al., 2021). A community shift in favour of macroalgae was observed as proximity with the CO_2 seep system increases. The hurricane event caused a decrease in diversity, with less species being present in the transects, although this effect was mainly observed in the latter part of the transects. The synergistic effect of the hurricane and OA led to a simplification effect. However, the species composition near the seep site endures less of a simplification compared to the species composition further away from the CO_2 seep due to the creation of a more homogenous environment caused by OA. This might indicate that the impact of storm events, such as Hurricane Maria, may have less of an effect in the future when simplification has already occurred consequential to ocean acidification. In other words, the species that show less impact by ocean acidification are the same species that are not gravely

affected by the hurricane impact. Both sponge and coral coverage showed a slower recovery rate near the seep site, suggesting that recovery is limited by the low pH and high pCO_2 measurements surrounding the CO_2 seep. The findings of this study concur with other research of community shifts in response to natural pCO_2 gradients. Furthermore, the study illustrates the need for more research investigating the combined effect of multiple climatic stressors on marine communities, which is an issue that has been addressed by others

4.5.1 Global perspective

Although this study was conducted in a tropical region, the results of this study demonstrate the same trends as observed in other studies (Hall-Spencer et al. 2008; Fabricus et al. 2011; Sunday et al., 2017), indicating that community shifts away from calcifying species and towards macroalgae can be applied to an extensive range of ecosystems. As of yet, studies of natural analogues in the Arctic region have not yet been investigated, although there is a potential for commencing such reseach (Rastrick et al. 2018). Gaining knowledge of how marine communities of the Artic respond to climate change is integral for understanding how these ecosystems and communities will respond to climate change. The Arctic region is predicted to experience a higher frequency of storms, as well as a strong impact of OA (IPCC, 2014; IPCC, 2021). Cold water corals are also important species contributing to habitat formation, and are through to be at risk of OA (Roberts et al. 2006), although the calcification rate might not be impacted by predicted pCO_2 levels (Maier et al. 2013). Additionally, temperate water corals already have a lower metabolic rate and growth rate (Holcomb, McCorkle & Cohen, 2009; Rodolfo-Metalpa et al., 2010) (Holcomb et al. 2010; Rodolfo-Metalpa et al. 2011), and may therefore not experience the impacts fluctuations in oceanic chemistry as strongly as tropical corals (Jokiel 2011). However, considering that the impacts of OA will be most dominant in the higher latitudes (Gruber 2011; IPCC 2014), and the combined effect of changing patterns of other climatic stressors, also these corals cannot be expected to do well. Moreover, extreme weather events such as coastal storms do not only impact the shallow marine communities, but are also found to have an impact in deep-sea ecosystems (Sanchez-Vidal et al. 2012). Such storm events may cause sequestration due to transportation of organic carbon from shallow waters to the deep sea, leading to abrasion or burying of benthic species (Sanchez-Vidal et al., 2012).

Research into responses of communities along natural pCO_2 gradients can also be viewed in light of carbon capture and storage projects. Currently, the impacts of climate change as a result of persistent anthropogenic release of GHG are predicted to be large (IPCC, 2021). To minimize the consequences of anthropogenic forcing, carbon capture and storage is now posed as a mitigating solution to reduce the effects of climate change (IPCC, 2021). However, the long-term biological consequences of carbon storage are not yet known. One of the most hazardous consequence of carbon storage could be leakage from the storage areas (e.g. Goulding et al. 2017). Should the deep-sea community respond similarly to the community observed in this study, a simplification could occur in response to leakage events. Importantly, deep-sea ecosystem functioning and services, as well as the community dynamics remain somewhat unexplored, with little knowledge of responses to climate change.

References

Agostini, S., Harvey, B.P., Milazzo, M., Wada, S., Kon, K., Floc, N., Mayumi, K., and Hall-, J.M. 2021. Simplification , not " tropicalization ", of temperate marine ecosystems under ocean warming and acidification. **00**: 1–14. doi:10.1111/gcb.15749.

Agostini, S., Wada, S., Kon, K., Omori, A., Kohtsuka, H., Fujimura, H., Tsuchiya, Y., Sato, T., Shinagawa, H., Yamada, Y., and Inaba, K. 2015. Geochemistry of two shallow CO2 seeps in Shikine Island (Japan) and their potential for ocean acidification research. Reg. Stud. Mar. Sci. **2**: 45–53. Elsevier. doi:10.1016/j.rsma.2015.07.004.

Airoldi, L. 1998. Roles of Disturbance, sediment stress, and substratum retention on spatial dominance in algal turf. Ecology **79**(8): 2759–2770. doi:10.1890/0012-9658.

Akaike, H. 1998. Information Theory and an Extension of the Maximum Likelihood Principle. *In* Selected Papers of Hirotugu Akaike. Springer Series in Statistics (Perspectives in Statistics). *Edited by* E. Parzen, K. Tanabe, and G. Kitagawa. Springer, New York, NY. pp. 199–213. doi:10.1007/978-1-4612-1694-0_15.

Albright, R., and Langdon, C. 2011. Ocean acidification impacts multiple early life history processes of the Caribbean coral Porites astreoides. Glob. Chang. Biol. **17**(7): 2478–2487. John Wiley & Sons, Ltd. doi:10.1111/J.1365-2486.2011.02404.X.

Allemand, D., Tambutté, É., Zoccola, D., and Tambutté, S. 2011. Coral Calcification, Cells to Reefs. *In* Coral Reefs: An Ecosystem in Transition. *Edited by* Z. Dubinsky and N. Stambler. Springer, Dordrecht. pp. 119–150. doi:10.1007/978-94-007-0114-4_9.

Alvarez-Filip, L., Dulvy, N.K., Côte, I.M., Watkinson, A.R., and Gill, J.A. 2011. Coral identity underpins architectural complexity on Caribbean reefs. Ecol. Appl. **21**(6): 2223–2231. doi:DOI: 10.2307/41416650.

Andersson, A.J., Mackenzie, F.T., and Bates, N.R. 2008. Life on the margin: implications of ocean acidification on Mg-calcite, high latitude and cold-water marine calcifiers. Mar. Ecol. Prog. Ser. **373**: 265–273. doi:10.3354/MEPS07639.

Anthony, K.R.N., Kline, D.I., Diaz-Pulido, G., Dove, S., and Hoegh-Guldberg, O. 2008. Ocean acidification causes bleaching and productivity loss in coral reef builders. Proc. Natl. Acad. Sci. U. S. A. **105**(45): 17442–17446. National Academy of Sciences. doi:10.1073/pnas.0804478105.

Ashur, M.M., Johnston, N.K., and Dixson, D.L. 2017. Impacts of Ocean Acidification on Sensory Function in Marine Organisms. Integr. Comp. Biol. **57**(1): 63–80. Oxford Academic. doi:10.1093/ICB/ICX010.

Barkley, H.C., Cohen, A.L., Golbuu, Y., Starczak, V.R., DeCarlo, T.M., and Shamberger, K.E.F. 2015. Changes in coral reef communities across a natural gradient in seawater pH. Sci. Adv. **1**(5): e1500328. American Association for the Advancement of Science. doi:10.1126/sciadv.1500328.

Bartoń K. 2020. MuMIn: Multi-Model Inference. R package version 1.43.17. https://CRAN.R-project.org/package=MuMIn

Baumann, H., Talmage, S.C., and Gobler, C.J. 2011. Reduced early life growth and survival in a fish in direct response to increased carbon dioxide. Nat. Clim. Chang. **2**(1): 38–41. Nature Publishing Group. doi:10.1038/nclimate1291.

Beaubien, S.E., Ciotoli, G., Coombs, P., Dictor, M.C., Krüger, M., Lombardi, S., Pearce, J.M., and West, J.M. 2008. The impact of a naturally occurring CO2 gas vent on the shallow ecosystem and soil chemistry of a Mediterranean pasture (Latera, Italy). Int. J. Greenh. Gas Control **2**(3): 373–387. Elsevier. doi:10.1016/j.ijggc.2008.03.005.

Bell, J.J., Bennett, H.M., Rovellini, A., and Webster, N.S. 2018. Sponges to Be Winners under Near-Future Climate Scenarios. Bioscience **68**(12): 955–968. Oxford Academic. doi:10.1093/BIOSCI/BIY142.

Bell, J.J., Davy, S.K., Jones, T., Taylor, M.W., and Webster, N.S. 2013. Could some coral reefs become sponge reefs as our climate changes? Glob. Chang. Biol. **19**(9): 2613–2624. John Wiley & Sons, Ltd. doi:10.1111/GCB.12212.

Bellwood, D.R., and Hughes, T.P. 2001. Regional-Scale Assembly Rules and Biodiversity of Coral Reefs. Science. **292**(5521): 1532–1535. American Association for the Advancement of Science. doi:10.1126/SCIENCE.1058635.

Bender, M.A., Knutson, T.R., Tuleya, R.E., Sirutis, J.J., Vecchi, G.A., Garner, S.T., and Held, I.M. 2010. Modeled impact of anthropogenic warming on the frequency of intense Atlantic hurricanes. Science. **327**(5964): 454–458. American Association for the Advancement of Science. doi:10.1126/science.1180568.

Bogaert, K.A., Delva, S., and De Clerck, O. 2020. Concise review of the genus Dictyota J.V. Lamouroux. J. Appl. Phycol. **32**(3): 1521–1543. Springer. doi:10.1007/S10811-020-02121-4.

Bornhold, B.D., and Milliman, J.D. 1973. Generic and Environmental Control of Carbonate Mineralogy in Serpulid (Polychaete) Tubes. J. Geol. **81**(3): 363–373. University of Chicago Press. doi:10.1086/627876.

Ter Braak, C.J.F. 1986. Canonical Correspondence Analysis: A New Eigenvector Technique for Multivariate Direct Gradient Analysis . Ecology **67**(5): 1167–1179. Available from http://links.jstor.org/sici?sici=0012-9658%28198610%2967%3A5%3C1167%3ACCAANE%3E2.0.C0%3B2-U [accessed 30 August 2021].

Brown, D., and Blake, E. 2017. Hurricane Maria Tropical Cyclone Update Report. Available from https://www.nhc.noaa.gov/archive/2017/al15/al152017.update.09182345.shtml [accessed 26 August 2021].

Brown, N.E.M., Milazzo, M., Rastrick, S.P.S., Hall-Spencer, J.M., Therriault, T.W., and Harley, C.D.G. 2017. Natural acidification changes the timing and rate of succession, alters community structure, and increases homogeneity in marine biofouling communities. Glob. Chang. Biol. **24**(1): e112–e127. doi:10.1111/gcb.13856.

Bruno, J.F., Selig, E.R., Casey, K.S., Page, C.A., Willis, B.L., Harvell, C.D., Sweatman, H., and Melendy, A.M. 2007. Thermal Stress and Coral Cover as Drivers of Coral Disease Outbreaks. PLOS Biol. **5**(6): e124. Public Library of Science. doi:10.1371/JOURNAL.PBIO.0050124.

Budd, A.F., Fukami, H., Smith, N.D., and Knowlton, N. 2012. Taxonomic classification of the reef coral family Mussidae (Cnidaria: Anthozoa: Scleractinia). Zool. J. Linn. Soc. **166**(3): 465–529. Oxford Academic. doi:10.1111/J.1096-3642.2012.00855.X.

Burke, L., Reytar, K., Spalding, M., and Perry, A. 2011. Reefs at Risk: Revisited. World Resources Institute.

Byrnes, J.E., Reed, D.C., Cardinale, B.J., Cavanaugh, K.C., Holbrook, S.J., and Schmitt, R.J. 2011. Climate-driven increases in storm frequency simplify kelp forest food webs. Glob. Chang. Biol. **17**(8): 2513–2524. John Wiley & Sons, Ltd. doi:10.1111/J.1365-2486.2011.02409.X.

Caldeira, K., and Wickett, M. 2005. Ocean model predictions of chemistry changes from carbon dioxide emissions to the atmosphere and ocean. J. Geophys. Res. C Ocean. **110**(9): 1–12. doi:10.1029/2004JC002671.

Caldeira, K., and Wickett, M.E. 2003. Anthropogenic carbon and ocean pH. Nature **425**(6956): 365. Nature Publishing Group. doi:10.1038/425365a.

Calosi, P., Rastrick, S.P.S., Graziano, M., Thomas, S.C., Baggini, C., Carter, H.A., Hall-Spencer, J.M., Milazzo, M., and Spicer, J.I. 2013a. Distribution of sea urchins living near shallow water CO2 vents is dependent upon species acid-base and ion-regulatory abilities. Mar. Pollut. Bull. **73**(2): 470–484. doi:10.1016/j.marpolbul.2012.11.040.

Calosi, P., Rastrick, S.P.S., Lombardi, C., de Guzman, H.J., Davidson, L., Jahnke, M., Giangrande, A., Hardege, J.D., Schulze, A., Spicer, J.I., and Gambi, M.C. 2013b. Adaptation and acclimatization to ocean acidification in marine ectotherms: An in situ transplant experiment with polychaetes at a shallow CO2 vent system. Philos. Trans. R. Soc. B Biol. Sci. **368**(1627). doi:10.1098/rstb.2012.0444.

Cantin, N.E., Cohen, A.L., Karnauskas, K.B., Tarrant, A.M., and McCorkle, D.C. 2010. Ocean Warming Slows Coral Growth in the Central Red Sea. Science. **329**(5989): 322–325. American Association for the Advancement of Science. doi:10.1126/SCIENCE.1190182.

Cardoso, P.G., Raffaelli, D., Lillebø, A.I., Verdelhos, T., and Pardal, M.A. 2008. The impact of extreme flooding events and anthropogenic stressors on the macrobenthic communities' dynamics. Estuar. Coast. Shelf Sci. **76**(3): 553–565. Academic Press. doi:10.1016/J.ECSS.2007.07.026.

Carpenter, R.C. 1981. Grazing by Diadema antillarum (Philippi) and its effects on the benthic algal community [Sea urchin damage]. J. Mar. Res. **49**(4): 749–765. Available from https://agris.fao.org/agris-search/search.do?recordID=US19830853749 [accessed 30 August 2021].

Cigliano, M., Gambi, M.C., Rodolfo-Metalpa, R., Patti, F.P., and Hall-Spencer, J.M. 2010. Effects of ocean acidification on invertebrate settlement at volcanic CO2 vents. Mar. Biol. 2010 15711 **157**(11): 2489–2502. Springer. doi:10.1007/S00227-010-1513-6.

Clerck, O. De, Leliaert, F., Verbruggen, H., Lane, C.E., Paula, J.C. De, Payo, D.A., and Coppejans, E. 2006. A Revised Classification of the Dictyoteae (Dictyotales, Phaeophyceae) Based on rbcL and 26S Ribosomal DNA Sequence Analyses. J. Phycol. **42**(6): 1271–1288. John Wiley & Sons, Ltd. doi:10.1111/J.1529-8817.2006.00279.X.

Clermont, A. 2008. Study I: Distribution and abundance of selected Demospongiae in Dominica . ITME Reasearch Reorts **27**: 1–6. Available from http://www.itme.org/reports/ITME_RReports27a.pdf [accessed 24 March 2021].

Cohen, A.L., and Holcomb, M. 2009. Why corals care about ocean acidification uncovering the mechanism. Oceanography **22**(SPL.ISS. 4): 118–127. doi:10.5670/OCEANOG.2009.102.

Cole, C., Finch, A.A., Hintz, C., Hintz, K., and Allison, N. 2018. Effects of seawater pCO2 and temperature on calcification and productivity in the coral genus Porites spp.: an exploration of potential interaction mechanisms. Coral Reefs **37**(2): 471–481. Springer Verlag. doi:10.1007/S00338-018-1672-3.

Collard, M., Rastrick, S.P.S., Calosi, P., Demolder, Y., Dille, J., Findlay, H.S., Hall-Spencer, J.M., Milazzo, M., Moulin, L., Widdicombe, S., Dehairs, F., and Dubois, P. 2016. The impact of ocean acidification and warming on the skeletal mechanical properties of the sea urchin Paracentrotus lividus from laboratory and field observations. ICES J. Mar. Sci. **73**(3): 727–738. Oxford Academic. doi:10.1093/ICESJMS/FSV018.

Colvard, N.B., and Edmunds, P.J. 2010. Decadal-scale changes in abundance of non-scleractinian invertebrates on a Caribbean coral reef. J. Exp. Mar. Bio. Ecol. **397**: 153–160. doi:10.1016/j.jembe.2010.11.015.

Crook, E.D., Potts, D., Rebolledo-Vieyra, M., Hernandez, L., and Paytan, A. 2011. Calcifying coral abundance near low-pH springs: implications for future ocean acidification. Coral Reefs **31**(1): 239–245. Springer. doi:10.1007/S00338-011-0839-Y.

Cyronak, T., Schulz, K.G., and Jokiel, P.L. 2016. The Omega myth: what really drives lower calcification rates in an acidifying ocean. ICES J. Mar. Sci. **73**(3): 558–562. Oxford Academic. doi:10.1093/ICESJMS/FSV075.

Davies, S.W., Marchetti, A., Ries, J.B., and Castillo, K.D. 2016. Thermal and pCO2 Stress Elicit Divergent Transcriptomic Responses in a Resilient Coral. Front. Mar. Sci.: 112.

Frontiers. doi:10.3389/FMARS.2016.00112.
De'ath, G., Fabricius, K.E., Sweatman, H., and Puotinen, M. 2012. The 27–year decline of coral cover on the Great Barrier Reef and its causes. Proc. Natl. Acad. Sci. **109**(44): 17995–17999. National Academy of Sciences. doi:10.1073/PNAS.1208909109.
Diaz, M.C., and Rützler, K. 2001. Sponges: An essential component of Caribbean coral reefs. Bull. Mar. Sci. **69**(2): 535–546.
Dickson, A.G., and Millero, F.J. 1987. A comparison of the equilibrium constants for the dissociation of carbonic acid in seawater media. Deep Sea Res. Part A. Oceanogr. Res. Pap. **34**(10): 1733–1743. Elsevier. doi:10.1016/0198-0149(87)90021-5.
Doney, S.C., Fabry, V.J., Feely, R.A., and Kleypas, J.A. 2009. Ocean acidification: The other CO2 problem. Annual Reviews . **1**: 169-192 doi:10.1146/annurev.marine.010908.163834.
Doney, S.C., Ruckelshaus, M., Emmett Duffy, J., Barry, J.P., Chan, F., English, C.A., Galindo, H.M., Grebmeier, J.M., Hollowed, A.B., Knowlton, N., Polovina, J., Rabalais, N.N., Sydeman, W.J., and Talley, L.D. 2012. Climate Change Impacts on Marine Ecosystems. Ann. Rev. Mar. Sci. **4**(1): 11–37. Annual Reviews. doi:10.1146/annurev-marine-041911-111611.
Duckworth, A.R., West, L., Vansach, T., Stubler, A., and Hardt, M. 2012. Effects of water temperature and pH on growth and metabolite biosynthesis of coral reef sponges. Mar. Ecol. Prog. Ser. **462**: 67–77. Available from https://www.int-res.com/articles/meps2012/462/m462p067.pdf [accessed 16 August 2021].
Edmunds, P.J. 2019. Three decades of degradation lead to diminished impacts of severe hurricanes on Caribbean reefs. Ecology **100**(3): e02587. John Wiley & Sons, Ltd. doi:10.1002/ECY.2587.
Emanuel, K. 2007. Environmental factors affecting tropical cyclone power dissipation. J. Clim. **20**(22): 5497–5509. American Meteorological Society. doi:10.1175/2007JCLI1571.1.
EN 16260. 2012. Water quality - Visual seabed surveys using remotely operated and/or towed observation gear for collection of environmental data. Available from https://standards.iteh.ai/catalog/standards/cen/f2fda660-7904-4757-a72a-45d61d061593/en-16260-2012 [accessed 1 September 2021].
Enochs, I.C., Formel, N., Manzello, D., Morris, J., Mayfield, A.B., Boyd, A., Kolodziej, G., Adams, G., and Hendee, J. 2020. Coral persistence despite extreme periodic pH fluctuations at a volcanically acidified Caribbean reef. Coral Reefs **39**(3): 523–528. Springer. doi:10.1007/s00338-020-01927-5.
Enochs, I.C., Manzello, D.P., Jones, P.J., Aguilar, C., Cohen, K., Valentino, L., Schopmeyer, S., Kolodziej, G., Jankulak, M., and Lirman, D. 2018. The influence of diel carbonate chemistry fluctuations on the calcification rate of Acropora cervicornis under present day and future acidification conditions. J. Exp. Mar. Bio. Ecol. **506**: 135–143. Elsevier. doi:10.1016/J.JEMBE.2018.06.007.
Erez, J., Reynaud, S., Silverman, J., Schneider, K., and Allemand, D. 2011. Coral calcification under ocean acidification and global change. *In* Coral Reefs: An Ecosystem in Transition. Springer Netherlands. pp. 151–176. doi:10.1007/978-94-007-0114-4_10.
Fabricius, K.E., Langdon, C., Uthicke, S., Humphrey, C., Noonan, S., De'ath, G., Okazaki, R., Muehllehner, N., Glas, M.S., and Lough, J.M. 2011. Losers and winners in coral reefs acclimatized to elevated carbon dioxide concentrations. Nat. Clim. Chang. **1**(3): 165–169. Nature Publishing Group. doi:10.1038/nclimate1122.
Fabry, V.J., Seibel, B.A., Feely, R.A., and Orr, J.C. 2008. Impacts of ocean acidification on marine fauna and ecosystem processes. ICES J. Mar. Sci. **65**(3): 414–432. Oxford Academic. doi:10.1093/ICESJMS/FSN048.

Fitzer, S.C., Caldwell, G.S., Close, A.J., Clare, A.S., Upstill-Goddard, R.C., and Bentley, M.G. 2012. Ocean acidification induces multi-generational decline in copepod naupliar production with possible conflict for reproductive resource allocation. J. Exp. Mar. Bio. Ecol. **418**–**419**: 30–36. Elsevier. doi:10.1016/J.JEMBE.2012.03.009.

Gardner, T.A., Côté, I.M., Gill, J.A., Grant, A., and Watkinson, A.R. 2005. Hurricanes and Caribbean Coral Reefs: Impacts, recovery patterns, and role in long-term decline. Ecology **86**(1): 174–184. John Wiley & Sons, Ltd. doi:10.1890/04-0141.

Gauch, H.G. 1982. Multivariate analysis in community ecology. Cambridge University Press, Cambridge. ISBN: 9780511623332.

Glynn, P.W. 1991, June 1. Coral reef bleaching in the 1980s and possible connections with global warming. Elsevier Current Trends. doi:10.1016/0169-5347(91)90208-F.

Glynn, P.W. 1993. Coral Reefs Coral reef bleaching: ecological perspectives. Coral Reefs **12**: 1–17. doi:10.1007/BF00303779.

Gochfeld, D.J., Olson, J.B., Chaves-Fonnegra, A., Smith, T.B., Ennis, R.S., and Brandt, M.E. 2020. Impacts of Hurricanes Irma and Maria on Coral Reef Sponge Communities in St. Thomas, U.S. Virgin Islands. Estuaries and Coasts **43**: 1235–1247. doi:10.1007/s12237-020-00694-4.

Goldenberg, S.B., Landsea, C.W., Mestas-Nuñez, A.M., and Gray, W.M. 2001. The Recent Increase in Atlantic Hurricane Activity: Causes and Implications. Science. **293**(5529): 474–479. American Association for the Advancement of Science. doi:10.1126/SCIENCE.1060040.

González-Rivero, M., Beijbom, O., Rodriguez-Ramirez, A., Bryant, D.E.P., Ganase, A., Gonzalez-Marrero, Y., Herrera-Reveles, A., Kennedy, E. V., Kim, C.J.S., Lopez-Marcano, S., Markey, K., Neal, B.P., Osborne, K., Reyes-Nivia, C., Sampayo, E.M., Stolberg, K., Taylor, A., Vercelloni, J., Wyatt, M., and Hoegh-Guldberg, O. 2020. Monitoring of Coral Reefs Using Artificial Intelligence: A Feasible and Cost-Effective Approach. Remote Sens. 2020, Vol. 12, Page 489 **12**(3): 489. Multidisciplinary Digital Publishing Institute. doi:10.3390/RS12030489.

Goulding, T.A., De Orte, M.R., Szalaj, D., Basallote, M.D., DelValls, T.A., and Cesar, A. 2017. Assessment of the environmental impacts of ocean acidification (OA) and carbon capture and storage (CCS) leaks using the amphipod Hyale youngi. Ecotoxicology **26**: 521–533. doi:10.1007/s10646-017-1783-6.

Graham, N.A.J., Chong-Seng, K.M., Huchery, C., Januchowski-Hartley, F.A., and Nash, K.L. 2014. Coral Reef Community Composition in the Context of Disturbance History on the Great Barrier Reef, Australia. PLoS One **9**(7): e101204. Public Library of Science. doi:10.1371/JOURNAL.PONE.0101204.

Graham, N.A.J., Robinson, J.P.W., Smith, S.E., Govinden, R., Gendron, G., and Wilson, S.K. 2020. Changing role of coral reef marine reserves in a warming climate. Nat. Commun. **11**(1): 1–8. Nature Research. doi:10.1038/s41467-020-15863-z.

Green, D., Edmunds, P., and Carpenter, R. 2008. Increasing relative abundance of Porites astreoides on Caribbean reefs mediated by an overall decline in coral cover. Mar. Ecol. Prog. Ser. **359**: 1–10. doi:10.3354/meps07454.

Gruber, N. 2011. Warming up, turning sour, losing breath: ocean biogeochemistry under global change. Philos. Trans. R. Soc. A Math. Phys. Eng. Sci. **369**(1943): 1980–1996. The Royal Society Publishing. doi:10.1098/RSTA.2011.0003.

Guinotte, J.M., and Fabry, V.J. 2008. Ocean Acidification and Its Potential Effects on Marine Ecosystems. Ann. N.Y. Acad. Sci. **1134**: 320–342. doi:10.1196/annals.1439.013.

Hall-Spencer, J.M., Rodolfo-Metalpa, R., Martin, S., Ransome, E., Fine, M., Turner, S.M., Rowley, S.J., Tedesco, D., and Buia, M.C. 2008. Volcanic carbon dioxide vents show ecosystem effects of ocean acidification. Nature **454**(7200): 96–99. Nature Publishing

Group. doi:10.1038/nature07051.
Harley, C.D.G., Hughes, A.R., Hultgren, K.M., Miner, B.G., Sorte, C.J.B., Thornber, C.S., Rodriguez, L.F., Tomanek, L., and Williams, S.L. 2006, February 1. The impacts of climate change in coastal marine systems. John Wiley & Sons, Ltd. doi:10.1111/j.1461-0248.2005.00871.x.
Harmelin-Vivien, M. 1994. The Effects of Storms and Cyclones on Coral Reefs: A Review. J. Coast. Res. Spec. Issue No. 12. Coast. HAZARDS PERCEPTION, SUSCEPTIBILITY Mitig. (12): 211–231. Available from http://www.jstor.org/stable/25735600. [accessed 23 August 2021].
Harvey, B.P., Kon, K., Agostini, S., Wada, S., and Hall-Spencer, J.M. 2021. Ocean acidification locks algal communities in a species-poor early successional stage. Glob. Chang. Biol. **27**(10): 2174–2187. John Wiley & Sons, Ltd. doi:10.1111/GCB.15455.
Harvey, B.P., McKeown, N.J., Rastrick, S.P.S., Bertolini, C., Foggo, A., Graham, H., Hall-Spencer, J.M., Milazzo, M., Shaw, P.W., Small, D.P., and Moore, P.J. 2016. Individual and population-level responses to ocean acidification. Sci. Rep. **6**(February 2016). Nature Publishing Group. doi:10.1038/srep20194.
Hernández-Delgado, E.A., Toledo-Hernández, C., Ruíz-Díaz, & C.P., Gómez-Andújar, & N., Medina-Muñiz, J.L., Canals-Silander, M.F., and Suleimán-Ramos, & S.E. 2020. Hurricane Impacts and the Resilience of the Invasive Sea Vine, Halophila stipulacea: a Case Study from Puerto Rico. Estuaries & Coasts **43**: 1263–1283. doi:10.1007/s12237-019-00673-4.
Hernández, C.A., Sangil, C., and Hernández, J.C. 2016. A new CO2vent for the study of ocean acidification in the Atlantic. Mar. Pollut. Bull. **109**(1): 419–426. Elsevier Inc. doi:10.1016/j.marpolbul.2016.05.040.
Highsmith, R.C., Riggs, A.C., and Antonio, C.M. D'. 1980. Survival of Hurricane-Generated Coral Fragments and a Disturbance Model of Reef Calcification/Growth Rates. Oecologia (Berl.) **46**: 322–329.
Hill, M.O. 1973. Diversity and Evenness: A Unifying Notation and Its Consequences. Ecology **54**(2): 427–432. John Wiley & Sons, Ltd. doi:10.2307/1934352.
Hill, M.O., and Gauch, H.G. 1980. Detrended correspondence analysis: An improved ordination technique. Vegetatio **42**(1): 47–58. Springer. doi:10.1007/BF00048870.
Ho, D.T.K. 2020. Implications of Climate Change on Marine Biodiversity Phytoremediation View project Microplastic and Nanoplastic Pollution View project Implications of Climate Change on Marine Biodiversity. Glob. J. Agric. Soil Sci. **1**(1). doi:https://www.researchgate.net/publication/339916763.
Hoegh-Guldberg, O. 2011. Coral reef ecosystems and anthropogenic climate change. Reg. Environ. Chang. **11**(SUPPL. 1): 215–227. Springer. doi:10.1007/s10113-010-0189-2.
Hoegh-Guldberg, O., Mumby, P.J., Hooten, A.J., Steneck, R.S., Greenfield, P., Gomez, E., Harvell, C.D., Sale, P.F., Edwards, A.J., Caldeira, K., Knowlton, N., Eakin, C.M., Iglesias-Prieto, R., Muthiga, N., Bradbury, R.H., Dubi, A., and Hatziolos, M.E. 2007. Coral reefs under rapid climate change and ocean acidification. Science. 318(5857): 1737-1742). doi:10.1126/science.1152509.
Hoegh-Guldberg, O., Poloczanska, E.S., Skirving, W., and Dove, S. 2017, May 29. Coral reef ecosystems under climate change and ocean acidification. Front. Mar. Sci. 4:158. doi:10.3389/fmars.2017.00158.
Hoffmann, A., and Parsons, P. 1991. Evolutionary genetics and environmental stress. Oxford University Press. Available from https://agris.fao.org/agris-search/search.do?recordID=US201300695279 [accessed 24 August 2021].
Holcomb, M., McCorkle, D.C., and Cohen, A.L. 2010. Long-term effects of nutrient and CO2 enrichment on the temperate coral Astrangia poculata (Ellis and Solander, 1786). J.

Exp. Mar. Bio. Ecol. **386**(1–2): 27–33. Elsevier. doi:10.1016/j.jembe.2010.02.007.
Hönisch, B., Ridgwell, A., Schmidt, D.N., Thomas, E., Gibbs, S.J., Sluijs, A., Zeebe, R., Kump, L., Martindale, R.C., Greene, S.E., Kiessling, W., Ries, J., Zachos, J.C., Royer, D.L., Barker, S., Marchitto, T.M., Moyer, R., Pelejero, C., Ziveri, P., Foster, G.L., and Williams, B. 2012a. The Geological Record of Ocean Acidification. Science. **335**(6072): 1058–1063. American Association for the Advancement of Science. doi:10.1126/SCIENCE.1208277.
Hönisch, B., Ridgwell, A., Schmidt, D.N., Thomas, E., Gibbs, S.J., Sluijs, A., Zeebe, R., Kump, L., Martindale, R.C., Greene, S.E., Kiessling, W., Ries, J., Zachos, J.C., Royer, D.L., Barker, S., Marchitto, T.M., Moyer, R., Pelejero, C., Ziveri, P., Foster, G.L., and Williams, B. 2012b. The Geological Record of Ocean Acidification. Science. **335**(6072): 1058–1063. American Association for the Advancement of Science. doi:10.1126/SCIENCE.1208277.
Hughes, T.P., and Connell, J.H. 1999. Multiple stressors on coral reefs: A long -term perspective. Limnol. Oceanogr. **44**(3part2): 932–940. John Wiley & Sons, Ltd. doi:10.4319/LO.1999.44.3_PART_2.0932.
Hughes, T.P., Keller, B.D., Jackson, J.B.C., and Boyle, M.J. 1985. Mass mortality of the echinoid Diadema antillarum Philippi in Jamaica. Bull. Mar. Sci. **36**(2): 377–384. Available from https://www.researchgate.net/publication/262908451 [accessed 30 August 2021].
Hughes, T.P., Rodrigues, M.J., Bellwood, D.R., Ceccarelli, D., Hoegh-Guldberg, O., McCook, L., Moltschaniwskyj, N., Pratchett, M.S., Steneck, R.S., and Willis, B. 2007. Phase Shifts, Herbivory, and the Resilience of Coral Reefs to Climate Change. Curr. Biol. **17**(4): 360–365. Cell Press. doi:10.1016/J.CUB.2006.12.049.
Idjadi, J.A., and Edmunds, P.J. 2006. Scleractinian corals as facilitators for other invertebrates on a Caribbean reef. Mar. Ecol. Prog. Ser. **319**: 117–127. doi:doi:10.3354/meps319117.
Inoue, S., Kayanne, H., Yamamoto, S., and Kurihara, H. 2013. Spatial community shift from hard to soft corals in acidified water. Nat. Clim. Chang. **3**(7): 683–687. Nature Publishing Group. doi:10.1038/nclimate1855.
IPCC. 2013. Climate Change 2013: The Physical Science Basis. Contribution of Working Group I to the Fifth Assessment Report of the Intergovern- mental Panel on Climate Change. *Edited By*T.F. Stocker, D. Qin, G.-K. Plattner, M. Tignor, S.K. Allen, J. Boschung, A. Nauels, Y. Xia, V. Bex, and P.M. Midgley. Cambridge University Press, United Kingdom and New York, NY, USA. Available from https://www.researchgate.net/profile/Abha_Chhabra2/publication/271702872_Carbon_and_Other_Biogeochemical_Cycles/links/54cf9ce80cf24601c094a45e/Carbon-and-Other-Biogeochemical-Cycles.pdf.
IPCC. 2014. Climate Change 2014: Synthesis report. Contribution of Working Groups I, II, and III to the Fifth Assessment Report of the Intergovernmental Panel on Climate Change. *Edited By*Core Writing Team, R.K. Pachauri, and L.A. Meyer. Geneva, Switzerland. Available from http://www.ipcc.ch. [accessed 17 March 2021].
IPCC. 2021. Summary for Policymakers. *In* Climate Change 2021: The Physical Science Basis. Contribution of Working Group I to the Sixth Assessment Report of the Intergovernmental Panel on Climate Change. *Edited by* V. Masson-Delmotte, P. Zhai, A. Pirani, S.L. Connors, C. Péan, S. Berger, N. Caud, Y. Chen, L. Goldfarb, M.I. Gomis, M. Huang, K. Leitzell, E. Lonnoy, J.B.R. Matthews, T.K. Maycock, T. Waterfield, O. Yelekçi, R. Yu, and B. Zhou. Cambridge University Press. In Press.
Jackson, J., Donovan, M., Cramer, K., and Lam, V. 2014. Status and Trends of Caribbean Coral Reefs: 1970-2012. Gland, Switzerland.

Jiang, L.Q., Carter, B.R., Feely, R.A., Lauvset, S.K., and Olsen, A. 2019. Surface ocean pH and buffer capacity: past, present and future. Sci. Rep. **9**(1): 1–11. Nature Research. doi:10.1038/s41598-019-55039-4.

Jokiel, P.L. 2011. Ocean Acidifcation and Control of Reef Coral Calcification by Boundary Layer Limitation of Proton Flux. Bull. Mar. Sci. **87**(3): 639–657. doi:10.5343/bms.2010.1107.

Joseph, E.P., Frey, H.M., Manon, M.R., Onyeali, M.M.C., DeFranco, K., Metzger, T., and Aragosa, C. 2019. Update on the fluid geochemistry monitoring time series for geothermal systems in Dominica, Lesser Antilles island arc: 2009–2017. J. Volcanol. Geotherm. Res. **376**: 86–103. Elsevier B.V. doi:10.1016/j.jvolgeores.2019.03.010.

Keller, B.D., Gleason, D.F., McLeod, E., Woodley, C.M., Airamé, S., Causey, B.D., Friedlander, A.M., Grober-Dunsmore, R., Johnson, J.E., Miller, S.L., and Steneck, R.S. 2009. Climate change, coral reef ecosystems, and management options for marine protected areas. Environmental Management. **44**: 1069–1088. Springer. doi:10.1007/s00267-009-9346-0.

Kenkel, C.D., Moya, A., Strahl, J., Humphrey, C., and Bay, L.K. 2018. Functional genomic analysis of corals from natural CO_2 -seeps reveals core molecular responses involved in acclimatization to ocean acidification. Glob. Chang. Biol. **24**(1): 158–171. Blackwell Publishing Ltd. doi:10.1111/gcb.13833.

Keppel, E.A., Scrosati, R.A., and Courtenay, S.C. 2012. Ocean Acidification Decreases Growth and Development in American Lobster (Homarus americanus) Larvae. J. Northw. Atl. Fish. Sci **44**: 61–66. doi:10.2960/J.v44.m683.

Kerrison, P., Hall-Spencer, J.M., Suggett, D.J., Hepburn, L.J., and Steinke, M. 2011. Assessment of pH variability at a coastal CO2 vent for ocean acidification studies. Estuar. Coast. Shelf Sci. **94**(2): 129–137. Academic Press. doi:10.1016/j.ecss.2011.05.025.

Knutson, T.R., McBride, J.L., Chan, J., Emanuel, K., Holland, G., Landsea, C., Held, I., Kossin, J.P., Srivastava, A.K., and Sugi, M. 2010, March 21. Tropical cyclones and climate change. Nature Geoscience. **3**(3). Nature Publishing Group. doi:10.1038/ngeo779.

Kramer, K.L., Cotton, S.P., Lamson, M.R., and Walsh, W.J. 2016. Bleaching and catastrophic mortality of reef-building corals along west Hawai‘i island: findings and future directions. Proc. 13th Int. Coral Reef Symp. Honolulu: 219–230. Available from http://coralreefs.org/wp-content/uploads/2019/01/Session-30-Kramer_etal_ICRS_Final-1-2.pdf [accessed 5 June 2020].

LaJeunesse, T.C., Parkinson, J.E., Gabrielson, P.W., Jeong, H.J., Reimer, J.D., Voolstra, C.R., and Santos, S.R. 2018. Systematic Revision of Symbiodiniaceae Highlights the Antiquity and Diversity of Coral Endosymbionts. Curr. Biol. **28**(16): 2570-2580.e6. Cell Press. doi:10.1016/j.cub.2018.07.008.

Lamare, M.D., Liddy, M., and Uthicke, S. 2016. In situ developmental responses of tropical sea urchin larvae to ocean acidification conditions at naturally elevated pCO2 vent sites. Proc. R. Soc. B Biol. Sci. **283**(1843). Royal Society of London. doi:10.1098/rspb.2016.1506.

Langdon, C., Albright, R., Baker, A.C., and Jones, P. 2018. Two threatened Caribbean coral species have contrasting responses to combined temperature and acidification stress. Limnol. Oceanogr. **63**(6): 2450–2464. John Wiley & Sons, Ltd. doi:10.1002/LNO.10952.

Legendre, P., and Gallagher, E.D. 2001. Ecologically meaningful transformations for ordination of species data. Oecologia **129**: 271–280. Available from http://adn.biol.umontreal.ca/~numericalecology/Reprints/Legendre_&_Gallagher.pdf

[accessed 28 July 2021].
Lenth R. V. 2021. emmeans: Estimated Marginal Means, aka Least-Squares Means. R package version 1.6.2-1. https://CRAN.R-project.org/package=emmeans
Lepš, J., and Šmilauer, P. 2003. Multivariate Analysis of Ecological Data using CANOCO. *In* Multivariate Analysis of Ecological Data using CANOCO. Cambridge University Press, Cambridge. doi:10.1017/CBO9780511615146.
Lewis, E., and Wallace, D. 1998. CO2SYS Dos Program Developed for CO2 System Calculations. ORNL/CDIAC-105 Carbon Dioxide Information Analysis Center, Oak Ridge National Laboratory, US Department of Energy, Oak Ridge, Tennessee. Available from https://www.ncei.noaa.gov/access/ocean-carbon-data-system/oceans/CO2SYS/co2rprt.html [accessed 1 August 2021].
Lin, Y.S., Lui, H.K., Lee, J., Chen, C.T.A., Burr, G.S., Chou, W.C., and Kuo, F.W. 2019. Fates of vent CO 2 and its impact on carbonate chemistry in the shallow-water hydrothermal field offshore Kueishantao Islet, NE Taiwan. Mar. Chem. **210**: 1–12. Elsevier B.V. doi:10.1016/j.marchem.2019.02.002.
Lindsay, J.M., Stasiuk, M. V., and Shepherd, J.B. 2003. Geological history and potential hazards of the late-Pleistocene to Recent Plat Pays volcanic complex, Dominica, Lesser Antilles. Bull. Volcanol. **65**(2–3): 201–220. Springer Verlag. doi:10.1007/s00445-002-0253-y.
Lirman, D. 2000. Fragmentation in the branching coral Acropora palmata (Lamarck): growth, survivorship, and reproduction of colonies and fragments. J. Exp. Mar. Bio. Ecol. **251**(1): 41–57. Elsevier. doi:10.1016/S0022-0981(00)00205-7.
Loya, Y., Sakai, K., Yamazato, K., Nakano, Y., Sambali, H., and van Woesik, R. 2001. Coral bleaching: the winners and the losers. Ecol. Lett. **4**(2): 122–131. John Wiley & Sons, Ltd. doi:10.1046/j.1461-0248.2001.00203.x.
Mackinder, L., Wheeler, G., Schroeder, D., Riebesell, U., and Brownlee, C. 2010. Molecular Mechanisms Underlying Calcification in Coccolithophores. http://dx.doi.org/10.1080/01490451003703014 **27**(6–7): 585–595. Taylor & Francis Group . doi:10.1080/01490451003703014.
Madin, J.S., Baird, A.H., Dornelas, M., and Connolly, S.R. 2014. Mechanical vulnerability explains size-dependent mortality of reef corals. Ecol. Lett. **17**(8): 1008–1015. John Wiley & Sons, Ltd. doi:10.1111/ELE.12306.
Mah, A.J., and Stearn, C.W. 1986. The effect of Hurricane Allen on the Bellairs fringing reef, Barbados. Coral Reefs **4**(3): 169–176. Springer-Verlag. doi:10.1007/BF00427938.
Maier, C., Schubert, A., Sànchez, M.M.B., Weinbauer, M.G., Watremez, P., and Gattuso, J.-P. 2013. End of the Century pCO2 Levels Do Not Impact Calcification in Mediterranean Cold-Water Corals. PLoS One **8**(4): e62655. Public Library of Science. doi:10.1371/JOURNAL.PONE.0062655.
Maliao, R.J., Turingan, R.G., and Lin, J. 2008. Phase-shift in coral reef communities in the Florida Keys National Marine Sanctuary (FKNMS), USA. Mar. Biol. **154**(5): 841–853. Springer. doi:10.1007/S00227-008-0977-0.
Manzello, D., Enochs, I., Musielewicz, S., Carlton, R., and Gledhill, D. 2013. Tropical cyclones cause CaCO3 undersaturation of coral reef seawater in a high-CO2 world. J. Geophys. Res. Ocean. **118**(10): 5312–5321. John Wiley & Sons, Ltd. doi:10.1002/JGRC.20378.
Manzello, D.P., Matz, M. V., Enochs, I.C., Valentino, L., Carlton, R.D., Kolodziej, G., Serrano, X., Towle, E.K., and Jankulak, M. 2019. Role of host genetics and heat-tolerant algal symbionts in sustaining populations of the endangered coral Orbicella faveolata in the Florida Keys with ocean warming. Glob. Chang. Biol. **25**(3): 1016–1031. John Wiley & Sons, Ltd. doi:10.1111/GCB.14545.

Mccarthy, K.T., Pichler, T., and Price, R.E. 2005. Geochemistry of Champagne Hot Springs shallow hydrothermal vent field and associated sediments, Dominica, Lesser Antilles. Chem. Geol. **224**: 55–68. doi:10.1016/j.chemgeo.2005.07.014.

McCullagh, P. (Peter), and Nelder, J.A. 1989. Generalized linear models. *In* 2nd Edition, Chapman and Hall, London. http://dx.doi.org/10.1007/978-1-4899-3242-6

McCulloch, M., Falter, J., Trotter, J., and Montagna, P. 2012a. Coral resilience to ocean acidification and global warming through pH up-regulation. Nat. Clim. Chang. 2012 28 **2**(8): 623–627. Nature Publishing Group. doi:10.1038/nclimate1473.

McCulloch, M., Trotter, J., Montagna, P., Falter, J., Dunbar, R., Freiwald, A., Försterra, G., López Correa, M., Maier, C., Rüggeberg, A., and Taviani, M. 2012b. Resilience of cold-water scleractinian corals to ocean acidification: Boron isotopic systematics of pH and saturation state up-regulation. Geochim. Cosmochim. Acta **87**: 21–34. Pergamon. doi:10.1016/J.GCA.2012.03.027.

McMurray, S.E., Henkel, T.P., and Pawlik, J.R. 2010. Demographics of increasing populations of the giant barrel sponge Xestospongia muta in the Florida Keys. Ecology **91**(2): 560–570. doi:10.1890/08-2060.1.

McNeil, B.I., and Sasse, T.P. 2016. Future ocean hypercapnia driven by anthropogenic amplification of the natural CO2 cycle. Nat. 2016 5297586 **529**(7586): 383–386. Nature Publishing Group. doi:10.1038/nature16156.

Mumby, P.J., Hedley, J.D., Zychaluk, K., Harborne, A.R., and Blackwell, P.G. 2006. Revisiting the catastrophic die-off of the urchin Diadema antillarum on Caribbean coral reefs: Fresh insights on resilience from a simulation model. Ecol. Modell. **196**(1–2): 131–148. Elsevier. doi:10.1016/j.ecolmodel.2005.11.035.

National Academies of Sciences Engineering and Medicine. 2016. Attribution of Extreme Weather Events in the Context of Climate Change. *In* Attribution of Extreme Weather Events in the Context of Climate Change. National Academies Press, Washington, DC. doi:10.17226/21852.

Nelson, H.R., and Altieri, A.H. 2019. Oxygen: the universal currency on coral reefs. Coral Reefs **38**: 177–198. doi:10.1007/s00338-019-01765-0.

Newman, S.P., Meesters, E.H., Dryden, C.S., Williams, S.M., Sanchez, C., Mumby, P.J., and Polunin, N.V.C. 2015. Reef flattening effects on total richness and species responses in the Caribbean. J. Anim. Ecol. **84**(6): 1678–1689. John Wiley & Sons, Ltd. doi:10.1111/1365-2656.12429.

Oksanen, J. 2015. Multivariate Analysis of Ecological Communities in R: vegan tutorial. URL https://www.mooreecology.com/uploads/2/4/2/1/24213970/vegantutor.pdf [Accessed: 01.07.21]

Oksanen, J. 2020. Vegan: ecological diversity. URL https://cran.r-project.org/web/packages/vegan/vignettes/diversity-vegan.pdf [Accessed: 24.06.21]

Oksanen J., F. Guillaume Blanchet, Michael Friendly, Roeland Kindt, Pierre Legendre, Dan McGlinn, Peter R. Minchin, R. B. O'Hara, Gavin L. Simpson, Peter Solymos, M. Henry H. Stevens, Eduard Szoecs and Helene Wagner (2020). vegan: Community Ecology Package. R package version 2.5-7. https://CRAN.R-project.org/package=vegan

Otaño-Cruz, A., Montañez-Acuña, A.A., García-Rodríguez, N.M., Díaz-Morales, D.M., Benson, E., Cuevas, E., Ortiz-Zayas, J., and Hernández-Delgado, E.A. 2019. Caribbean Near-Shore Coral Reef Benthic Community Response to Changes on Sedimentation Dynamics and Environmental Conditions. Front. Mar. Sci. **6**: 551. Frontiers Media S.A. doi:10.3389/fmars.2019.00551.

Peña, V., Harvey, B.P., Agostini, S., Porzio, L., Milazzo, M., Horta, P., Le, L., and Jason, G. 2021. Major loss of coralline algal diversity in response to ocean acidification. (June): 1–14. doi:10.1111/gcb.15757.

Pengsakun, S., Yeemin, T., Sutthacheep, M., Samsuvan, W., Klinthong, W., and Chamchoy, C. 2019. Monitoring of coral communities in the inner Gulf of Thailand influenced by the elevated seawater temperature and flooding. Acta Oceanol. Sin. 2019 381 **38**(1): 102–111. Springer. doi:10.1007/S13131-019-1376-8.

Perry, C.T., Murphy, G.N., Kench, P.S., Smithers, S.G., Edinger, E.N., Steneck, R.S., and Mumby, P.J. 2013. Caribbean-wide decline in carbonate production threatens coral reef growth. Nat. Commun. 2013 41 **4**(1): 1–7. Nature Publishing Group. doi:10.1038/ncomms2409.

Pielou, E.C. 1966. The measurement of diversity in different types of biological collections. J. Theor. Biol. **13**(C): 131–144. Academic Press. doi:10.1016/0022-5193(66)90013-0.

Pinnegar, J.K., Engelhard, G.H., Norris, N.J., Theophille, D., Sebastien, R.D., and Hidalgo, M. 2019. Assessing vulnerability and adaptive capacity of the fisheries sector in Dominica: Long-term climate change and catastrophic hurricanes. ICES Journal of Marine Science. **76**(5): 1353–1367. Oxford University Press. doi:10.1093/icesjms/fsz052.

Plaisance, L., Caley, M.J., Brainard, R.E., and Knowlton, N. 2011. The Diversity of Coral Reefs: What Are We Missing? PLoS One **6**(10): 25026. doi:10.1371/journal.pone.0025026.

Poloczanska, E.S., Brown, C.J., Sydeman, W.J., Kiessling, W., Schoeman, D.S., Moore, P.J., Brander, K., Bruno, J.F., Buckley, L.B., Burrows, M.T., Duarte, C.M., Halpern, B.S., Holding, J., Kappel, C. V., O'Connor, M.I., Pandolfi, J.M., Parmesan, C., Schwing, F., Thompson, S.A., and Richardson, A.J. 2013. Global imprint of climate change on marine life. Nat. Clim. Chang. **3**([Published Online]). doi:10.1038/NCLIMATE1958.

Pörtner, H.O., and Farrell, A.P. 2008. Physiology and Climate Change . Science. **322**(5902): 690–692. Available from https://www.jstor.org/stable/20145158?seq=1#metadata_info_tab_contents [accessed 24 August 2021].

Precht, L., and Precht, W. 2015. The sea urchin Diadema antillarum – keystone herbivore or redundant species? PeerJ Prepr. doi:10.7287/PEERJ.PREPRINTS.1565.

Przeslawski, R., Ahyong, S., Byrne, M., Wörheide, G., and Hutchings, P. 2008. Beyond corals and fish: The effects of climate change on noncoral benthic invertebrates of tropical reefs. Glob. Chang. Biol. **14**(12): 2773–2795. doi:10.1111/J.1365-2486.2008.01693.X.

Quan-Young, L.I., and Espinoza-Avalos, J. 2006. Reduction of zooxanthellae density, chlorophyll a concentration, and tissue thickness of the coral Montastraea faveolata (Scleractinia) when competing with mixed turf algae. Limnol. Oceanogr. **51**(2): 1159–1166. John Wiley & Sons, Ltd. doi:10.4319/LO.2006.51.2.1159.

R Core Team (2021). R: A language and environment for statistical computing. R Foundation for Statistical Computing, Vienna, Austria. URL https://www.R-project.org/.

Rao, C.R. 1964. The Use and Interpretation of Principal Component Analysis in Applied Research. Sankhyā Indian J. Stat. Ser. A **26**(4): 329–358. Available from https://www.jstor.org/stable/25049339?seq=1#metadata_info_tab_contents [accessed 30 August 2021].

Rastrick, S.S.P., Graham, H., Azetsu-Scott, K., Calosi, P., Chierici, M., Fransson, A., Hop, H., Hall-Spencer, J., Milazzo, M., Thor, P., and Kutti, T. 2018. Using natural analogues to investigate the effects of climate change and ocean acidification on Northern ecosystems. ICES J. Mar. Sci. **75**(7): 2299–2311. doi:10.1093/icesjms/fsy128.

Reaka-Kudla, M.L. 1997. Biodiversity II: Understanding and Protecting Our Biological Resources - Google Books. *Edited By*M.L. Reaka-Kudla, D.E. Wilson, and E.O. Wilson. Joseph Henry Press, Washington, DC. Available from

https://books.google.no/books?hl=en&lr=&id=-X5OAgAAQBAJ&oi=fnd&pg=PR1&ots=f2YimI109q&sig=Lyia7rQy91VZ6dNSvaC2HL1Kab0&redir_esc=y#v=onepage&q&f=false [accessed 4 June 2020].
Reaka-Kulda, M.L. 2005. Biodiversity of Caribbean coral reefs. *In* Caribbean Marine Biodiversity. *Edited by* P. Miloslavich and E. Klein. Des Tech Publishers, Lancaster, PA. pp. 259–276. Available from https://www.researchgate.net/publication/304216525 [accessed 20 May 2021].
Riebesell, U., and Gattuso, J.-P. 2014. Lessons learned from ocean acidification research. Nat. Clim. Chang. 2015 51 **5**(1): 12–14. Nature Publishing Group. doi:10.1038/nclimate2456.
Roberts, C.M., McClean, C.J., Veron, J.E.N., Hawkins, J.P., Allen, G.R., McAllister, D.E., Mittermeier, C.G., Schueler, F.W., Spalding, M., Wells, F., Vynne, C., and Werner, T.B. 2002. Marine biodiversity hotspots and conservation priorities for tropical reefs. Science. **295**(5558): 1280–1284. American Association for the Advancement of Science. doi:10.1126/science.1067728.
Roberts, J.M., Wheeler, A.J., and Freiwald, A. 2006. Reefs of the Deep: The Biology and Geology of Cold-Water Coral Ecosystems. Science. **312**(5773): 543–547. American Association for the Advancement of Science. doi:10.1126/SCIENCE.1119861.
Rodolfo-Metalpa, R., Houlbrèque, F., Tambutté, É., Boisson, F., Baggini, C., Patti, F.P., Jeffree, R., Fine, M., Foggo, A., Gattuso, J., and Hall-Spencer, J.M. 2011. Coral and mollusc resistance to ocean acidification adversely affected by warming. Nat. Clim. Chang. **1**: 308-312. doi:10.1038/NCLIMATE1200.
Roff, G., and Mumby, P.J. 2012. Global disparity in the resilience of coral reefs. Trends Ecol. Evol. **27**(7): 404–413. Elsevier Current Trends. doi:10.1016/J.TREE.2012.04.007.
Roleda, M.Y., Boyd, P.W., and Hurd, C.L. 2012. Before Ocean Acidification: Calcifier Chemistry Lessons. J. Phycol. **48**(4): 840–843. John Wiley & Sons, Ltd. doi:10.1111/J.1529-8817.2012.01195.X.
Rosell, D., and Uriz, M.J. 1992. Do associated zooxanthellae and the nature of the substratum affect survival, attachment and growth of Cliona viridis (Porifera: Hadromerida)? An experimental approach. Mar. Biol. 1992 1143 **114**(3): 503–507. Springer. doi:10.1007/BF00350042.
Roswell, M., Dushoff, J., and Winfree, R. 2021. A conceptual guide to measuring species diversity. Oikos **130**(3): 321–338. Blackwell Publishing Ltd. doi:10.1111/oik.07202.
Rützler, K. 2004. Sponges on Coral Reefs: A community shaped by competitive cooperation. Boll. Mus. Ist. Biol. Univ. Genova **68**: 85–148.
Saba, V.S., Griffies, S.M., Anderson, W.G., Winton, M., Alexander, M.A., Delworth, T.L., Hare, J.A., Harrison, M.J., Rosati, A., Vecchi, G.A., and Zhang, R. 2016. Enhanced warming of the <scp>N</scp> orthwest <scp>A</scp> tlantic <scp>O</scp> cean under climate change. J. Geophys. Res. Ocean. **121**(1): 118–132. doi:10.1002/2015JC011346.
Sabine, C.L., Feely, R.A., Gruber, N., Key, R.M., Lee, K., Bullister, J.L., Wanninkhof, R., Wong, C.S., Wallace, D.W.R., Tilbrook, B., Millero, F.J., Peng, T.-H., Kozyr, A., Ono, T., and Rios, A.F. 2004. The Oceanic Sink for Anthropogenic CO2. Science. **305**(5682): 367–371. American Association for the Advancement of Science. doi:10.1126/SCIENCE.1097403.
Sainsbury, N.C., Genner, M.J., Saville, G.R., Pinnegar, J.K., O'Neill, C.K., Simpson, S.D., and Turner, R.A. 2018. Changing storminess and global capture fisheries. Nature Publishing Group. doi:10.1038/s41558-018-0206-x.
Sanchez-Vidal, A., Canals, M., Calafat, A.M., Lastras, G., Pedrosa-Pàmies, R., Menéndez, M., Medina, R., Company, J.B., Hereu, B., Romero, J., and Alcoverro, T. 2012. Impacts

on the Deep-Sea Ecosystem by a Severe Coastal Storm. PLoS One **7**(1): e30395. Public Library of Science. doi:10.1371/JOURNAL.PONE.0030395.
Santhanam, R. 2020. Biology and Ecology of the Venomous Marine Anthozoans (Class Anthozoa). *In* Biology and Ecology of Venomous Marine Cnidarians. Springer, Singapore. pp. 169–285. doi:10.1007/978-981-15-1603-0_6.
Selig, E.R., Casey, K.S., and Bruno, J.F. 2012. Temperature-driven coral decline: the role of marine protected areas. Glob. Chang. Biol. **18**(5): 1561–1570. John Wiley & Sons, Ltd. doi:10.1111/j.1365-2486.2012.02658.x.
Simmons, K.R., Eggleston, D.B., and Bohnenstiehl, D.R. 2021. Hurricane impacts on a coral reef soundscape. PLoS One **16**(2): e0244599. Public Library of Science. doi:10.1371/JOURNAL.PONE.0244599.
Simpson G. L. 2019. ggvegan: 'ggplot2' Plots for the 'vegan' Package. R package version 0.1-0.
Slinger-Friedman, V. 2017. Dominica. *In* Landscapes and Landforms of the Lesser Antilles. *Edited by* C.D. Allen. Springer International Publishing, Cham. pp. 153–171. doi:10.1007/978-3-319-55787-8_11.
Small, D.P., Milazzo, M., Bertolini, C., Graham, H., Hauton, C., Hall-Spencer, J.M., and Rastrick, S.P.S. 2016. Temporal fluctuations in seawater pCO2 may be as important as mean differences when determining physiological sensitivity in natural systems. ICES J. Mar. Sci. **73**(3): 604–612. doi:10.1093/icesjms/fsv232.
Sokal, R.R., and Rohlf, F.J. 1995. Biometry : the principles and practice of statistics in biological research. *In* 3rd edition. Freeman, New York. Available from https://searchworks.stanford.edu/view/2950400 [accessed 31 August 2021].
Steiner, S.C.C. 2003. Stony corals and reefs of Dominica. Atoll Res. Bull. **498**: 1–15. doi:https://doi.org/10.5479/si.00775630.498.1.
Steiner, S.C.C. 2015a. Coral Reefs of Dominica (Lesser Antilles). *In* Ann. Naturhist. Mus. Wien, B.
Steiner, S.C.C. 2015b. Coral Reefs of Dominica (Lesser Antilles). Ann. des Naturhistorischen Museums Wien, B **117**: 47–119. Available from https://www.researchgate.net/publication/340511458_Coral_Reefs_of_Dominica_Lesser_Antilles [accessed 11 March 2021].
Steiner, S.C.C., and Willette, D.A. 2010. Distribution and size of benthic marine habitats in Dominica, Lesser Antilles. Rev. Biol. Trop. **58**(2). Available from https://www.scielo.sa.cr/scielo.php?script=sci_arttext&pid=S0034-77442010000200005 [accessed 5 April 2021].
Steiner, S.C.C., Willette, D.A., Wallover, N.J., Wilson, K.R., Price, L.M., and Macfarlane, K.J. 2007. First Large Scale Survey of Marine Habitat Categories in Dominica. *In* Research Reports-Number. Roseau, Commonwealth of Dominica. Available from www.itme.org [accessed 22 March 2021].
Steiner, S.C.C., and Williams, S.M. 2006. The density and size distribution of Diadema antillarum in Dominica (Lesser Antilles): 2001–2004. Mar. Biol. **149**(5): 1071–1078. Springer Science and Business Media LLC. doi:10.1007/s00227-006-0279-3.
Stephenson, D.B. 2008. Definition, diagnosis, and origin of extreme weather and climate events. *In* Climate Extremes and Society. *Edited by* H.F. Diaz and R.J. Murnane. Cambridge University Press, Cambridge. pp. 11–23. doi:10.1017/CBO9780511535840.004.
Sunday, J.M., Calosi, P., Dupont, S., Munday, P.L., Stillman, J.H., and Reusch, T.B.H. 2014. Evolution in an acidifying ocean. Trends Ecol. Evol. **29**(2): 117–125. Elsevier Current Trends. doi:10.1016/J.TREE.2013.11.001.
Teece, M.A., Estes, B., Gelsleichter, E., and Lirman, D. 2011. Heterotrophic and autotrophic

assimilation of fatty acids by two scleractinian corals, Montastraea faveolata and Porites astreoides. Limnol. Oceanogr. **56**(4): 1285–1296. John Wiley & Sons, Ltd. doi:10.4319/LO.2011.56.4.1285.
Thomas, A., and Benjamin, L. 2018. Policies and mechanisms to address climate-induced migration and displacement in Pacific and Caribbean small island developing states. Int. J. Clim. Chang. Strateg. Manag. **10**(1): 86–104. doi:10.1108/IJCCSM-03-2017-0055.
Ting, M., Kossin, J.P., Camargo, S.J., and Li, C. 2019. Past and Future Hurricane Intensity Change along the U.S. East Coast. Sci. Reports 2019 91 **9**(1): 1–8. Nature Publishing Group. doi:10.1038/s41598-019-44252-w.
Törnroos, A., Bonsdorff, E., Bremner, J., Blomqvist, M., Josefson, A.B., Garcia, C., and Warzocha, J. 2015. Marine benthic ecological functioning over decreasing taxonomic richness. J. Sea Res. **98**: 49–56. Elsevier. doi:10.1016/J.SEARES.2014.04.010.
Towle, E.K., Enochs, I.C., and Langdon, C. 2015. Threatened Caribbean Coral Is Able to Mitigate the Adverse Effects of Ocean Acidification on Calcification by Increasing Feeding Rate. PLoS One **10**(4): e0123394. Public Library of Science. doi:10.1371/JOURNAL.PONE.0123394.
Trenberth, K.E., Fasullo, J.T., and Shepherd, T.G. 2015. Attribution of climate extreme events. Nat. Clim. Chang. **5**: 725–730. Nature Publishing Group. doi:10.1038/nclimate2657.
Vermeij, M.J.A., van Moorselaar, I., Engelhard, S., Hörnlein, C., Vonk, S.M., and Visser, P.M. 2010. The Effects of Nutrient Enrichment and Herbivore Abundance on the Ability of Turf Algae to Overgrow Coral in the Caribbean. PLoS One **5**(12): e14312. Public Library of Science. doi:10.1371/journal.pone.0014312.
Vicente, J., Silbiger, N.J., Beckley, B.A., Raczkowski, C.W., and Hill, R.T. 2016. Impact of high pCO2 and warmer temperatures on the process of silica biomineralization in the sponge Mycale grandis. ICES J. Mar. Sci. **73**(3): 704–714. Oxford Academic. doi:10.1093/ICESJMS/FSV235.
Villamizar, E., Díaz, M.C., Rützler, K., and De Nóbrega, R. 2014. Biodiversity, ecological structure, and change in the sponge community of different geomorphological zones of the barrier fore reef at Carrie Bow Cay, Belize. Mar. Ecol. **35**(4): 425–435. Blackwell Publishing Ltd. doi:10.1111/MAEC.12099.
Wagenmakers, E.-J., and Farrell, S. 2004. AIC model selection using Akaike weights. Psychon. Bull. Rev. **11**(1): 192–196. doi:https://doi.org/10.3758/BF03206482.
Wei T. and Simko V. 2021. R package 'corrplot': Visualization of a Correlation Matrix (Version 0.90). Available from https://github.com/taiyun/corrplot
Wernberg, T., Bennett, S., Babcock, R.C., Bettignies, T. de, Cure, K., Depczynski, M., Dufois, F., Fromont, J., Fulton, C.J., Hovey, R.K., Harvey, E.S., Holmes, T.H., Kendrick, G.A., Radford, B., Santana-Garcon, J., Saunders, B.J., Smale, D.A., Thomsen, M.S., Tuckett, C.A., Tuya, F., Vanderklift, M.A., and Wilson, S. 2016. Climate-driven regime shift of a temperate marine ecosystem. Science. **353**(6295): 169–172. American Association for the Advancement of Science. doi:10.1126/SCIENCE.AAD8745.
Wernberg, T., Smale, D.A., Tuya, F., Thomsen, M.S., Langlois, T.J., De Bettignies, T., Bennett, S., and Rousseaux, C.S. 2013. An extreme climatic event alters marine ecosystem structure in a global biodiversity hotspot. Nat. Clim. Chang. **3**(1): 78–82. doi:10.1038/NCLIMATE1627.
Wickham. H. 2016 ggplot2: Elegant Graphics for Data Analysis. Springer-Verlag New York.
Wijgerde, T., Silva, C., Scherders, V., van Bleijswijk, J., and Osinga, R. 2014. Coral calcification under daily oxygen saturation and pH dynamics reveals the important role of oxygen. Biol. Open **3**(6): 489–493. Biol Open. doi:10.1242/BIO.20147922.
Williams, E.H., Bunkley-Williams, L., and Washington, U. 1990. The Worldwide Coral Reef

Bleaching Cycle and Related Sources of Coral Mortality. Atoll Res. Bull. **335**.
Worm, B., Barbier, E.B., Beaumont, N., Duffy, J.E., Folke, C., Halpern, B.S., Jackson, J.B.C., Lotze, H.K., Micheli, F., Palumbi, S.R., Sala, E., Selkoe, K.A., Stachowicz, J.J., and Watson, R. 2006. Impacts of biodiversity loss on ocean ecosystem services. Science. **314**(5800): 787–790. American Association for the Advancement of Science. doi:10.1126/science.1132294.
Zea, S. 1993. Cover of sponges and other sessile organisms in rocky and coral reef habitats of Santa Marta, Colombian Caribbean Sea. Caribb. J. Sci. **29**(1–2): 75–88. Available from https://www.researchgate.net/publication/235754324_Cover_of_sponges_and_other_sessile_organisms_in_rocky_and_coral_reef_habitats_of_Santa_Marta_Colombian_Caribbean_Sea [accessed 2 August 2021].
Zheng, M. Di, and Cao, L. 2014. Simulation of global ocean acidification and chemical habitats of shallow- and cold-water coral reefs. Adv. Clim. Chang. Res. **5**(4): 189–196. Elsevier. doi:10.1016/J.ACCRE.2015.05.002.

Appendix

Appendix 1: Figure of Ocean Acidification

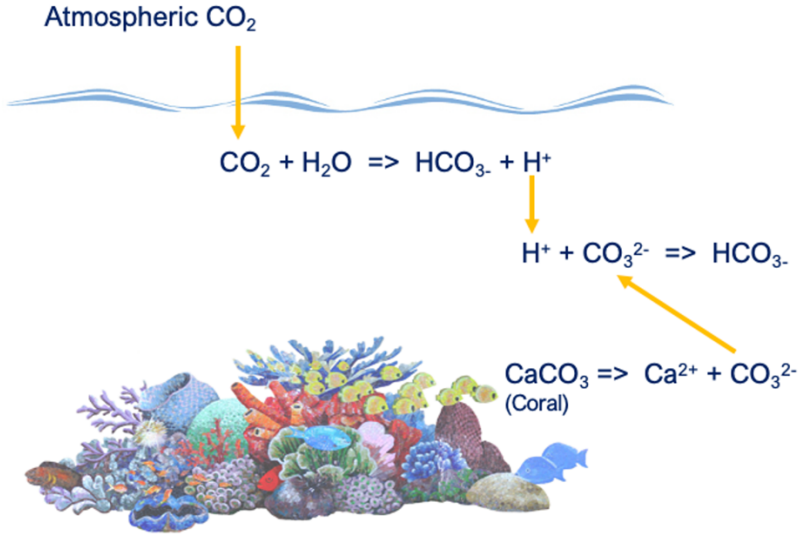

Figure 16: The Process of Ocean Acidfication. Adapted from Hoegh-Guldberg et al., 2007

Appendix 2: Model Selection for Total Alkalinity

Table 6: Results of model selection for Total Alkalinity. A linear model was selected by comparing the two independent variables with and without an interaction term. Model in bold text signifies the selected model. Akaike Information Criterium (AICc) is a measure of goodness of fit for models, where a lower number suggests a better fit model. Probability of having a true model is given with the AIC weight. The adjusted R-squared value describes the variance of the independent variables fitted, where a higher number indicates a better fitted model.

Response variable	Model (Independent variables)	AIC	AIC weights	Adjusted R-squared
Total alkalinity	Site * year	598.6424	0.079	0.4802
	Site + year	593.7436	0.921	0.5024

Appendix 3: Correlation plot for Environmental Variables

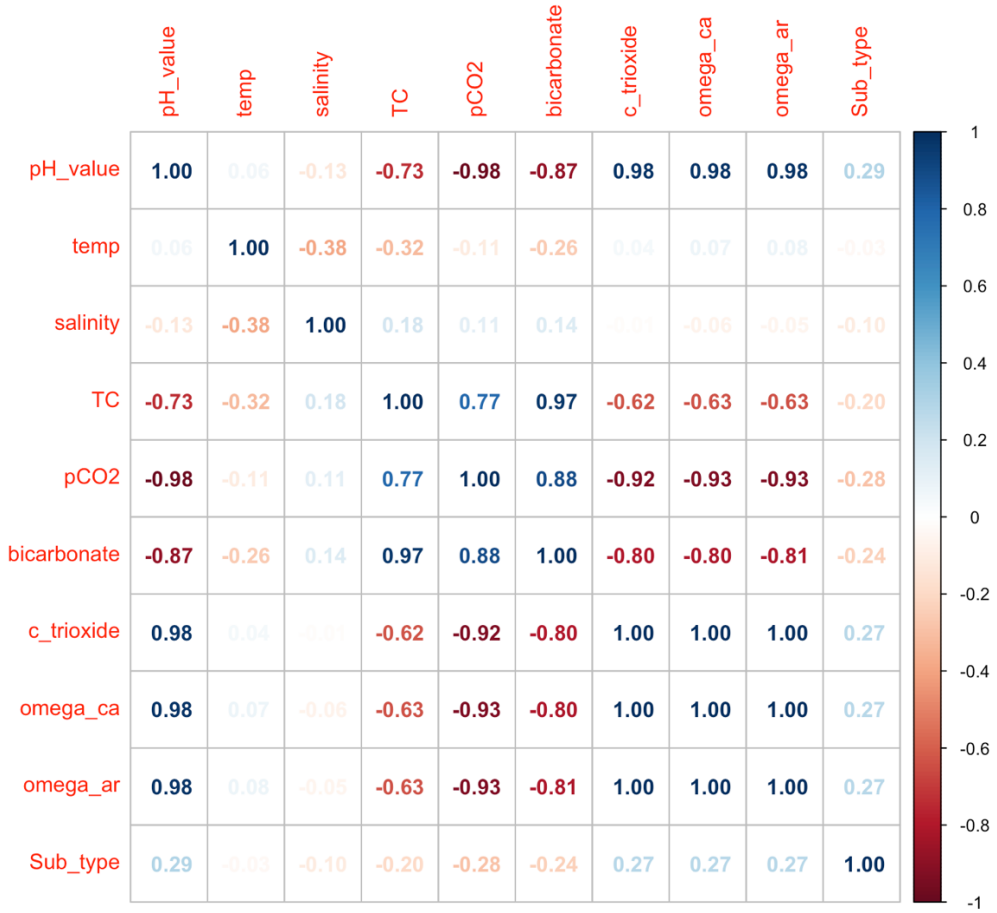

	pH_value	temp	salinity	TC	pCO2	bicarbonate	c_trioxide	omega_ca	omega_ar	Sub_type
pH_value	1.00	0.06	-0.13	-0.73	-0.98	-0.87	0.98	0.98	0.98	0.29
temp	0.06	1.00	-0.38	-0.32	-0.11	-0.26	0.04	0.07	0.08	-0.03
salinity	-0.13	-0.38	1.00	0.18	0.11	0.14	-0.01	-0.06	-0.05	-0.10
TC	-0.73	-0.32	0.18	1.00	0.77	0.97	-0.62	-0.63	-0.63	-0.20
pCO2	-0.98	-0.11	0.11	0.77	1.00	0.88	-0.92	-0.93	-0.93	-0.28
bicarbonate	-0.87	-0.26	0.14	0.97	0.88	1.00	-0.80	-0.80	-0.81	-0.24
c_trioxide	0.98	0.04	-0.01	-0.62	-0.92	-0.80	1.00	1.00	1.00	0.27
omega_ca	0.98	0.07	-0.06	-0.63	-0.93	-0.80	1.00	1.00	1.00	0.27
omega_ar	0.98	0.08	-0.05	-0.63	-0.93	-0.81	1.00	1.00	1.00	0.27
Sub_type	0.29	-0.03	-0.10	-0.20	-0.28	-0.24	0.27	0.27	0.27	1.00

Figure 17: Correlation plot for environmental variables. Positive correlations are displayed in blue colours, while negative correlations are displayed in red. Colour intensity indicates the strength of the correlation. Each environmental variable is plotted against each other. The environmental variables include pH level, temperature, salinity, total carbon (TC), surface ocean partial pressure of CO_2 (pCO_2), bicarbonate, carbonate trioxide (c_trioxide), calcium carbonate saturation (omega_ca), aragonite saturation (omega_ar) and substrate category (Sub_type; Hard or Mixed). The correlation plot was plotted using the 'corrplot' package (Wei & Simko 2021) in the statistical programming language 'R'.

Appendix 4: Raw pCO_2 gradient

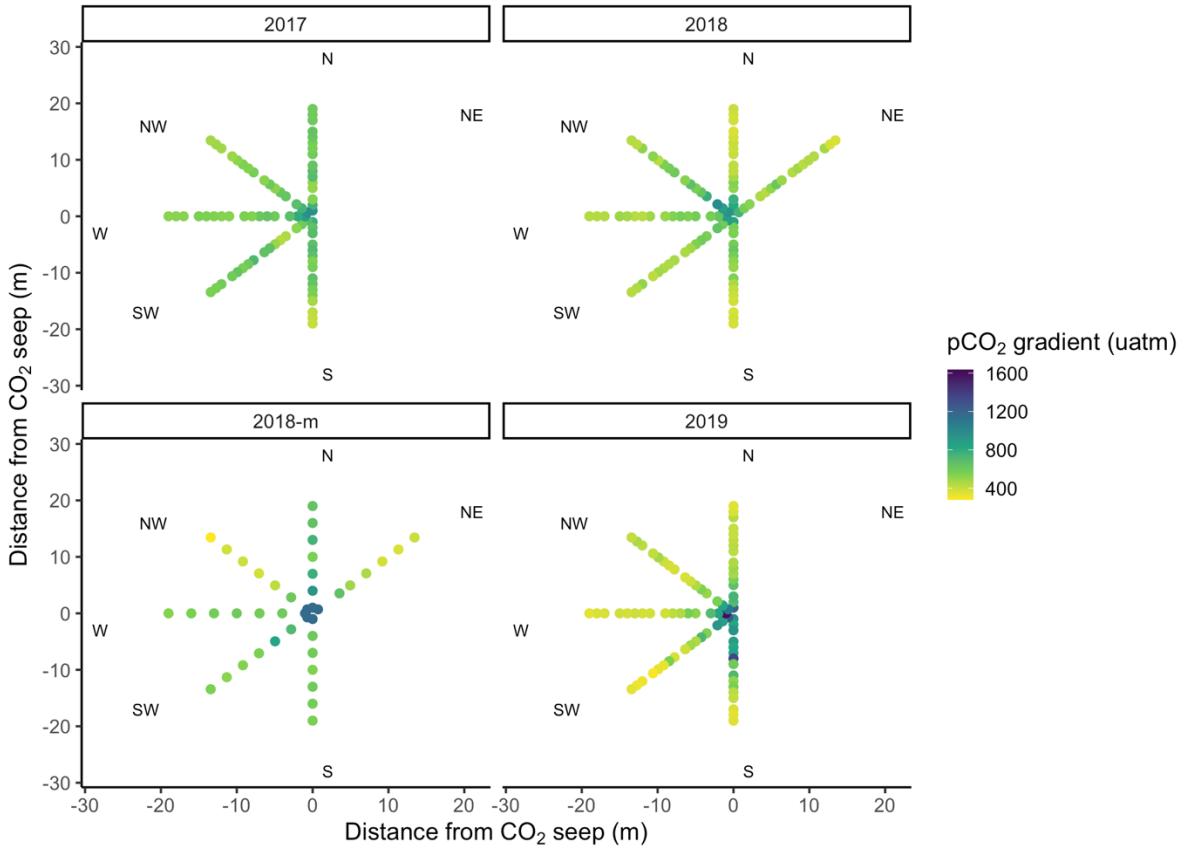

Figure 18: Raw pCO_2 gradient from all survey time points. pCO_2 (µtam) was measured for every cardinal direction, as displayed by labels NE for North East, S for South, SW for South West, W for West, NW for North West and N for North. This was plotted for every survey time point, as indicated by the panes on top of the graphs, with 2017 for the summer of 2017, 2018-m for March of 2018, 2018 for the summer of 2018 and 2019 for the summer of 2019.

Appendix 5: Coefficients table for Total Alkalinity

Table 7: Coefficients table for linear model for total alkalinity. Treatment contrasts of estimated regression parameters, standard errors, t-value and P-values for the linear model.

	Estimate	**Standard Error (SE)**	**t-value**	**p-value**
(Intercept)	2372.475	19.683	120.535	< 2e-16
siteseep	-22.425	17.018	-1.318	0.194
year2018	-120.059	21.922	-5.477	1.56e-06
year2018m	21.895	26.380	0.830	0.411
year2019	-8.137	28.063	-0.290	0.773

Appendix 6: Post Hoc Tukey test for the Linear Model for Total Alkalinity

Table 8: Post-hoc Tukey test for linear model of Total alkalinity. All survey time points are pairwise compared with one another, as indicated by the 'contrast' column. The estimate, standard error, degrees of freedom, t-ratio and p-values are reported for each of the pairwise comparisons. Results are averaged by site (reference site or seep site).

Contrast	Estimate	Standard Error (SE)	Degrees of Freedom (df)	t-ratio	p-value
2017 – 2018	120.06	21.9	48	5.477	<.0001
2017 – (2018-m)	-21.90	26.4	48	-0.830	0.8400
2017 – 2019	8.14	28.1	48	0.290	0.9914
2018 – (2018-m)	-141.95	23.3	48	-6.093	<.0001
2018 – 2019	-111.92	25.3	48	-4.431	0.0003
(2018-m) – 2019	30.03	29.2	48	1.028	0.7339

Appendix 7: Coefficients table for Species Richness

Table 9: Coefficients table from species richness model. Treatment contrasts of estimated regression parameters, standard errors, z-values and P-values for the quasi-Poisson GLM.

	Estimate	Standard Error (SE)	z-ratio	p-value
(Intercept)	2.482	0.04643	53.464	< 0.05
March, 2018	-0.5411	0.02771	-19.529	< 0.05
2018	-0.5548	0.02785	-19.918	< 0.05
2019	-0.3341	0.02810	-11.890	< 0.05
pCO2	-0.0005688	0.00006898	-8.246	< 0.05
Substrate: Mixed	0.04052	0.02121	1.911	0.0564
Substrate: Soft	-0.02448	0.09903	-0.247	0.8048

Appendix 8: Post Hoc Tukey test for Species Richness GLM

Table 10: Post-hoc Tukey test for the generalized linear model for species richness. All survey time points are pairwise compared with one another, as indicated by the 'contrast' column. The estimate, standard error, degrees of freedom, z-ratio and p-values are reported for each of the pairwise comparisons. Results are averaged by levels of substrate category ('hard', 'mixed' or 'soft').

Contrast	Estimate	Standard Error (SE)	Degrees of Freedom (df)	z-ratio	p-value
2017 - 2018	0.5548	0.0279	Inf	19.918	<.0001
2017 - (2018-m)	0.5411	0.0277	Inf	19.529	<.0001
2017 - 2019	0.3341	0.0281	Inf	11.890	<.0001
2018 - (2018-m)	-0.0137	0.0305	Inf	-0.448	0.9700
2018 - 2019	-0.2207	0.0298	Inf	-7.414	<.0001
(2018-m) - 2019	-0.2070	0.0307	Inf	-6.738	<.0001

Appendix 9: Coefficients table for Coral Richness

Table 11: Coefficients table from coral richness model. Treatment contrasts of estimated regression parameters, standard errors, z-values and P-values for the quasi-Poisson GLM.

	Estimate	Standard Error (SE)	z-ratio	p-value
(Intercept)	1.4875089	0.1001818	14.848	< 0.05
March, 2018	-0.7864316	0.0587076	-13.396	< 0.05
2018	-0.7329013	0.0576697	-12.709	< 0.05
2019	-0.5973962	0.0599964	-9.957	< 0.05
pCO2	-0.0007696	0.0001526	-5.043	< 0.05
Substrate: Mixed	-0.0415384	0.0449888	-0.923	0.356
Substrate: Soft	-0.0129902	0.2042630	-0.064	0.949

Appendix 10: Post Hoc Tukey test for Coral Richness GLM

Table 12: Post-hoc Tukey test for the generalized linear model for coral richness. All survey time points are pairwise compared with one another, as indicated by the 'contrast' column. The estimate, standard error, degrees of freedom, z-ratio and p-values are reported for each of the pairwise comparisons. Results are averaged by levels of substrate category ('hard', 'mixed' or 'soft').

Contrast	Estimate	Standard Error (SE)	Degrees of Freedom (df)	z-ratio	p-value
2017 - 2018	0.7329	0.0577	Inf	12.709	<.0001
2017 - (2018-m)	0.7864	0.0587	Inf	13.396	<.0001
2017 - 2019	0.5974	0.0600	Inf	9.957	<.0001
2018 - (2018-m)	0.0535	0.0663	Inf	0.807	0.8511
2018 - 2019	-0.1355	0.0651	Inf	-2.083	0.1587
(2018-m) - 2019	-0.1890	0.0684	Inf	-2.765	0.0291

Appendix 11: Coefficients table for Sponge Richness

Table 13: Coefficients table from sponge richness model. Treatment contrasts of estimated regression parameters, standard errors, z-values and P-values for the quasi-Poisson GLM.

	Estimate	Standard Error (SE)	z-ratio	p-value
(Intercept)	2.0715275	0.1792281	11.558	< 0.05
March, 2018	-1.0511354	0.0928491	-11.321	< 0.05
2018	-1.4953014	0.1043586	-14.328	< 0.05
2019	-0.7744472	0.0915655	-8.458	< 0.05
pCO2	-0.0024712	0.0002897	-8.531	< 0.05
Substrate: Mixed	0.0125419	0.0696545	0.180	0.857
Substrate: Soft	-0.0311263	0.3207686	-0.097	0.923

Appendix 12: Post Hoc Tukey test for Sponge Richness GLM

Table 14: Post-hoc Tukey test for the generalized linear model for sponge richness. All survey time points are pairwise compared with one another, as indicated by the 'contrast' column. The estimate, standard error, degrees of freedom, z-ratio and p-values are reported for each of the pairwise comparisons. Results are averaged by levels of substrate category ('hard', 'mixed' or 'soft').

Contrast	Estimate	Standard Error (SE)	Degrees of Freedom (df)	z-ratio	p-value
2017 - 2018	1.495	0.1044	Inf	14.328	<.0001
2017 - (2018-m)	1.051	0.0928	Inf	11.321	<.0001
2017 - 2019	0.774	0.0916	Inf	8.458	<.0001
2018 - (2018-m)	-0.444	0.1186	Inf	-3.745	0.0010
2018 - 2019	-0.721	0.1120	Inf	-6.436	<.0001
(2018-m) - 2019	-0.277	0.1070	Inf	-2.587	0.0477

Appendix 13: Coefficient table for Hill-Shannon Diversity LM

Table 15: Coefficients table for linear model of Hill-Shannon diversity. Treatment contrasts of estimated regression parameters, standard errors, t-values and P-values for the fitted linear model.

	Estimate	Standard Error (SE)	t-ratio	p-value
(Intercept)	3.2793235	0.0990570	33.105	< 0.05
March, 2018	-1.2722606	0.0632806	-20.105	< 0.05
2018	-1.0761012	0.0639514	-16.827	< 0.05
2019	-0.9194729	0.0675661	-13.608	< 0.05
pCO2	-0.0010000	0.0001381	-7.239	< 0.05
Substrate: Mixed	0.1151428	0.0478168	2.408	< 0.05
Substrate: Soft	-0.3292637	0.2159516	-1.525	0.1276

Appendix 14: Post Hoc Tukey test for Hill-Shannon Diversity LM

Table 16: Post-hoc Tukey test for linear model of Hill-Shannon diversity. All survey time points are pairwise compared with one another, as indicated by the 'contrast' column. The estimate, standard error, degrees of freedom, t-ratio and p-values are reported for each of the pairwise comparisons. Results are averaged over the levels of Substrate categories ('Hard', 'Mixed' and 'Soft').

Contrast	Estimate	Standard Error (SE)	Degrees of Freedom (df)	t-ratio	p-value
2017 - 2018	1.076	0.0640	1259	16.827	<.0001
2017 - (2018-m)	1.272	0.0633	1259	20.105	<.0001
2017 - 2019	0.919	0.0676	1259	13.608	<.0001
2018 - (2018-m)	0.196	0.0620	1259	3.165	0.0086
2018 - 2019	-0.157	0.0646	1259	-2.426	0.0728
(2018-m) - 2019	-0.353	0.0656	1259	-5.381	<.0001

Appendix 15: Coefficient table for Hill-Simpson Diversity LM

Table 17: Coefficients table for linear model of Hill-Simpson diversity. Treatment contrasts of estimated regression parameters, standard errors, t-values and P-values for the fitted linear model.

	Estimate	Standard Error (SE)	t-ratio	p-value
(Intercept)	2.231	0.06205	35.951	< 0.05
March, 2018	-0.7162	0.03964	-18.067	< 0.05
2018	-0.5843	0.04006	-14.586	< 0.05
2019	-0.5372	0.04232	-12.693	< 0.05
pCO2	-0.0005627	0.00008653	-6.503	< 0.05
Substrate: Mixed	0.05106	0.02995	1.705	0.0885
Substrate: Soft	-0.2116	0.1353	-1.564	0.1180

Appendix 16: Post Hoc Tukey test for Hill-Simpson Diversity LM

Table 18: Post-hoc Tukey test for linear model of Hill-Simpson diversity. All survey time points are pairwise compared with one another, as indicated by the 'contrast' column. The estimate, standard error, degrees of freedom, t-ratio and p-values are reported for each of the pairwise comparisons. Results are averaged over the levels of Substrate categories ('Hard', 'Mixed' and 'Soft').

Contrast	Estimate	Standard Error (SE)	Degrees of Freedom (df)	t-ratio	p-value
2017 - 2018	0.5843	0.0401	1259	14.586	<.0001
2017 - (2018-m)	0.7162	0.0396	1259	18.067	<.0001
2017 - 2019	0.5372	0.0423	1259	12.693	<.0001
2018 - (2018-m)	0.1318	0.0388	1259	3.397	0.0039
2018 - 2019	-0.0471	0.0405	1259	-1.164	0.6498
(2018-m) - 2019	-0.1789	0.0411	1259	-4.357	0.0001

Appendix 17: Coefficient table for Pielou's Evenness Diversity LM

Table 19: Coefficients table for linear model of Hill-Simpson diversity. Treatment contrasts of estimated regression parameters, standard errors, t-values and P-values for the fitted linear model.

	Estimate	Standard Error (SE)	t-ratio	p-value
(Intercept)	0.5153	0.01632	31.576	< 0.05
March, 2018	-0.1862	0.01043	-17.860	< 0.05
2018	-0.1059	0.01053	-10.057	< 0.05
2019	-0.1195	0.01112	-10.745	< 0.05
pCO2	-0.0002152	0.00002276	-9.455	< 0.05
Substrate: Mixed	0.03708	0.007881	4.705	< 0.05
Substrate: Soft	-0.05649	0.03556	-1.589	0.112

Appendix 18: Post Hoc Tukey test for Pielou's Evenness LM

Table 20: Post-hoc Tukey test for linear model of Pielou's Evenness. All survey time points are pairwise compared with one another, as indicated by the 'contrast' column. The estimate, standard error, degrees of freedom, t-ratio and p-values are reported for each of the pairwise comparisons. Results are averaged over the levels of Substrate categories ('Hard', 'Mixed' and 'Soft').

Contrast	Estimate	Standard Error (SE)	Degrees of Freedom (df)	t-ratio	p-value
2017 - 2018	0.1059	0.0105	1258	10.057	<.0001
2017 - (2018-m)	0.1862	0.0104	1258	17.860	<.0001
2017 - 2019	0.1195	0.0111	1258	10.745	<.0001
2018 - (2018-m)	0.0803	0.0102	1258	7.866	<.0001
2018 - 2019	0.0136	0.0106	1258	1.282	0.5743
(2018-m) - 2019	-0.0667	0.0108	1258	-6.172	<.0001

Appendix 19: Species codes for ordination plots

Table 21: Species codes for ordination plots. Species were given shorter codes to make it easier to interpret ordination plots.

Scientific Name	Species Code
HARD CORALS - Scleractinia	
Colpophyllia natans	Col.nat
Diploria sp.	Dip.spp.
Madracis mirabilis	Mad.mir
Montastraea cavernosa	Mon.cav
Orbicella annularis	Orb.ann
Orbicella faveolata	Orb.fav
Porites astreoides	Por.ast
Porites divaricata	Por.div
Porites porites	Por.por
Siderastrea siderea	Sid.sid
Siderastrea radians	Sid.rad
Solenastrea bournoni	Sol.bou.
Stephanocoenia intersepta	Ste.int
CORALS – Anthoathecata (hydrocoral)	
Millepora spp.	Mil.spp.
CORALS - Alcyonacea	
Gorgonia spp.	Gor.spp.
Pseudopterogorgia spp.	Pse.spp.
SPONGES – Demospongia / PORIFERA	
Agelas spp.	Age.spp.
Amphimedon compressa	Amp.com.
Aplysina cauliformis	Apl.cau.
Aplysina fistularis	Apl.fis
Chondrilla nucula	Cho.nuc.
Cliona spp.	Cli.spp.
Iotrochota birotulata	Iot.bir
Ircinia felix	Iri.fel
Ircinia spp.	Iri.spp.
Oceanapia bartschi	Oce.bar.
Siphonodictyon spp.	Sip.spp.
Svenzea spp.	Sve.spp.
Verongula rigida	Ver.rig.
Verongula spp.	Ver.spp.
Xestospongia muta	Xes.mut.

MACROALGAE	
Dictyota spp.	Dic.spp.
Brown turf algae	brown.alg
Calcifying algae	calc.alg
Green turf algae	green.turf
Unidentified green algae	green.alg
CNIDARIAN	
Stichodactyla helianthus	Sti.hel.
ECHINODERMATA	
Diadema antillarum	Did.ant.
POLYCHAETA	
Loimia medusa	Loi.med.
Hermodice spp.	Her.spp.
Sabellastarte spp.	Sab.spp.
Bispira spp.	Bis.spp.

Appendix 20: RDA of species in 2017, including brown turf algae

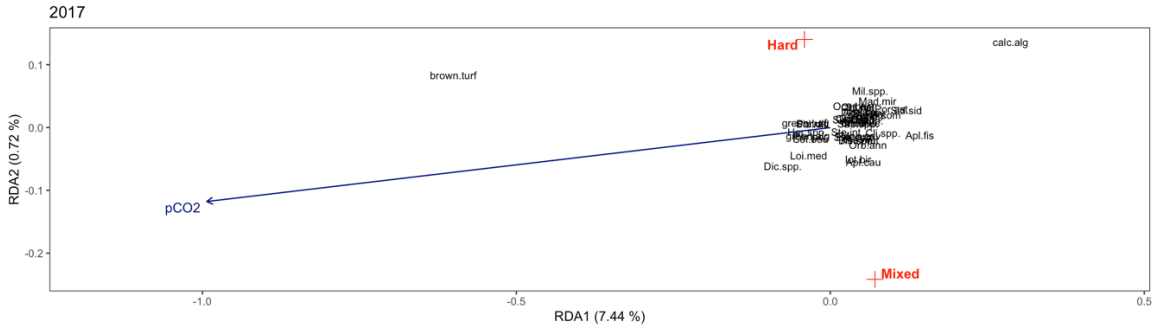

Figure 19: Redundancy analysis (RDA) for all species in the summer of 2017. A biplot was made to display the species responses to the response to environmental variables. Factor level variable substrate category (indicated by labels 'Hard' or 'Mixed') are indicated by red crosses. pCO_2 measurements are represented by the blue arrow, with arrow length and direction corresponds with the variance which can be explained by that explanatory variable. The direction of the arrows indicates an increasing magnitude of the variable.

Appendix 21: RDA of species in March of 2018, including brown turf algae

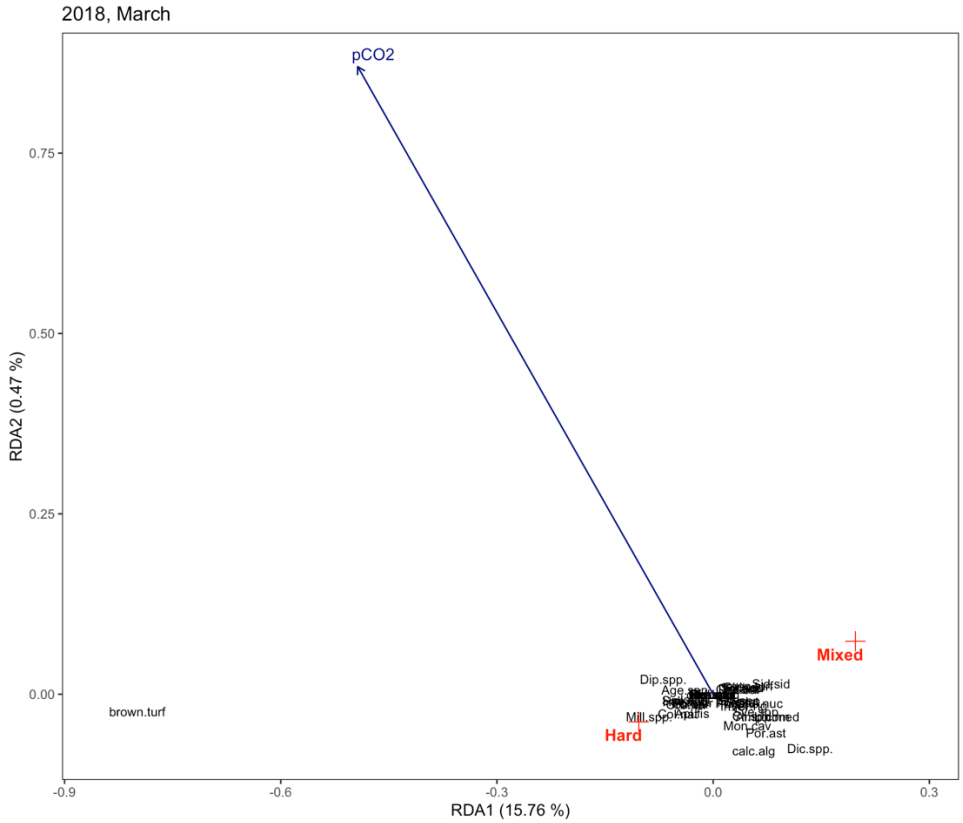

Figure 20: Redundancy analysis (RDA) for all species in March of 2018. A biplot was made to display the species responses to the response to environmental variables. Factor level variable substrate category (indicated by labels 'Hard' or 'Mixed') are indicated by red crosses. pCO_2 measurements are represented by the blue arrow, with arrow length and direction corresponds with the variance which can be explained by that explanatory variable. The direction of the arrows indicates an increasing magnitude of the variable.

Appendix 22: RDA of species in summer of 2018, including brown turf algae

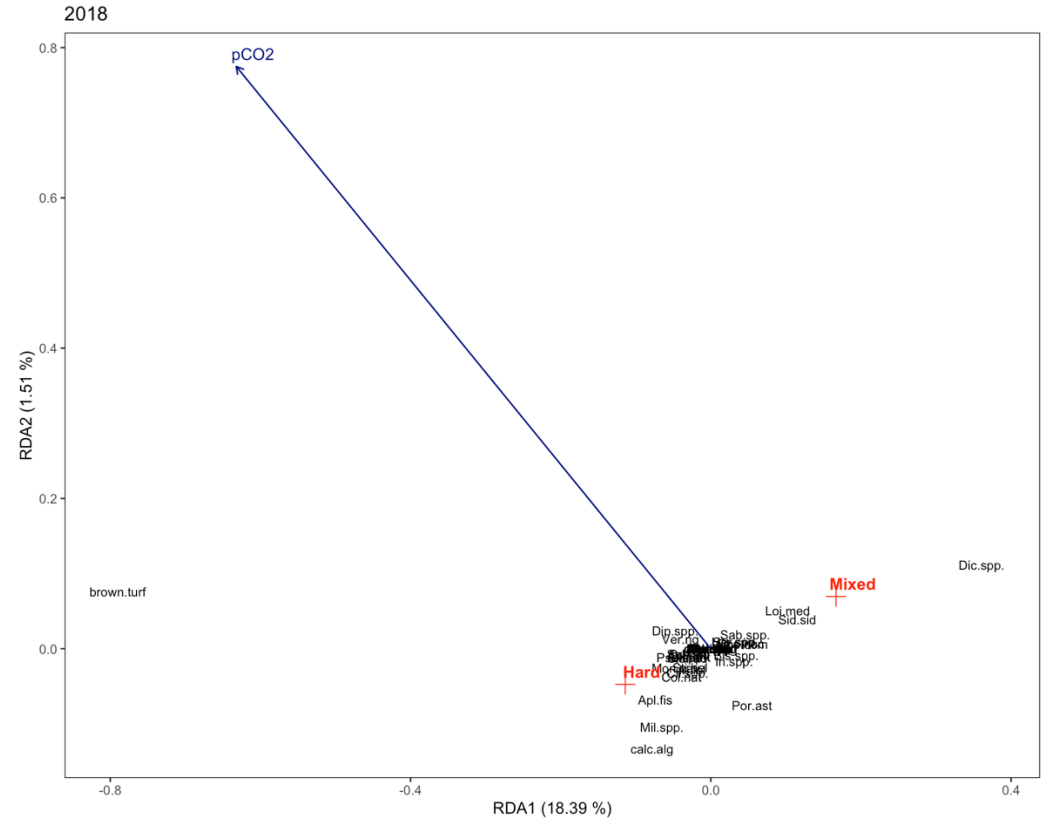

Figure 21: Redundancy analysis (RDA) for all species in the summer of 2018. A biplot was made to display the species response to the environmental variables. Factor level variable substrate category (indicated by labels 'Hard' or 'Mixed') are indicated by red crosses. pCO_2 measurements are represented by the blue arrow, with arrow length and direction corresponds with the variance which can be explained by that explanatory variable. The direction of the arrows indicates an increasing magnitude of the variable.

Appendix 23: RDA of species in 2019, including brown turf algae

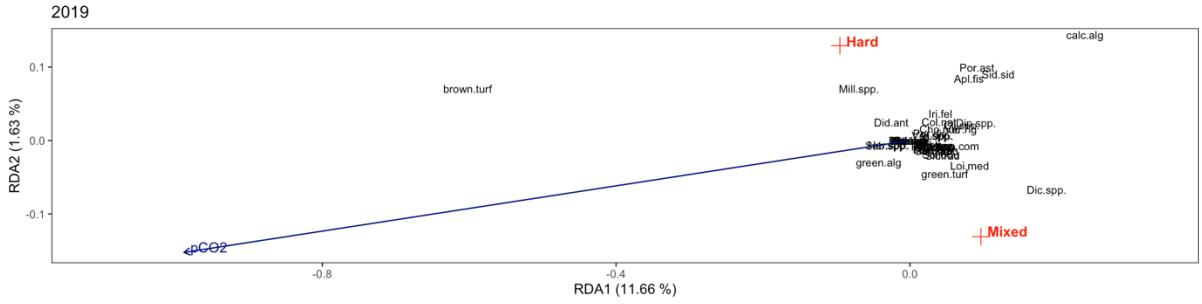

Figure 22: Redundancy analysis (RDA) for all species in the summer of 2018. A biplot was made to display the species response to the environmental variables. Factor level variable substrate category (indicated by labels 'Hard' or 'Mixed') are indicated by red crosses. pCO_2 measurements are represented by the blue arrow, with arrow length and direction corresponds with the variance which can be explained by that explanatory variable. The direction of the arrows indicates an increasing magnitude of the variable.

Appendix 24: Table of Partitioning of Variance in RDA models

Table 22: Partitioning of variance from all RDA models. Constrained variance includes the variance explained by the predictor variables in the model. Unconstrained variance includes all of the variance that could not be explained by these variables. Total variance is the sum of all the variance. The proportions of each of these variance categories is given in the "Proportion" column.

Year:	Partitioning of variance:	Inertia (variance)	Proportion
2017	Total	0.21613	1.00000
	Constrained	0.01759	0.08140
	Unconstrained	0.19854	0.91860
2018, March	Total	0.09029	1.0000
	Constrained	0.01459	0.16160
	Unconstrained	0.07570	0.83840
2018	Total	0.08500	1.00000
	Constrained	0.01692	0.19902
	Unconstrained	0.06808	0.80098
2019	Total	0.09691	1.00000
	Constrained	0.01286	0.13268
	Unconstrained	0.08405	0.86732
All survey time points	Total	0.13666	1.00000
	Constrained	0.02638	0.19305
	Unconstrained	0.11028	0.80695

Appendix 25: Table of Summary Output from RDA

Table 23: Summary outcome of all Redundancy Analyses (RDAs). Predictor variables included in the five fitted models are shown with degreed of freedom (Df), variance, a pseudo-F statistic and a p-value.

Model:	Predictor variable	Df	Variance	Pseudo-F	p
RDA for 2017					
	pCO2	1	0.014870	11.609	0.001
	Substrate category	1	0.001775	1.386	0.194
	Residual	155	0.198537		
RDA for 2018, March					
	pCO2	1	0.002093	4.508	0.009
	Substrate category	1	0.010825	23.309	0.001
	Residual	163	0.075700		
RDA for 2018					
	pCO2	1	0.003408	8.359	0.001
	Substrate category	1	0.009900	24.283	0.001
	Residual	167	0.068085		
RDA for 2019					
	pCO2	1	0.007853	12.894	0.001
	Substrate category	1	0.001805	2.964	0.014
	Residual	138	0.084052		
RDA for all years					
	Survey time point	3	0.015804	29.665	0.001
	pCO2	1	0.003721	20.952	0.001
	Substrate category	1	0.005029	28.319	0.001
	Residual	621	0.110281		

Appendix 26: Eigenvalues of constrained axes for CCAs without brown turf algae

Table 24: Eigenvalues for constrained and unconstrained axes for canonical correspondence analysis (CCA) without brown turf algae. Number of axes are listed for both constrained and unconstrained axes. Eigenvalues of the two constrained axes with the largest values and the three unconstrained axes with the largest eigenvalues.

Model:	**Eigenvalues for constrained axes**			**Eigenvalues for unconstrained axes**			
	Number of axes	CCA1	CCA2	Number of axes	CA1	CA2	CA3
2017	2	0.06367	0.03917	40	0.4372	0.3256	0.2617
2018, March	2	0.08524	0.02651	31	0.3821	0.3441	0.3380
2018	2	0.08071	0.02008	26	0.3405	0.3092	0.2721
2019	2	0.05608	0.03467	31	0.3130	0.2869	0.2646
All years	5	0.10267	0.04572	40	0.3708	0.2789	0.2680
Macro	6	0.22306	0.14094	6	0.8308	0.6552	0.5808

Appendix 27: Eigenvalues of constrained axes for RDAs with brown turf algae

Table 25: Eigenvalues for constrained and unconstrained axes for redundancy analysis (RDA) with brown turf algae. Number of axes are listed for both constrained and unconstrained axes. Eigenvalues of the two constrained axes with the largest values and the three unconstrained axes with the largest eigenvalues.

Model:	**Eigenvalues for constrained axes**			**Eigenvalues for unconstrained axes**			
	Number of axes	RDA1	RDA2	Number of axes	PC1	PC2	PC3
2017	2	0.01602	0.00158	44	0.09480	0.01634	0.01182
2018, March	2	0.01417	0.00042	34	0.03995	0.00646	0.00500
2018	2	0.01563	0.00128	28	0.02375	0.01203	0.00704
2019	2	0.01128	0.00158	34	0.02838	0.01161	0.00843
All years	5	0.01912	0.00523	44	0.04619	0.01115	0.00751

Appendix 28: Table of Partitioning of Variance in CCA models

Table 26: Partitioning of variance from all CCA models. Constrained variance includes the variance explained by the predictor variables in the model. Unconstrained variance includes all of the variance that could not be explained by these variables. Inertia is a scales Chi-squared value. The proportions of each of these inertia categories is given in the "Proportion" column.

Year:	**Partitioning of variance:**	**Inertia (scaled Chi-square)**	**Proportion**
2017	Total	4.4691	1.0000
	Constrained	0.1028	0.0230
	Unconstrained	4.3662	0.9770
2018, March	Total	5.4073	1.0000
	Constrained	0.1118	0.0207
	Unconstrained	5.2955	0.9793
2018	Total	3.7325	1.0000
	Constrained	0.1008	0.0270
	Unconstrained	3.6317	0.9730
2019	Total	3.7451	1.0000
	Constrained	0.0908	0.0242
	Unconstrained	3.6544	0.9758

All survey time points	Total	5.7801	1.0000
	Constrained	0.2025	0.0350
	Unconstrained	5.5777	0.9650
Macro count model	Total	3.5859	1.0000
	Constrained	0.4123	0.1150
	Unconstrained	3.1735	0.8850

Appendix 29: Table of Summary Output from CCAs

Table 27: Summary outcome of all Canonical Correspondence Analysis (CCAs). Predictor variables included in the five fitted models are shown with degreed of freedom (Df), Chi-square value, a pseudo-F statistic and a p-value.

Model:	Predictor variable	Df	Chi-square	Pseudo-F	p
CCA for 2017					
	pCO2	1	0.0637	2.2603	0.002
	Substrate category	1	0.0397	1.4087	0.068
	Residual	155	4.3662		
CCA for 2018, March					
	pCO2	1	0.0456	1.3964	0.097
	Substrate category	1	0.0555	1.6968	0.004
	Residual	162	5.2955		
CCA for 2018					
	pCO2	1	0.0300	1.3813	0.142
	Substrate category	1	0.0792	3.6402	0.001
	Residual	167	3.6317		
CCA for 2019					
	pCO2	1	0.0501	1.8935	0.015
	Substrate category	1	0.0503	1.8976	0.003
	Residual	138	3.6544		
CCA for all years					
	Survey time point	3	0.1554	5.7597	0.001
	pCO2	1	0.0236	2.6256	0.001
	Substrate category	1	0.0266	2.9592	0.001
	Residual	620	5.5776		
Macro count model					
	Survey time point	3	0.3314	21.2322	0.001
	pCO2	1	0.0195	3.7545	0.009
	Substrate category	1	0.0537	5.1563	0.010
	Residual	610	3.1735		